Aus der Medizinischen Klinik und Poliklinik IV der Ludwig-Maximilians-Universität München

Direktor: Prof. Dr. med. Martin Reincke

Membrane-anchored chemokine fusion proteins as adjuvants for tumor therapy

Dissertation

zum Erwerb des Doktorgrades der Naturwissenschaften

an der Medizinischen Fakultät

der Ludwig-Maximilians-Universität München

vorgelegt von

Jan Niklas Münchmeier

aus Dachau

2011

Gedruckt mit Genehmigung der Medizinischen Fakultät

der Ludwig-Maximilians-Universität München

Betreuer der Arbeit:	Prof. Dr. Peter Jon Nelson
Zweitgutachter:	Prof. Dr. Judith Johnson
Dekan:	Prof. Dr. med. Dr. h.c. Maximilian Reiser, FACR, FRCR
Tag der mündlichen Prüfung:	14.02.2012

Table of contents

Zusammenfassung

Maligne Tumorerkrankungen sind eine der häufigsten Todesursachen der Welt und neue Therapiemöglichkeiten werden dementsprechend dringend benötigt. Einen vielversprechenden Ansatz stellt der adoptive Transfer von Immun-Effektorzellen in Tumorpatienten dar. Die Effizienz dieser Therapieform wird jedoch häufig durch eine unzureichende Rekrutierung der transferierten Leukozyten in das Tumorgewebe eingeschränkt. Aus diesem Grunde wurden in der vorliegenden Studie neuartige Fusionsproteine entwickelt, die spezifisch die Rekrutierung bestimmter Leukozyten verstärken sollten. Die Proteine setzten sich zusammen aus einer N-terminalen Chemokindomäne, der Muzindomäne des membrangebundenen Chemokins CX3CL1 sowie einem C-terminalen Glykosylphosphatidylinositol (GPI) Membrananker, der die Transmembrandomäne von CX3CL1 ersetzte. Nach Injektion in einen Tumor sollten sich die Proteine aufgrund des GPI-Ankers in die Zellmembranen von Endothel-, Tumor- und Stromazellen integrieren. Dabei sollte die Chemokindomäne im Zusammenspiel mit der Muzindomäne selektiv Leukozyten rekrutieren, die den korrespondierenden Chemokinrezeptor exprimieren. Für die Rekrutierung zytotoxischer T-Zellen und NK-Zellen wurde zunächst ein Fusionsprotein mit einer CXCL10 Chemokindomäne generiert (CXCL10-mucin-GPI), sowie diverse Varianten des Proteins als Kontrollen. Die Fusionsproteine wurden in eukaryotischen Zellen exprimiert und konnten anschließend mittels FACS und Immunfluoreszenz-Mikroskopie auf der Zellmembran der transfizierten Zellen nachgewiesen werden. Weitere Versuche zeigten, dass die CXCL10 Fusionsproteine den korrespondierenden Chemokinrezeptor CXCR3 aktivieren können. Dies führte in CXCR3-positiven Zellen zu einer Mobilisation von intrazellulärem Calcium, einer Internalisierung von CXCR3 sowie zu einer Verstärkung der Adhäsion an Zelloberflächen. Die GPI-verankerten Fusionsproteine wurden anschließend mittels Affinitätschromatographie aufgereinigt und es konnte gezeigt werden, dass sich die gereinigten Proteine aufgrund ihres GPI-Ankers spontan in Zellmembranen integrieren. In einem *in vitro* Modell für Rekrutierungsprozesse in Blutgefäßen konnten Endothelzellen nach Behandlung mit CXCL10-mucin-GPI effektiv NK-Zellen in Gegenwart physiologischer Scherkräfte rekrutieren. Vergleiche mit entsprechenden Varianten von CXCL10-mucin-GPI zeigten, dass die Muzindomäne unabdingbar für diesen Effekt war. Im Gegensatz zu NK-Zellen wurden T-Zellen weniger effizient rekrutiert. In einem *in vivo* Tumor-Modell zeigte sich, dass eine intratumorale Injektion von CXCL10-mucin-GPI zu einer wesentlich stärkeren Rekrutierung von NK-Zellen führt als eine Injektion von löslichem CXCL10. Aus den Versuchen der vorliegenden Studie kann demnach die Schlussfolgerung gezogen werden, dass Fusionsproteine wie CXCL10-mucin-GPI eine vielversprechende Möglichkeit für die gezielte Verstärkung der Rekrutierung von Leukozyten im Rahmen zellulärer Immuntherapien darstellen.

Summary

Cancer is one of the leading causes of death worldwide and novel therapeutic approaches for the treatment of this disease are urgently needed. The adoptive transfer of immune effector cells represents a promising therapeutic strategy. However, the efficacy of this therapy can be hampered by insufficient infiltration of the tumor by the transferred cells. To help address this problem, a novel class of reagents was developed to enhance leukocyte recruitment to tumor environments. This class of fusion proteins was designed to selectively recruit specific leukocyte subsets based on their expression of a given chemokine receptor. The proteins were composed of an N-terminal chemokine head and the mucin domain taken from the membrane-anchored chemokine CX3CL1, with a C-terminal glycosylphosphatidylinositol (GPI) membrane anchor replacing the normal transmembrane domain. When purified and injected into a tumor, these proteins integrate into cell membranes of tumor, stromal and endothelial cells by means of their GPI anchor. The mucin domain in conjunction with the chemokine head acts to specifically recruit leukocytes that express the corresponding chemokine receptor, e.g. adoptively transferred T or NK cells. A fusion protein comprising a CXCL10 chemokine head (CXCL10-mucin-GPI) was studied as the proof of concept of this approach, with a series of control proteins generated in parallel. The proteins were expressed in a mammalian system and it was verified that the GPI anchor signal sequence could correctly target them to the cell membrane. The ability of the CXCL10 fusion proteins to trigger the CXCR3 receptor was further verified using assays that measured receptor internalization, calcium mobilization and enhanced adhesion of T cells to cell monolayers as readouts. Following the identification of a suitable detergent for solubilization, the various proteins were isolated from cell extracts using affinity chromatography. Purified proteins were found to efficiently integrate into cell membranes in a process dependent upon the GPI anchor. *In vitro* models of leukocyte recruitment showed that endothelial cells incubated with CXCL10-mucin-GPI efficiently recruited NK cells under conditions of physiologic flow. This process was found to be dependent on the presence of the mucin domain. T cells were in contrast not recruited as effectively. When injected into experimental murine tumors *in vivo*, CXCL10-mucin-GPI was more efficient in recruiting NK cells than soluble CXCL10. Thus, fusion proteins such as CXCL10-mucin-GPI represent promising candidates for novel adjuvants to be used in cellular immunotherapy.

1 Introduction

1.1 Immunotherapy of cancer

The medical term cancer describes a group of diseases which are all associated with an uncontrolled growth of transformed cells. It is one of the leading causes of death, accounting in 2008 worldwide for 7.6 million deaths (about 13% of all deaths). Despite many advances in the field of cancer therapies, deaths from cancer are projected to rise to 11 millions in 2030 (WHO 2011). Besides surgical resection of the tumor mass and radiation therapy, the current medicamentous treatment options for cancer patients can be grouped into four major categories: (i) chemotherapy, which involves the administration of cytotoxic drugs, (ii) hormonal therapy that interferes with hormone receptors on the cancerous cells, (iii) targeted therapy using novel antibodies and small molecules that specifically affect proteins involved in growth signaling pathways and (iv) immunotherapy (Lesterhuis et al. 2011).

Immunotherapy builds upon the body´s ability to recognize and destroy transformed cells. Early therapeutic approaches were already described more than a century ago. In 1891 William Coley treated a sarcoma patient with intratumoral injections of two bacterial strains, which subsequently triggered an inflammatory reaction that was followed by a complete disappearance of the tumor (Coley 1910). Today, much is known about the immune system and its diverse interactions with a growing tumor. An immune cell infiltrate consisting of monocytes, macrophages, neutrophils, dendritic cells, natural killer (NK) cells and T cells is found in diverse cancer settings (Becker 1993; Di Carlo et al. 2001; Bingle et al. 2002; Pages et al. 2010; Levy et al. 2011; Ruffell et al. 2011). However, the immune reaction evoked by the tumor is often not adequate to control tumor growth, as evidenced by the outgrowth of the tumor. In some cases, the infiltrating cells have also been shown to promote tumor growth by creating a tumor-permissive microenvironment (Figel et al. 2011; Meyer et al. 2011). The general aim of cancer immunotherapy is focused on moderating the immune response against the tumor so that efficient tumor recognition and destruction is induced. Several different approaches have been taken in order to achieve this goal, some examples of which are listed in the next section.

1.1.1 Adjuvants, antibodies and small proteins

In order to enhance the immune response against the tumor, immune-stimulatory cytokines such as interleukin-2 (IL-2) or interferon α (IFNα) have been administered. This was first shown to be effective in melanoma patients (Parkinson et al. 1990; Kirkwood et al. 1996). In addition, adjuvants like CpG oligonucleotides (Garbi et al. 2004) or bacillus Calmette-Guerin (Sylvester et al. 2010) are sometimes used to strengthen the endogenous immune reaction.

Secondly, inhibitory pathways that downregulate the immune response can be targeted, as exemplified by the antibody Ipilimumab. This reagent blocks the inhibitory receptor cytotoxic T lymphocyte associated antigen 4 (CTLA-4) on T cells, thus enhancing their activity. It has recently been approved by the food and drug administration (FDA) of the United States for treatment of advanced-stage melanoma following a successful phase III clinical trial (Hodi et al. 2010).

Third, growth factor receptors such as the epidermal growth factor receptor (EGFR) which are actively used by some cancer cells can be targeted by blocking antibodies (e.g. the humanized antibody Trastuzumab) (Slamon et al. 2001). Antibodies like these mediate their effects not only by blocking the respective receptors or altering their signal transduction cascades, but also by inducing antibody-dependent cellular toxicity through the activation of Fc-receptor expressing cells, and by complement activation. The degree with which each effect contributes to the therapeutic outcome varies between the different antibodies (Borghaei et al. 2009).

Also cell type-specific antigens like CD20, a common B cell marker that is also expressed on many non-Hodgkin lymphomas, have successfully been used as antigens for antibody-based immunotherapy (McLaughlin et al. 1998).

An emerging class of antibody-based drugs consists of bispecific antibody reagents. These are designed to recognize either two different tumor antigens simultaneously or to recognize one tumor antigen with one of their arms and the invariant T cell activating molecule CD3 with the other arm [reviewed in (Beck et al. 2010; Müller and Kontermann 2010)]. The latter approach allows redirecting the polyclonal T cell pool of the patient towards a specific tumor antigen, irrespective of T cell specificities. These antibodies are referred to as BiTEs (Bispecific T cell engager) and include Catumaxomab, which binds to CD3 and the epithelial cell adhesion molecule (EpCAM) that is often overexpressed on tumor cells. Catumaxomab was approved in 2009 by the European medicines agency for the treatment of malignant ascites [reviewed in (Linke et al. 2010)].

In addition to the approaches detailed above that are generally based on the use of bioactive proteins or adjuvants, a major focus of immunotherapy is also directed towards the use of immune cells themselves as anti-cancer agents, as discussed below.

1.1.2 Cell-based immunotherapies

1.1.2.1 Therapeutic approaches using NK cells

The central premise of cell-based immunotherapy is focused on harnessing the natural cytotoxic potential of immune cells to eliminate their target cells in a highly specific and efficient manner. For this purpose, both natural killer (NK) and cytotoxic T cells are under active investigation. NK cells recognize their target cells by a combination of (i) missing inhibitory signals like major histocompatibility complex I (MHC I) proteins, (ii) the presence of activating signals such as the stress-

induced protein MICA binding to the NKG2D receptor, and (iii) activating cytokines. This combined stimulation leads to degranulation of the cytotoxic vesicles and ultimately destruction of the target cell. In addition, NK cells can also be triggered via their Fc receptors (FCγRIII/ CD16) (Leibson 1997) and have therefore been implicated in the mechanism of action of various therapeutic antibodies [e.g. for the above mentioned Trastuzumab (Musolino et al. 2008)]. As immunotherapeutic tools, they have mostly been studied in the context of hematologic malignancies, e.g. in combination with hematopoietic stem cell transplantation. In this setting it has been shown that NK cells can mediate graft-versus-leukemia effects, especially when the NK cell inhibitory ligands of donor and recipient are mismatched, so that inhibitory molecules on the leukemic cells are ineffective against donor NK cells (Ruggeri et al. 2002). Recent studies have also investigated the potential of NK cell therapy in the treatment of solid tumors, for example in non-small cell lung cancer, melanoma and renal cell cancer patients. Here, first encouraging results were obtained in phase I clinical trials (Arai et al. 2008; Cho et al. 2010; Iliopoulou et al. 2010). A recent phase II study in patients with ovarian and breast cancer has shown a transient donor chimerism after infusion of *ex vivo* expanded haploidentical NK cells, suggesting the need for further investigations to enhance NK cell persistence and expansion (Geller et al. 2011). The major focus of cell-based immunotherapy lies, however, on cytotoxic $CD8^+$ T cells.

1.1.2.2 Therapeutic approaches using $CD8^+$ T cells

In contrast to NK cells, $CD8^+$ T cells recognize specific peptides bound to MHC I on the surface of the target cells via their T cell receptor (TCR). The rationale to use $CD8^+$ T cells as anti-tumor agents was based on the observation that in some patients, melanoma lesions undergo spontaneous regression (Everson 1964; McGovern 1975). Later this regression was associated with a clonal expansion of T cells (Ferradini et al. 1993). In addition, the presence of a robust T cell infiltrate within the tumor correlated with a favorable prognosis in some cancers including melanoma, colon cancer and ovarian cancer (Clark et al. 1989; Clemente et al. 1996; Naito et al. 1998; Sato et al. 2005). Of note, it was observed that only the presence of T cells within the tumor had a beneficial effect, whereas T cells present at the tumor margin did not alter the probability of survival (Naito et al. 1998). This finding suggested that efficient infiltration of the tumor mass is required for the tumoricidal effects of $CD8^+$ T cells. This requirement represents a significant hurdle for many current therapeutic strategies as will be discussed in more detail later.

To generate tumor-reactive T cells, two mechanistically distinct approaches have been taken: Either T cells are primed *in situ* by vaccination protocols, or expanded *in vitro* and subsequently reinfused into the patient. The potential of vaccinating tumor patients against their tumors was enhanced by the identification of tumor-associated antigens recognized by tumor-infiltrating lymphocytes in the early 1990s (van der Bruggen et al. 1991; Kawakami et al. 1994). This has lead to development of

cancer vaccines based on different techniques. To date, one of the most successful vaccines is the recently FDA approved sipuleucel-T, used for the treatment of metastatic prostate cancer. It consists of enriched blood antigen presenting cells cultured *in vitro* with a fusion protein consisting of prostatic acid phosphatase and granulocyte macrophage colony stimulating factor (GM-CSF). In a phase III clinical trial, this agent prolonged the median survival by 4.1 months and reduced the risk of death by 22% (Kantoff et al. 2010). Another successful example is a peptide vaccine targeting gp100, a protein expressed in melanoma cells as well as normal melanocytes. In a recent phase III clinical study, metastatic melanoma patients were treated either with high-dose IL-2 alone, or with IL-2 in conjunction with the vaccine in incomplete Freud´s adjuvant. The vaccine group displayed a 6.7 months longer median overall survival than the group receiving only IL-2 (Schwartzentruber et al. 2011). However, clinical trials generally showed disappointing results, although frequently a tumor-specific immune response could be generated [reviewed in (Klebanoff et al. 2011; Palucka et al. 2011)]. Importantly, vaccination protocols rely on the endogenous T cell repertoire, which represents a major drawback of this technique as many tumor-associated antigens are self antigens, for which the reactive T cells have either been clonally deleted in the thymus or display an anergic or regulatory phenotype [reviewed in (Paul et al. 2007)].

An appealing different approach makes use of adoptive T cell therapy. Here, T cells are isolated either from the peripheral blood or from tumor-infiltrating lymphocytes (TILs), expanded *in vitro* and subsequently reinfused into the patient. During the *in vitro* culture period, the cells can be selected for efficient tumor recognition or transduced with a novel receptor to overcome clonal deletion and in order to confer a defined tumor-specificity as depicted in Figure 1 [reviewed in (Turtle and Riddell 2011)].

The first clinical trial of adoptive T cell therapy was performed in 1985 with IL-2 activated peripheral blood lymphocytes (Rosenberg et al. 1985). Complete regression of the tumor in one patient with metastatic melanoma was observed. Following the observation that mice could be cured from metastatic colon carcinomas by the infusion of IL-2 expanded TILs (Rosenberg et al. 1986), the anti-tumor effect of TILs was further investigated in the clinic in 20 melanoma patients, of which 11 displayed tumor regression (Rosenberg et al. 1988). Since then, many trials including randomized clinical studies have followed in various cancer settings like gastric cancer, hepatocellular carcinoma, renal cell cancer, lung cancer and melanoma. However, many of these trials have not shown a statistically significant positive effect of the infused T cells, especially in cancers other than melanoma [reviewed in (June 2007)].

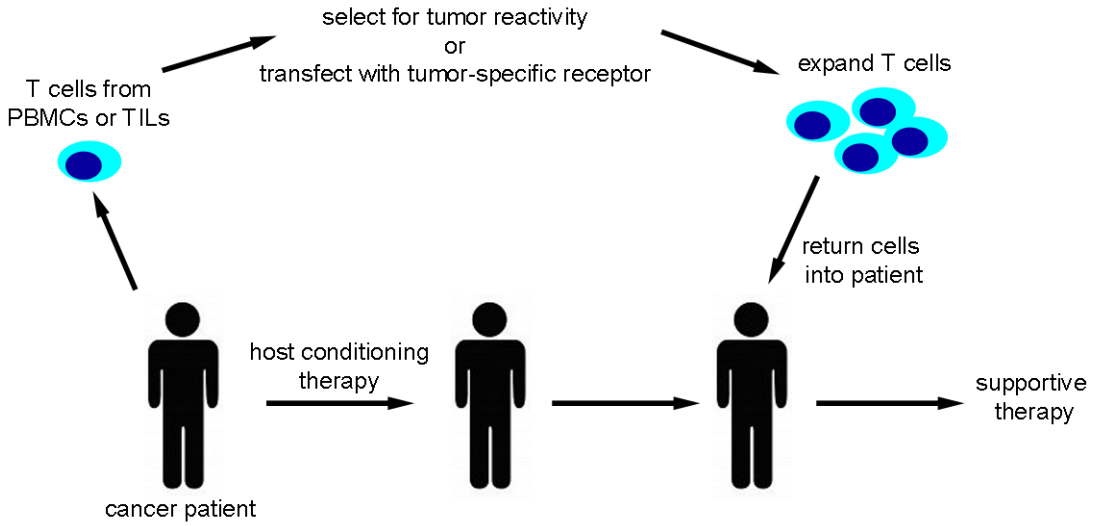

Figure 1: Principle of adoptive T cell therapy. Adoptive T cell therapy relies on the ability of T cells to specifically recognize and destroy tumor cells. T cells are isolated from a cancer patient either using peripheral blood (PBMCs, peripheral blood mononuclear cells) or tumor biopsies (TILs, tumor infiltrating lymphocytes). The cells can be selected for tumor reactivity or transduced with a novel receptor to confer tumor specificity. Subsequently, the cells are expanded (e.g. using IL-2 in combination with activating CD3-specific antibodies) and reinfused into the patient. In order to promote expansion and survival of the transferred cells, the patient can be treated with non-myeloablative lymphodepleting chemotherapy and/or radiation prior to infusion of the cells.

Many potential reasons for this lack of reproducible efficiency have been identified. These include a general immunosuppressive milieu within the tumor mediated by immunosuppressive cytokines like transforming growth factor β (TGF-β), regulatory T cells (Tregs), myeloid suppressor cells and oxygen limitation as well as evasion mechanisms by the tumor cells themselves such as MHC I down-regulation, expression of apoptosis-inducing ligands and others [reviewed in (Quezada et al. 2011) and (Leen et al. 2007)]. An additional important factor is a general lack of efficient infiltration of the transferred cells into the tumor milieu as detailed below.

1.1.3 Lack of infiltration as a reason for the failure of cell-based immunotherapies

Tumor growth is intimately associated with neoangiogenesis, a process in which new blood vessels are formed. Angiogenesis is required to provide the growing tumor cells with sufficient nutrients and oxygen. In order to stimulate angiogenesis, tumors release pro-angiogenic cytokines like vascular endothelial growth factor (VEGF) or basic fibroblast growth factor (bFGF) and pro-angiogenic chemokines like CXCL8, which in turn induce proliferation and migration of endothelial cells [reviewed in (De Luca et al. 2008)]. The degree of angiogenesis *in vivo* can be correlated with the amount of VEGF released by various melanoma cell lines (Danielsen and Rofstad 1998), and angiogenesis was shown to be required for the outgrowth of micrometastases *in vivo* (Gimbrone et al. 1972; Holmgren et al. 1995).

Angiogenesis not only keeps the tumor provided with nutrients and oxygen, it also acts as an important mechanism of immune escape. Endothelial cells exposed to the pro-angiogenic factors released by tumor cells have a markedly reduced expression of adhesion molecules. Intercellular adhesion molecule 1 and 2 (ICAM-1 and -2) as well as vascular endothelial cell adhesion molecule 1 (VCAM-1) have been found to be downregulated on endothelial cells isolated from human solid tumors, as well as on endothelial cells treated *in vitro* with bFGF or VEGF (Griffioen et al. 1996a; Griffioen et al. 1996b). Additionally, upregulation of endothelial adhesion molecules in response to proinflammatory cytokines such as interleukin-1β (IL-1β) and tumor necrosis factor α (TNFα) is inhibited in tumor endothelial cells. This phenomenon has been termed endothelial cell anergy in analogy to T cells that can no longer react to stimuli via their T cell receptor (Griffioen et al. 1996a). This endothelial cell anergy is problematic as the presence and upregulation of ICAM and VCAM are centrally important for efficient leukocyte recruitment from the blood stream. These molecules moderate the adhesion of leukocytes to the blood vessel wall and foster their subsequent extravasation because they act as receptors for integrin molecules on the migrating leukocytes as detailed in chapter 1.2 (Springer 1994). Consequently, in many tumor models, a reduced interaction of leukocytes with the blood vessel wall has been observed, along with defective infiltration of the tumors (Wu et al. 1992; Griffioen et al. 1999; Tromp et al. 2000; Dirkx et al. 2003). Lack of infiltration has also been proposed as a potential explanation for the limited success of adoptive T cell therapy in some clinical studies (Pockaj et al. 1994; Mukai et al. 1999; Huang et al. 2002), and blockade of VEGF-mediated angiogenesis by monoclonal antibodies in combination with adoptive T cell therapy has been shown to have an additive beneficial effect in a murine melanoma model (Shrimali et al. 2010).

In addition to the angiogenesis-related phenomenon described above, proteoglycan molecules on endothelial cells in tumors undergo dramatic changes on transcriptional and post-translational levels, the latter occurring through shedding and enzymatic modifications [reviewed in (Sanderson et al. 2005)]. During the complex cascade of events that represent leukocyte recruitment, proteoglycans are needed for the immobilization and presentation of chemokines at the luminal side of endothelial cells. Without properly presented chemokines, leukocytes cannot undergo tight adhesion or subsequent diapedesis (Kuschert et al. 1999; Proudfoot et al. 2003). Consequently, elevated levels of shed proteoglycans in the serum of myeloma and lung cancer patients have been associated with poor prognosis (Seidel et al. 2000; Joensuu et al. 2002). The dysregulated expression of proteoglycan molecules in the tumor microenvironment may thus represent an additional barrier for adoptively transferred leukocytes to infiltrate the tumor mass because it prevents appropriate chemokine signaling. These phenomena suggest the need to find solutions to overcome the deficiency in leukocyte recruitment into tumors, especially with regards to the disappointing results generally

obtained to date with adoptive T cell therapy. The approach that should be investigated in the current study to solve this problem will be outlined below.

1.2 Leukocyte recruitment and chemokines

Chemokines (chemotactic cytokines) comprise a family of about 50, mostly small secreted proteins. They classically act through binding to G-protein coupled receptors with seven transmembrane domains. Chemokines have been grouped into four major subfamilies based on the positioning of the first two Cysteine residues near the N-terminus: In chemokines of the CC subfamily, the two Cysteines lie directly adjacent to each other, while in the CXC subfamily the residues are separated by one amino acid. The majority of the currently known chemokines can be grouped into one of these two subfamilies. The C subfamily lacks the second Cysteine residue and contains only two members, and CX3CL1 is the only member of the CX3C subfamily, where the first two Cysteines are separated by three amino acids (Mantovani et al. 2006). Figure 2 gives an overview of the currently known chemokines and the respective subfamilies.

Chemokines can be produced by many different cell types and orchestrate the migration of virtually every cell type in the body, both under homeostatic and pathogenic conditions. In a classical inflammatory setting, cytokines such as IL-1β and TNFα are produced, e.g. by cells of the innate immune system like macrophages. These cytokines activate endothelial cells of neighboring microvascular blood vessels as depicted in Figure 3. The “inflamed” endothelial cells then express selectin molecules (usually primarily P-selectin followed by E-selectin) and upregulate the expression of ICAM and VCAM molecules as well as proteoglycans (Pober 1987; Klein et al. 1992; Grone et al. 1999; von Hundelshausen et al. 2001). The selectins induced on the endothelial surface bind to sialylated Lewis-X residues on glycoproteins constitutively expressed by leukocytes. This interaction leads to a phenomenon called rolling adhesion where the leukocyte is captured from the blood stream and subsequently slowly rolls along the vessel wall due to rapid formation and dissociation of bonds in the context of continuous blood flow [(Lawrence and Springer 1991), reviewed in (McEver and Zhu 2010)]. At the same time, chemokines are released at the infection site, e.g. also by cells of the innate immune system, and transcytosed through the endothelial cell layer to the luminal side (Middleton et al. 1997). There, the chemokines are immobilized by binding to proteoglycan molecules, and once immobilized, they can engage matching chemokine receptors on rolling leukocytes. For example, the chemokine CXCL10 is involved in the recruitment of activated T cells and NK cells, as it binds to the CXCR3 receptor found on these cell types.

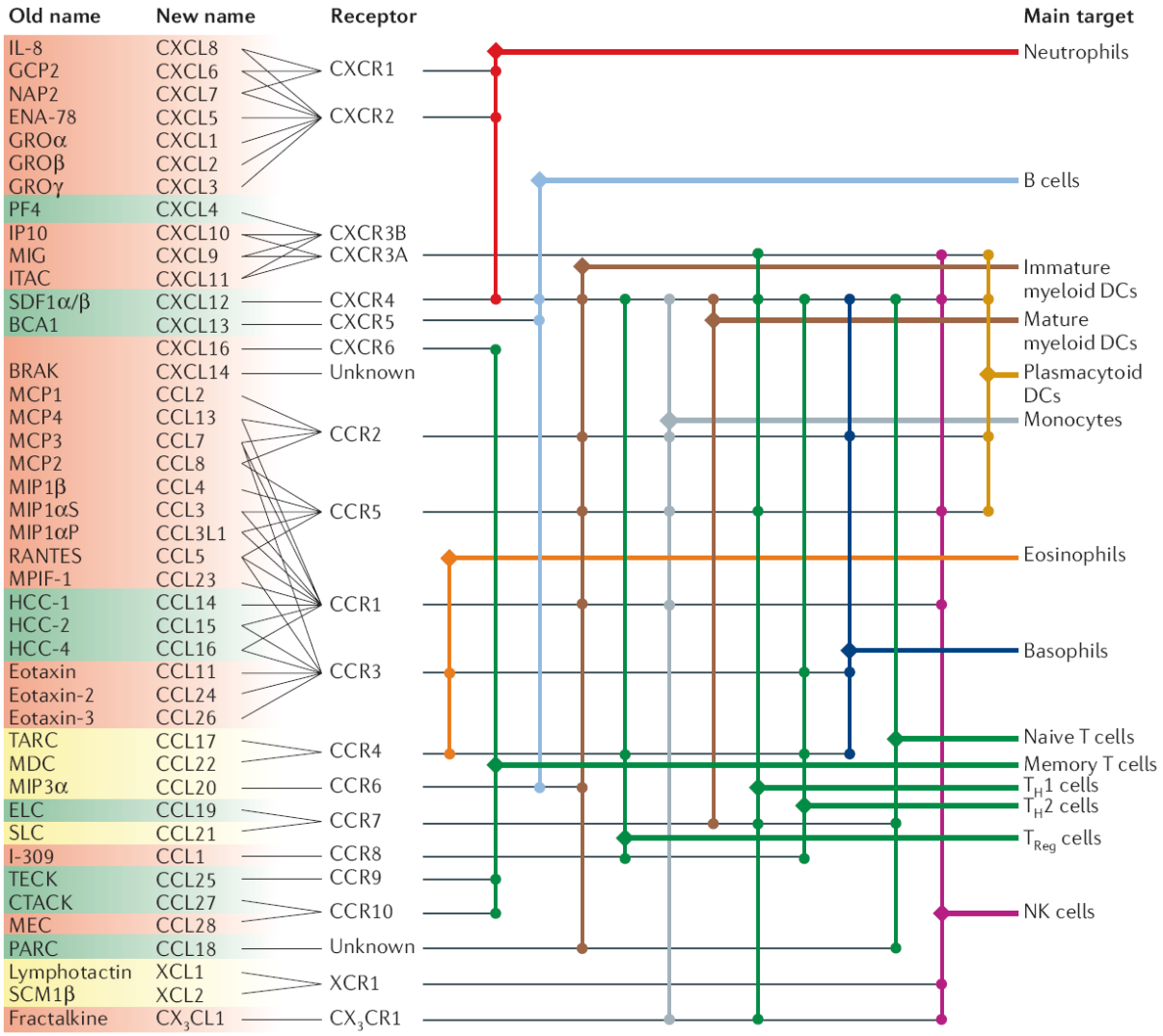

Figure 2: The chemokine family of proteins. An overview of the currently known chemokines is given in the first and second columns. The single proteins are arranged according to the four subfamilies (CXC, CC, C and CX3C subfamily), to which they are assigned based on the composition of a conserved sequence motif near the N-terminus. The respective subfamily of each chemokine also reflects in its systematic name (e.g. CXCL8 or CCL2). Additionally, the historic names are given because they are sometimes still used in the literature. Chemokines classically act by binding to G-protein coupled receptors with seven transmembrane domains, and the receptors for each chemokine are listed in the third column. One chemokine can bind to several receptors and one receptor can be triggered by several chemokines, by which a considerable combinatorial complexity is generated. On the right side of the figure, various leukocyte types are given and the chemokine receptors expressed by each type are indicated by small dots in the respective color. Figure from (Mantovani et al. 2006).

Chemokine receptor signaling then results in a conformational change of the leukocyte´s integrin molecules that leads to a much increased affinity for their ligands – immunoglobulin superfamily molecules like ICAM-1/2 and VCAM-1 on the endothelial cells. This increase in affinity enables the leukocyte to tightly adhere to the endothelial cell surfaces (Tanaka et al. 1993; Shamri et al. 2005). Once tight adherence is established, the leukocyte crawls along the endothelium until eventually it extravasates into the interstitium, a process termed diapedesis (Ryschich et al. 2006). Intraluminal

crawling is thought to be required to find optimal extravasation routes, as diapedesis is delayed if crawling is inhibited (Phillipson et al. 2006), and for crawling and diapedesis proteoglycan-presented chemokines on the endothelial cells are indispensable (Cinamon et al. 2001; Shulman et al. 2009). Following diapedesis, leukocytes can either follow soluble or immobilized chemokine gradients towards the inflammation site [reviewed in (Friedl and Weigelin 2008)]. In the latter process termed haptotaxis, the locally produced chemokines are immobilized on extracellular matrix proteins like collagens and presented to the leukocyte, which moves in an amoeboid manner through the tissue (Rot 1993; Proudfoot et al. 2003; Kohrgruber et al. 2004). Figure 3 summarizes the steps involved in the classical cascade of leukocyte recruitment. The chemokines CXCL8, CXCL10 and CX3CL1 were used in the current study. Each of these chemokines play unique roles in leukocyte trafficking as detailed below.

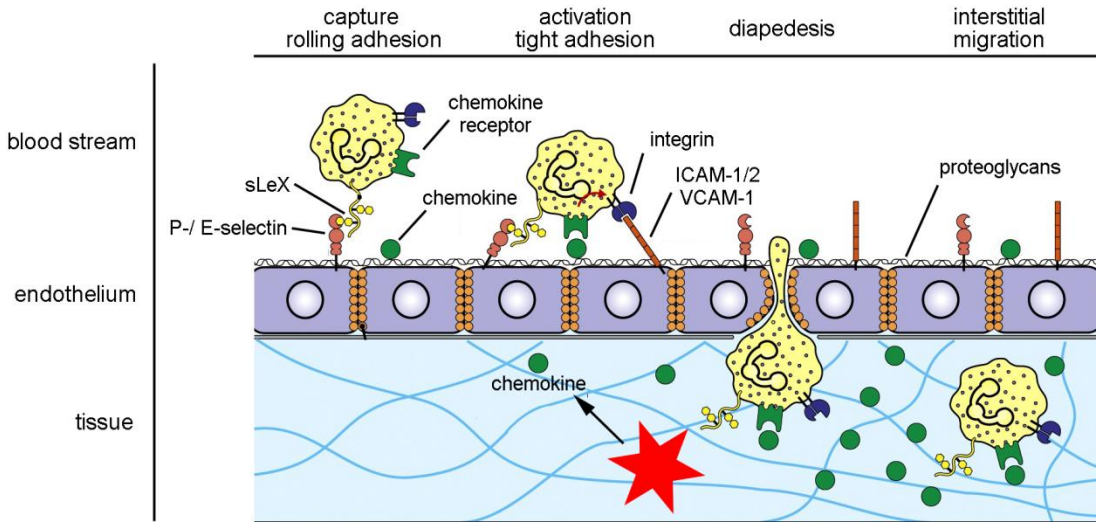

Figure 3: Leukocyte recruitment from the blood stream. In the course of an inflammatory reaction (red asterisk), inflammatory cytokines (not depicted) are produced that activate the endothelium. The activated endothelial cells subsequently express selectin molecules on their surface that bind to sialylated LewisX (sLeX) residues on glycoproteins on the leukocyte surface, leading to leukocyte rolling along the vessel wall. Simultaneously, chemokines that can either be produced at the inflammation site and transcytosed through the endothelium or be produced by endothelial cells themselves are immobilized on proteoglycan molecules on the endothelial surface. In this state, they can trigger matching chemokine receptors on rolling leukocytes leading to an increased affinity of the leukocytes´ integrins. This activation enables the leukocyte to tightly adhere to immunoglobulin superfamily molecules like ICAM-1 and -2 or VCAM-1 on the vessel wall, which is followed by chemokine-guided intraluminal crawling (not depicted) and diapedesis through the endothelium. For the subsequent interstitial migration towards the inflammation site, the leukocyte follows an immobilized chemokine gradient in a process termed haptotaxis. Figure modified from figure 2-49 in (Murphy et al. 2007).

1.2.1 The chemokine CXCL10 and its receptor CXCR3

CXCL10 was originally discovered in 1985 as a gene upregulated by interferon γ (IFNγ) in monocytes, fibroblasts and endothelial cells (Luster et al. 1985). It encodes a protein of roughly 10 kDa which was first named IFN γ-inducible protein 10 or IP-10. In 2002, the CXCL10 structure was solved by nuclear magnetic resonance (NMR) revealing a classical chemokine fold consisting of a flexible N-terminus which includes the CXC motif preceding a short three amino acid helix followed by three anti-parallel beta-sheets and a C-terminal alpha-helix packed across the beta-sheets (Booth et al. 2002).

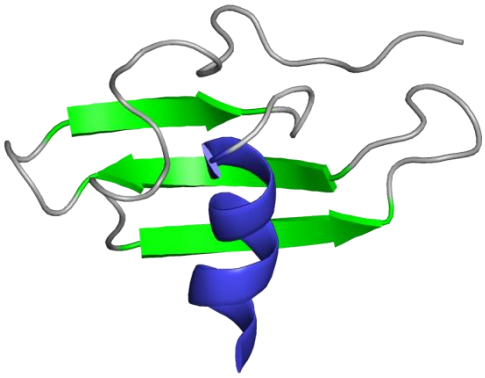

Figure 4: Molecular structure of CXCL10. The structure of CXCL10 was solved in 2002 (Booth et al. 2002). It consists of a flexible N-terminus followed by three antiparallel beta-sheets (green) and a C-terminal alpha helix (blue). The figure was generated from the structural data deposited by Booth et al. in the Protein Data Bank (http://www.pdb.org) under the accession number 1LV9 using PyMol.

This structure is common to most chemokines including CXCL8, CXCL12, CCL4 and CCL5 (Chung et al. 1995). Human and murine CXCL0 share the same tertiary structure and have 70% amino acid identity (83% homology) (Jabeen et al. 2008). CXCL10 binds to, and activates the receptor CXCR3, which it shares with the two other ligands CXCL9 (MIG) and CXCL11 (I-TAC) (Loetscher et al. 1996). CXCR3 is expressed on activated T cells expressing the CD45RO isoform of the CD45 antigen (Loetscher et al. 1998; Qin et al. 1998). Specifically, CXCR3 expression in T cells is associated with a Th1 skewed phenotype as it is highly expressed on Th1 polarized $CD4^+$ as well as on $CD8^+$ T cells (Qin et al. 1998; Sebastiani et al. 2001). CXCL10 bound to activated endothelial surfaces induces rapid adhesion and transmigration of T cells via CXCR3 (Piali et al. 1998; Manes et al. 2006). Consequently, CXCR3 has been shown to play a major role in the recruitment of effector cells in various Th1 dependent diseases like acute allograft rejection (Hancock et al. 2000; Zhao et al. 2002) and viral infections (Dufour et al. 2002), and blockade of CXCR3 with antibodies results in diminished recruitment of Th1 T cells into sites of inflammation (Xie 2003). Importantly, in a murine tumor model, intratumoral expression of CXCL10 was demonstrated to synergize with adoptive T cell therapy, leading to the eradication of established tumors and survival rates of 90% (Huang et al. 2002).

In addition to T cells, CXCR3 is also present on virtually all NK cells at varying expression levels, most pronounced within one of the two major subsets ($CD56^{bright}$ $CD16^{dim}$) of these cells [(Campbell et al. 2001), reviewed in (Cooper et al. 2001)]. A homologous subset exists in the murine system, defined as $CXCR3^{+}$ $CD27^{bright}$ NK cells (Marquardt et al. 2010). CXCL10-stimulated murine NK cells have been shown to contribute to tumor rejection, partly by activating T cells (Saudemont et al. 2005). Moreover, CXCL10 has been shown to enhance exocytosis of cytotoxic granules in NK cells, a property it shares with a variety of other chemokines [(Taub et al. 1995; Taub et al. 1996), reviewed in (Robertson 2002)]. CXCR3 has also been reported to be expressed on subsets of plasmacytoid and myeloid DCs (Cella et al. 1999; Garcia-Lopez et al. 2001), and eosinophils (Jinquan et al. 2000).

In addition to leukocytes, CXCL10 also has effects on other cell types, in particular, endothelial cells. CXCL10 can inhibit proliferation of endothelial cells *in vitro* (Luster et al. 1995; Feldman et al. 2006) as well as angiogenesis *in vivo* (Angiolillo et al. 1995; Strieter et al. 1995). It may even cause the dissociation of newly-formed blood vessels (Bodnar et al. 2009). Based on these effects, CXCL10 can delay wound healing and reduce tumor growth *in vivo* (Luster and Leder 1993; Luster et al. 1998). There is some controversy about how CXCL10 may mediate these effects, especially because CXCR3 is mostly absent on microvascular endothelial cells, or is only expressed during specific stages of the cell cycle (Romagnani et al. 2001). In 2004, an alternative variant of CXCR3 named CXCR3-B was described that is generated by alternative splicing (Lasagni et al. 2003). This receptor carries 48 additional amino acids at the N-terminus and, importantly, was demonstrated to be expressed on primary endothelial cells as opposed to the classical receptor CXCR3-A. Overexpression of CXCR3-B in an endothelial cell line resulted in CXCL10 inhibiting proliferation, whereas the proliferation of cells overexpressing CXCR3-A was stimulated by CXCL10 (Lasagni et al. 2003). However, Campanella et al. showed that CXCR3-B cannot exist in the murine system because of an in-frame stop codon and that the proliferation of endothelial cells isolated from CXCR3(-A) deficient mice is still inhibited by CXCL10 (Campanella et al. 2010). These findings suggest that there must be additional ways of signaling for CXCL10 beyond chemokine receptor triggering that have not yet been identified.

A third variant of the CXCR3 receptor named CXCR3-alt was described in peripheral blood mononuclear cells (Ehlert et al. 2004). CXCR3-alt is generated by exon-skipping and displays a much shorter C-terminus lacking one or two entire transmembrane domains. To date the only functional ligand known for CXCR3-alt is CXCL11. However, the exact cell type expressing this receptor variant remained elusive and the functionality of the receptor was only verified in transfected cells.

1.2.2 The chemokine CXCL8 and its receptors CXCR1 and CXCR2

CXCL8 or interleukin-8 (IL-8) was originally identified as a neutrophil-activating cytokine (Walz et al. 1987; Baggiolini et al. 1989). It is produced upon stimulation with inflammatory cytokines or lipopolysaccharide (LPS) by a variety of cells including fibroblasts, epithelial and endothelial cells,

hepatocytes, mononuclear phagocytes and others (Walz et al. 1987; Yoshimura et al. 1987; Strieter et al. 1988). CXCL8 is a small protein of about 8 kDa which is secreted primarily as a 79 amino acid (aa) protein. The amino terminus can be further processed by proteolytic cleavage yielding various forms ranging from 69 to 79 aa with the 72 aa form being the predominant one *in vivo* [reviewed in (Baggiolini and Clark-Lewis 1992)]. Structurally, CXCL8 displays the classical chemokine fold as detailed for CXCL10 in 1.2.1 with a flexible N-terminus, three antiparallel beta-sheets and a C-terminal alpha-helix (Baldwin et al. 1991). The two known receptors for CXCL8, CXCR1 and CXCR2, are expressed primarily on neutrophils. CXCL8 not only induces migration in these cells, but can also trigger granule exocytosis and respiratory burst [reviewed in (Baggiolini and Clark-Lewis 1992)]. In 2002, Hess and colleagues described a subset of $CD8^+$ T cells as an additional target for CXCL8 (Hess et al. 2004). This subset was enriched in perforin, granzyme B and IFNγ and thus had a high cytotoxic potential. The ability to target this highly cytotoxic subset of T cells makes CXCL8 a potential candidate for use in cancer immunotherapy. Additionally, neutrophils, co-recruited by CXCL8, have been proposed as anti-cancer effector cells due to their ability to release cytotoxic mediators as well as chemokines and cytokines (Di Carlo et al. 2001), which can in turn recruit other effector cells. Finally, CXCL8 also acts on endothelial cells, where it stimulates proliferation, migration and angiogenesis (Li et al. 2003). In contrast to CXCL8 and CXCL10, which both represent classical chemokines, the chemokine CX3CL1 displays unique structural and mechanistic features.

1.2.3 The chemokine CX3CL1 and its receptor CX3CR1

CX3CL1, also termed Fractalkine, was discovered in 1997 by homology searches in expressed-sequence tags. The gene identified was found to be expressed primarily in endothelial cells stimulated with IL-1 or TNF (Bazan et al. 1997). The mature CX3CL1 protein is far bigger than other chemokines – it consists of 373 amino acids. In this relatively large protein, the N-terminal 76 aa generate a chemokine domain that structurally resembles other chemokines. But unlike most other chemokines, the chemokine domain of CX3CL1 is fused to a 241 aa long mucin-like domain that connects to a single hydrophobic transmembrane domain and a 37 aa intracellular tail. Thus, CX3CL1 is a membrane anchored chemokine, a characteristic shared only with CXCL16. In addition to the membrane-bound version, CX3CL1 can also be shed from the surface by proteolytic cleavage and exist as a soluble molecule (Bazan et al. 1997; Hundhausen et al. 2003).

The molecular structure of the chemokine domain of CX3CL1 was solved in 1999, confirming the prediction that it resembles, in large part, the structure common to other chemokines (see structure described for CXCL10 in 1.2.1) (Mizoue et al. 1999). The mucin-like domain fused to the chemokine head is rich in Serine and Threonine residues that are predicted to be O-glycosylated (Bazan et al. 1997), and it has been shown that CX3CL1 contains 10-20 kDa of O-linked carbohydrates (Fong et al. 2000). Electron microscopy has revealed that the mucin domain forms an extended stalk that

protrudes 26 nm away from the cell membrane, displaying the 3 nm chemokine domain at its end (Fong et al. 2000). Figure 5 schematically summarizes the structure of CX3CL1.

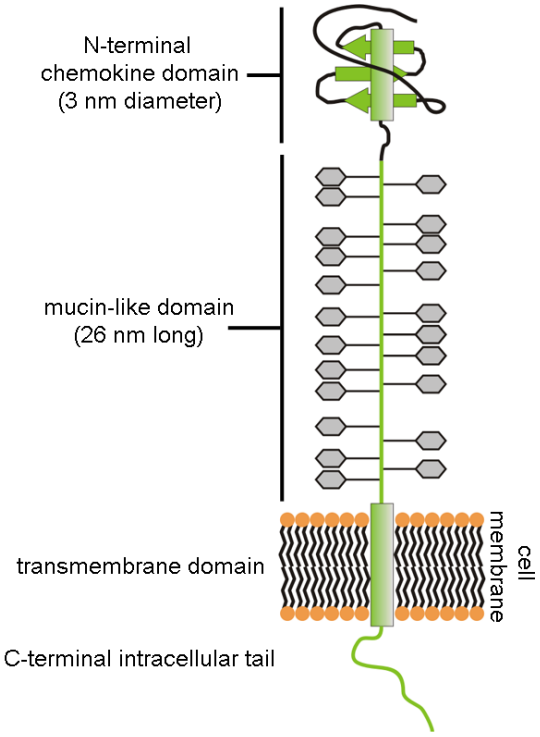

Figure 5: Architecture of the membrane-bound chemokine CX3CL1. A schematic representation is shown. CX3CL1 consists of an N-terminal chemokine domain (3 nm in diameter) that is connected to a 26 nm long mucin-like stalk, which is O-glycosylated at various positions (grey hexagons). The mucin domain is tethered to the cell membrane via a single hydrophobic transmembrane domain that is followed by a 37 amino acid intracellular tail.

This exceptional architecture is also responsible for another unique characteristic of CX3CL1: In the first paper describing the CX3CL1 receptor, CX3CR1, it was noted that the CX3CL1 protein can not only mediate chemotactic migration as seen with other chemokines, but it can also induce the adhesion of CX3CR1-epressing cells *in vitro* (Imai et al. 1997). This is in strong contrast to other chemokines that can only induce adhesion in rolling leukocytes by upregulating integrin affinity, not by acting as an adhesion molecule themselves. Notably, while the migration induced by soluble CX3CL1 required G-protein signaling, the induction of adhesion by surface-bound protein did not (Imai et al. 1997; Haskell et al. 1999). Leukocyte capture by CX3CL1 also occurred efficiently under conditions of physiologic flow (Fong et al. 1998), and CX3CL1-mediated tight adhesion was found to take place in the absence of other adhesion molecules such as ICAM-1 or VCAM-1. Moreover, activation of CX3CR1 did not lead to an upregulation of integrin affinity, which suggests that the adhesion molecules classically involved in leukocyte recruitment are dispensable for CX3CL1-mediated recruitment (Haskell et al. 1999). Figure 6 summarizes the classical cascade of leukocyte recruitment in comparison with leukocyte recruitment as mediated by CX3CL1.

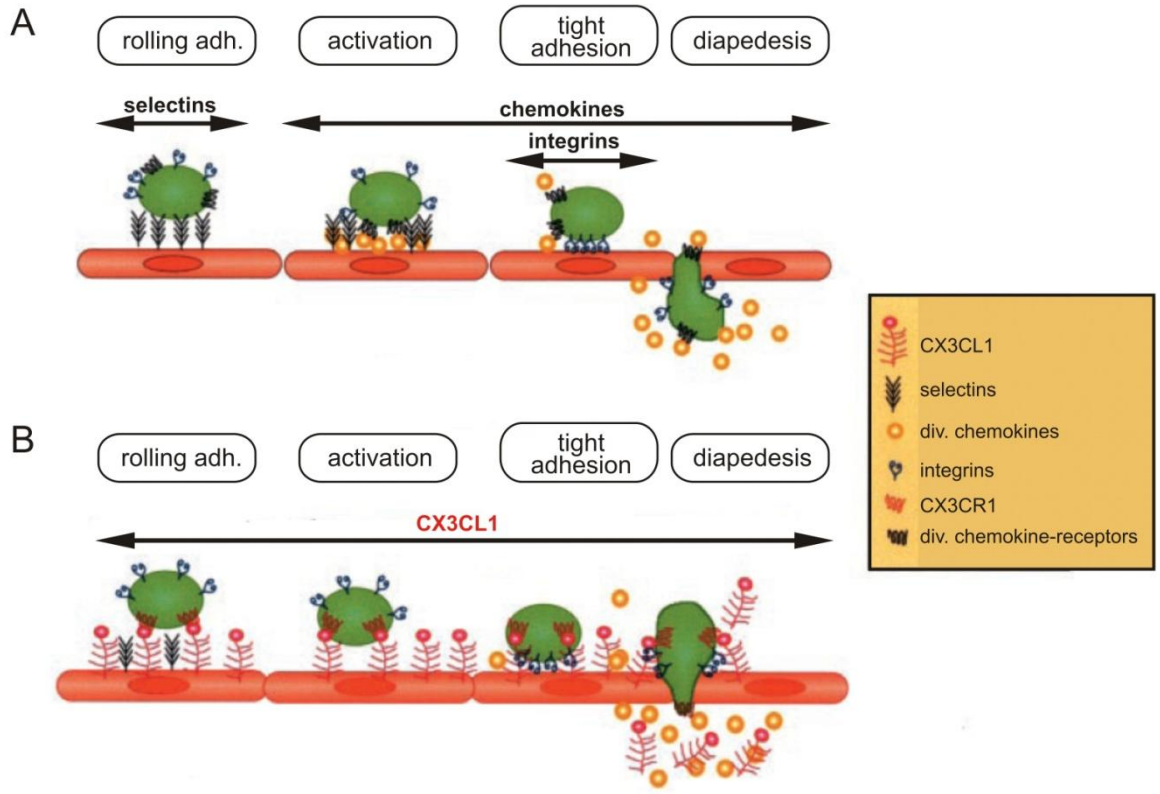

Figure 6: Classical scheme of leukocyte recruitment in comparison with recruitment by CX3CL1. **A:** The classical cascade of leukocyte recruitment relies on selectins expressed by activated endothelial cells to induce rolling adhesion. At the same time chemokines are immobilized on glycosaminoglycan molecules also expressed by endothelial cells. In this immobilized state, the chemokines can trigger matching receptors on the rolling leukocyte which leads to an upregulation of integrin affinity towards immunoglobulin superfamily molecules (not depicted) on the endothelial cells. The increased affinity enables the leukocyte to tightly adhere to the endothelium. Subsequently, diapedesis through the endothelium is initiated, a process which also requires chemokine signaling. **B:** CX3CL1 is able to mediate all steps of leukocyte recruitment including the initiation of rolling adhesion, tight adhesion and diapedesis. Figure modified from (Umehara et al. 2004).

The molecular basis for this feature of CX3CL1 has been a subject of debate. The elevation of the chemokine domain by the mucin domain is thought to be a critical parameter for CX3CL1-mediated leukocyte capture as this activity is retained if the mucin domain is replaced with six short consensus repeat segments from E-selectin that also build a 26 nm extended structure (but lack adhesive capacity themselves). In contrast, the activity is dramatically reduced if the mucin domain is deleted. The mucin domain alone, without a chemokine head, does not appear to induce adhesion (Fong et al. 2000).

As stated above, CX3CL1 is primarily expressed on endothelial cells as a reaction to proinflammatory cytokines like IL-1β or TNFα, whereas it is rarely found to be expressed in leukocytes (Bazan et al. 1997; Foussat et al. 2000). The CX3CR1 receptor however is expressed in several human leukocyte types including monocytes (also microglial cells in the central nervous system), $CD56^{dim}$ $CD16^{bright}$ NK cells, B cells, and plasmacytoid as well as myeloid DCs (Jung et al. 2000; Campbell et al. 2001;

Corcione et al. 2009). It is also found on both activated ($CD45RO^+$) and resting ($CD45RO^-$) $CD8^+$ and activated $CD45RO^+$ $CD4^+$ human T cells (Foussat et al. 2000). In mice, however, CX3CR1 expression in T cells is controversial. Some studies reported that CXCR3 is absent on T lymphocytes (Jung et al. 2000; Haskell et al. 2001), whereas others reported it to be expressed on a small percentage of T cells (Harcourt et al. 2006).

CX3CL1 has also been implicated in the activation of NK cells. Here it has been shown that CX3CL1 can activate CX3CR1-positive NK cells leading to higher efficiencies of cell-mediated lysis. (Zhang et al. 2006; Zhang et al. 2007).

An observation important for the current study was made by the Yoshie group. They assessed the ability of CX3CL1 to capture leukocytes transfected with various chemokine receptors. As expected, they found that CX3CL1 could only recruit cells that were transfected with CX3CR1. However, they also generated proteins where they exchanged the chemokine head of CX3CL1 by the chemokine CCL17 (also named TARC), leaving the mucin domain unchanged. This novel CCL17-mucin fusion protein displayed a redirected specifity - it captured cells expressing CCR4, the receptor for CCL17 and no longer CX3CR1-transfected cells. Both the mucin domain alone as well as the two chemokine domains alone were unable to capture significant amounts of cells, irrespective of the receptor that these cells expressed. Furthermore, the efficiency of recruitment was similar for wildtype CX3CL1 in combination with $CX3CR1^+$ cells and for CCL17-mucin in combination with $CCR4^+$ cells (Imai et al. 1997). Another study showed that CXCL8 fused to the mucin domain of CX3CL1 can induce rolling adhesion of cells expressing the CXCL8-receptor CXCR1 under conditions of physiologic flow. The same was true for a CCL2-mucin fusion protein in combination with $CCR2^+$ cells, although the efficiency of recruitment was reported to lack behind that of wildtype CX3CL1 (Haskell et al. 2000). Thus, the specificity of CX3CL1 can be redirected by exchanging the chemokine domain by another, unrelated chemokine. This possibility was exploited in the current study by fusing different chemokine heads to the mucin domain of CX3CL1 as will be detailed in chapter 1.4. Furthermore, we combined that approach with the technique of cell painting which will be introduced in the next section.

1.3 GPI-anchored proteins and cell painting

Glycosylphosphatidylinositol- (GPI-) anchors are membrane anchors that tether proteins to the outer leaflet of the cell membrane. Numerous membrane-associated proteins in eukaryotes are known to be GPI-anchored, such as alkaline phosphatase, decay accelerating factor (DAF), heparan sulfate proteoglycans or the adhesion molecule lymphocyte function antigen 3 (LFA-3) [reviewed in (Brown and Waneck 1992)]. The anchor itself consists of a phosphatidylinositol group that is linked via a carbohydrate core to the C-terminus of the respective protein. This core structure contains a

glucosamine residue that is linked to the phosphatidylinositol lipid group and connects α1,4 glycosidically to three mannose residues. The last mannose rest is connected via a phosphoryl group to ethanolamine that is in turn directly attached to the protein´s C-terminus (Homans et al. 1988). The mannose residues as well as the inositol ring of the phosphatidylinositol moiety can be substituted with various rests depending on the species as well the respective protein, but the above described backbone is relatively conserved (Brown and Waneck 1992). Figure 7 schematically depicts the composition of a GPI anchor.

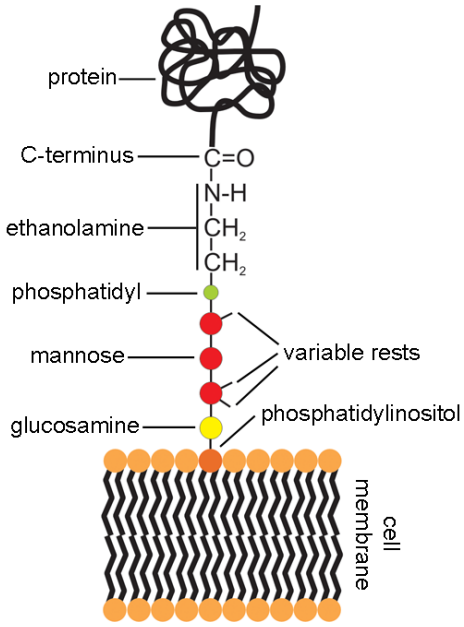

Figure 7: Schematic representation of the composition of a GPI anchor. The protein is linked via its C-terminus to ethanolamine, the latter being connected through a phosphatidyl residue to three mannose rests. A glucosamine moiety connects the mannose rests to phosphatidylinositol, the fatty acids of which anchor the protein to the outer cell membrane leaflet. The mannose rests as well as the inositol ring of phosphatidylinositol can be substituted at various positions, depending on the respective species and GPI-anchored protein.

GPI-anchored proteins are expressed with two signal peptides in their primary structure. The first one is an N-terminal signal peptide directs the synthesis of the proteins into the endoplasmatic reticulum and is subsequently cleaved from the protein, analogous to what is observed for secreted proteins and type I transmembrane proteins. For GPI-anchored proteins however, a second signal sequence is present at the C-terminus. It contains a stretch of 15-30 hydrophobic amino acids (Gerber et al. 1992). Once synthesis of the nascent protein has reached this sequence, the protein is cleaved from the signal sequence and transferred via a transamidase complex onto a preformed GPI anchor (Hiroi et al. 2000). There is considerable variance among the C-terminal signal peptides of different GPI-anchored proteins and the various sequences have been shown to differ in their efficiency of mediating GPI attachment (Chen et al. 2001).

It has been shown that purified GPI-anchored proteins possess the ability to integrate spontaneously into the cell membranes of virtually any other cell. Following this incorporation, they can still exert their natural activity. This technique has been referred to as “cell painting” because the proteins are “painted” directly onto the surface of the cell without any transfection process needed (Medof et al. 1984; Medof et al. 1996; Hoessli and Robinson 1998). Almost any protein can be expressed in a GPI-anchored version by fusing the gene sequence to appropriate signal sequences (Legler et al. 2005). Thus, the activity of any given protein can be transferred to any cell surface.

Cell painting represents a powerful alternative to conventional gene transfer for several reasons. First, it can be used with cells that are hard to transfect. Second, the surface modification occurs directly, without the need for cultivation or incubation, and the amount of protein that is transferred can be precisely controlled. Third, it avoids the safety concerns associated with gene transfer such as random integration and potential carcinogenic side effects by oncogene activation, which is especially important with regards to *in vivo* applications (Medof et al. 1996). For these reasons, cell painting is an attractive tool to be used for the development of novel treatment options, and it was also used in the current study, the rationale of which will be outlined below.

1.4 Rationale of this study

As outlined above, the recruitment of effector cells represents a crucial step and major hurdle for the efficient immunological treatment of tumors. We sought to overcome this problem by generating a novel, flexible class of reagents that could be used for the targeted modification of tissue micromilieus. The reagents described in this study were designed to selectively enhance recruitment and activation of specific leukocyte subsets in tumors, although the general applicability of the underlying concept also extends to other settings. They consisted of three different protein domains that were combined into novel fusion proteins as detailed below:

- The N-terminus of the proteins comprised a chemokine head (e.g. CXCL10 or CXCL8) that would direct the specificity of the fusion proteins towards cells expressing the respective chemokine receptor.
- The mucin domain of CX3CL1 fused to the chemokine head would assist in the recruitment process by lowering the requirement for additional adhesion molecules. In a tumor setting, this could also help overcome endothelial cell anergy, and lead to a larger number of leukocytes extravasating into the tumor tissue.
- The addition of a GPI anchor at the C-terminus would allow the recombinant proteins to directly integrate into virtually every cell membrane when added exogenously into a tissue.

The composition of the envisioned recombinant fusion proteins is exemplarily shown in Figure 8. The scheme depicts CXCL10-mucin-GPI, a fusion protein containing a CXCL10 chemokine head.

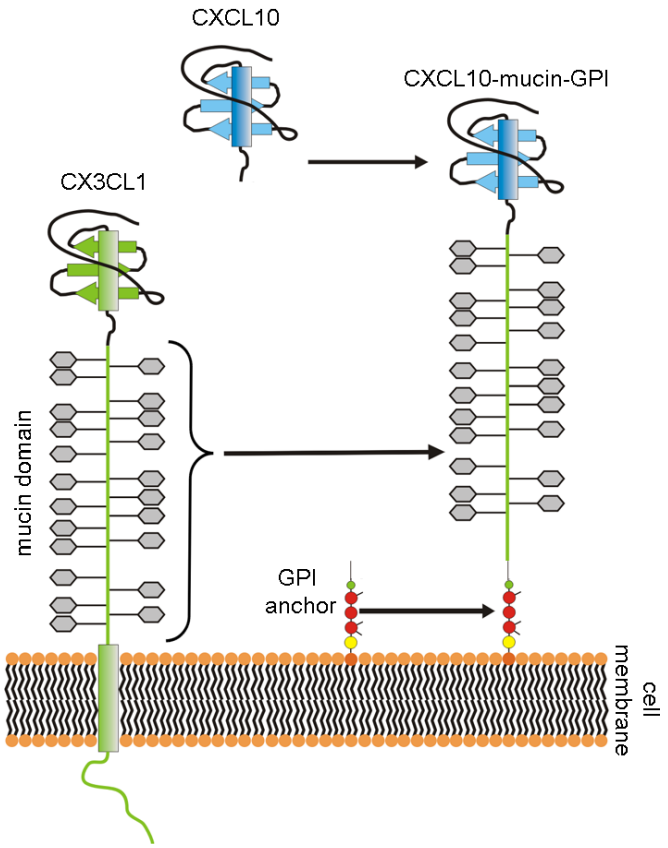

Figure 8: Composition of CXCL10-mucin-GPI as an example for a novel class of GPI-anchored chemokine fusion proteins. For the generation of CXCL10-mucin-GPI, the mucin domain of CX3CL1 was combined with a GPI anchor and a CXCL10 chemokine head in order to generate a flexible tool for the modification of tumor micromilieus capable of selectively stimulating the recruitment of $CXCR3^+$ leukocytes. The chemokine head would direct the specificity towards $CXCR3^+$ leukocytes, while the mucin domain would assist in the recruitment process and lower the requirement for other adhesion molecules. Inclusion of a GPI anchor would allow the fusion protein to integrate into the cell membranes of tumor, stromal and endothelial cells when applied exogenously, thus superseding the transfer of genetic material into the tumor.

According to our hypothesis, recombinant fusion proteins such as CXCL10-mucin-GPI would, if injected into a solid tumor, incorporate into the cell membranes of tumor, stromal and endothelial cells. Thereby, they would generate a stable, immobilized chemokine gradient to help facilitate leukocyte migration into the tumor. When present on tumor endothelial cells, the proteins would help overcome endothelial cell anergy by specifically recruiting leukocytes that express the matching chemokine receptor with limited requirement for other adhesion molecules.

The major part of the current study related to CXCL10-mucin-GPI. This protein would be specific for $CXCR3^+$ cells such as cytotoxic T cells or NK cells. Treatment with CXCL10-mucin-GPI could therefore be especially useful in conjunction with adoptive T or NK cell therapy to enhance recruitment of

transferred cells into the tumor. In a second part of the study, an additional set of fusion proteins was generated using the same architecture as described above but with a CXCL8 chemokine head instead of CXCL10. Thereby, the applicability of the reagents should be extended to the recruitment of other leukocyte subsets.

1.5 Specific aims and scope

The scope of the study was directed toward the following specific aims:

- *Cloning of recombinant constructs encoding required fusion proteins.* These included a fusion protein consisting of a CXCL10 chemokine head, followed by the mucin domain taken from CX3CL1 and a GPI anchor signal sequence derived from LFA-3 (CXCL10-mucin-GPI). A variant lacking the mucin domain (CXCL10-GPI) would act as a control to assess the biologic effects of the mucin domain. Soluble versions of both proteins (CXCL10-mucin-Stop and CXCL10-Stop) served as controls for effects mediated by the GPI anchor. Proteins with a CXCL8 chemokine domain instead of CXCL10 (CXCL8-mucin-GPI and CXCL8-GPI) should allow assessing broader applicability of the underlying concept. A GPI-anchored negative control protein lacking function in leukocyte recruitment should additionally be generated. All proteins should contain a c-myc epitope tag to facilitate detection and purification.
- *Expression of the recombinant constructs in Chinese hamster ovary cells.* Successful expression should be validated by FACS, and correct targeting to the cell membrane should be further assessed by immunofluorescence microscopy.
- *Verification of the bioactivity of CXCL10-GPI and CXCL10-mucin-GPI.* The bioactivity of the proteins should be tested to ensure proper expression, folding and processing of the fusion proteins.
- *Development of purification protocols.* Protocols for the solubilization and purification of the recombinant proteins from overexpressing CHO cells should be established.
- *Analysis of the incorporation process.* The capacity of purified GPI-anchored proteins to integrate into cell membranes and the dependency of the incorporation process on the GPI anchor should be verified.
- *Evaluation of bioactivity in vitro*. The bioactivity of CXCL10-mucin-GPI following incorporation into the cell membranes of endothelial cells should be evaluated in assays that mimic leukocyte recruitment *in vitro*. The experiments should assess if the incorporated proteins were able to facilitate NK or T cell adhesion under conditions of physiologic flow and the potential contribution of the mucin domain to this effect.
- *Evaluation of bioactivity in vivo.* Finally, an *in vivo* tumor model should be established to test if injection of CXCL10-mucin-GPI could enhance recruitment of NK and T cells.

2 Materials and Methods

2.1 Materials

2.1.1 Cell culture

2.1.1.1 Media and Supplements

Media:

CD CHO	Invitrogen, Carlsbad
DMEM	Invitrogen, Carlsbad
HAM-F12	Invitrogen, Carlsbad
Endothelial cell growth medium, microvascular (ECGM MV)	Promocell, Heidelberg
MEM alpha medium (MEMα)	Invitrogen, Carlsbad
RPMI 1640	Invitrogen, Carlsbad
RPMI 1640, Phenol red free	Invitrogen, Carlsbad
Serum-free freezing medium *Cryo-SFM*	Promocell, Heidelberg

Supplements:

2-Mercaptoethanol (2-ME), 55 mM	Invitrogen, Carlsbad
Endothelial cell growth supplement (ECGS), microvascular	Promocell, Heidelberg
Fetal calf serum (FCS)	Biochrom AG, Berlin
Fetal calf serum, dialyzed (dFCS)	Biochrom AG, Berlin
Fetal calf serum, ultra-low IgG (FCS IgG_{low})	PAN, Aidenbach
Glucose, 35%	Sigma Aldrich, Taufkirchen
HEPES, 1 M	Invitrogen, Carlsbad
HT-supplement, 50x	Invitrogen, Carlsbad
Human serum	Provided by Prof. Noessner, Helmholtz Zentrum Munich
L-Glutamine, 200 mM	Biochrom AG, Berlin
Na-Pyruvate, 100 mM	Invitrogen, Carlsbad
Non-essential amino acids (NEAA), 10 mM	Invitrogen, Carlsbad
Penicillin/ Streptomycin (P/S), 100x	PAA Laboratories, Pasching

Other reagents:

Collagen G, 4 mg/ml	Biochrom AG, Berlin
Dimethylsulfoxide (DMSO)	Merck, Darmstadt
Dulbecco´s PBS (without Ca^{2+} and Mg^{2+}, 1x or 10x)	PAA Laboratories, Pasching
EDTA, 1% in PBS	Biochrom AG, Berlin
Trypan blue	Sigma Aldrich, Taufkirchen
Trypsin-EDTA in PBS, 1x	PAA Laboratories, Pasching

2.1.1.2 Cell lines and primary cells

Cell line / growth	Description	Source	Medium	Supplements
291 cells	B cell lymphoma line from c-myc transgenic C57/Bl6 mice	Provided by R. Mocikat, Helmholtz Zentrum Munich	RPMI 1640	+ 5% FCS + 0.1 mM NEAA + 55 µM 2-ME + 1 mM Na-Pyruvate
9E10 hybridoma cells, suspension	Hybridoma cells expressing anti c-myc antibody 9E10	Provided by W. Uckert, MDC Berlin	RPMI 1640	+ 10% FCS IgG_{low} + 3,5 g/l Glucose + 2 mM L-Glutamine + 2,383 g/l HEPES + 110 g/l Na-Pyruvate
A5.12.14 hybridoma cells, suspension	Hybridoma cells expressing anti CXCL8 antibody A5.12.14	LGC Standards, Teddington	50% DMEM, 50% HAM-F12	+ 5% FCS IgG_{low}
Chinese hamster ovary (CHO) cells, adherent	Ovary cells from chinese hamster, Dhfr deficient	ATCC, USA	MEMα	+ 10% dFCS + 1% P/S non-transfected cells additionally : + 1% HT supplement
DS4 cells, suspension	Human alloreactive $CD8^+$ effector T cell clone	Provided by E. Noessner, Helmholtz Zentrum Munich Obtained freshly for each assay		
HDBEC, adherent	Microvascular endothelial cells from blood vessels of fetal foreskin	Promocell, Heidelberg	ECGM MV	+ ECGS, microvascular
HMEC, adherent	Microvascular endothelial cells, SV40-immortalized	Provided by H.-J. Gröne, DKFZ Heidelberg	DMEM	+ 10% FCS
Human NK cells, suspension	Human NK cells, isolated from peripheral blood (see 2.2.5.5)	Isolated in house	AIM-V	+ 10% human serum overnight activation: + 500 U/ml IL-2
JB4 cells, suspension	Human HLA-A2 alloreactive $CD8^+$ effector T cell clone	Provided by E. Noessner, Helmholtz Zentrum Munich Obtained freshly for each assay		
Murine T cells, suspension	Murine CD19-specific $CD4^+$ T cell clone	Provided by F. Lehmann, Helmholtz Zentrum Munich Obtained freshly for each assay		
Murine NK cells, suspension	Murine NK cells, isolated from spleens of C57/Bl6 mice	Provided by J. Pötzl, Helmholtz Zentrum Munich Isolated freshly for each assay		
YT cells, suspension	Human NK cell line established from acute lympho-blastic lymphoma	Provided by C. Clayberger, Stanford Univ.	RPMI 1640	+ 20% FCS

2.1.2 Bacteria

E. coli DH5alpha; Genotype: supE44, ΔlacU169 (Φ80 lacZΔM15) hsdR17 recA1 endA1 gyrA96 thi-1 relA1

E. coli XL1-blue supercompetent cells for site-directed mutagenesis kit: Fermentas, St. Leon-Rot

2.1.3 Buffers and solutions

If not stated otherwise, all buffers were prepared in ultra-pure H_2O, except all buffers used for chromatography (2.1.3.1), which were prepared using injection-grade water (Aqua ad iniectabilia).

2.1.3.1 Chromatography

Buffers for anti c-myc column:	
Equilibration buffer	1x PBS + 0.025% Triton X-100h
Washing buffer	145 mM NaCl in 1 x PBS (cell culture grade, Invitrogen)
Elution buffer	0.01 mg/ml c-myc peptide in equilibration buffer
Regeneration buffer	0.17 M Glycine in H_2O, pH 2.3
Storage buffer	0.1% NaN_3 (w/v) in 1x PBS (cell culture grade, Invitrogen)

Buffers for Protein A column:	
Equilibration buffer	20 mM Na_2HPO_4/ NaH_2PO_4, pH 7.4 (4°C)
Elution buffer	20 mM citrate buffer, pH 3.6 (4°C)

Other buffers:	
Extraction buffer	4 mM n-Dodecyl-β-D-maltoside 50 mM Tris/HCl, pH 7.5 100 mM NaCl 1 protease inhibitor cocktail tablet / 50ml
Tris/HCl, 1 M, pH 7.5 (4°C)	Commercially available; Invitrogen, Carlsbad

2.1.3.2 SDS-PAGE and western blot

Buffers and solutions prepared in house:	
Ammoniumpersulfate (APS)	10% APS (w/v)
Blocking solution	5% skimmed milk powder (w/v) in TBST
Coomassie staining solution	0.02% ServaBlue R (w/v) 0.25% methanol (v/v) 10% acetic acid (v/v)
Electrophoresis buffer	1.9 M Glycine 0.25 M Tris 1% SDS (w/v)
Laemmli buffer, 3x	150 mM Tris/HCl, pH 6.8 (rt) 30% Glycerine (v/v) 6% SDS (w/v) 0.3% Bromphenol blue (w/v) 7.5% β-mercaptoethanol (v/v)

Sodiumdodecylsulfate (SDS), 10%	10% SDS (w/v)
Tris, 1 M, pH 6.8	1 M Tris, pH 6.8 (rt)
Tris, 1.5 M, pH 8.8	1.5 M Tris, pH 8.8 (rt)
Tris-buffered saline (TBS), 10x	1.5 M NaCl 100 mM Tris 10 mM NaN_3
Tris-buffered saline with Tween (TBST)	0.05% Tween20 (v/v) in 1x TBS

Commercially available buffers and solutions:

Acrylamide/ Bisacrylamide solution, 30%	Roth, Karlsruhe
ECL-substrate for western blot	Pierce, Rockford
NuPAGE LDS sample buffer, 4x	Invitrogen, Carlsbad
NuPAGE transfer buffer, 50x	Invitrogen, Carlsbad
PageBlue protein staining solution	Fermentas, St. Leon Rot
WesternBreeze® Blocking solution	Invitrogen, Carlsbad

2.1.3.3 Molecular biology

Buffers and solutions prepared in house:

EGTA-Solution	100 mM EGTA, pH 8.0 (rt)
Loading buffer for agarose gels, 6x	0.25% Bromphenol blue (w/v) 0.25% Xylen-Cyanol FF (w/v) 30% Glycerin (v/v)
Tris-borate-EDTA (TBE) buffer, 1x	90 mM Tris, 2 mM boric acid 0.01 M EDTA pH 8.0 (rt)

Commercially available buffers:

Buffers for DNA restriction enzymes, 10x	NEB, Frankfurt
First strand buffer, 5x	Invitrogen, Carlsbad
SpeedAmp PCR buffer, 10x	Analytik Jena, Jena
ThermoPol buffer for Taq polymerase, 10x	NEB, Frankfurt

2.1.3.4 Microbiology

Agar, 2x	3% Agar-Agar (w/v), autoclaved
Ampicillin solution	50 mg/ml Ampicillin in 70% ethanol (w/v)
$CaCl_2$ solution (for preparation of competent bacteria)	60 mM $CaCl_2$ 15% Glycerin (v/v) 10 mM PIPES, pH 7 (rt) sterile filtered (0.2 µm)
Freezing solution for bacteria, 10x	132.3 mM KH_2PO_4 21 mM Sodiumcitrate 3.7 mM $MgSO_4$*7 H_2O 68.1 mM $(NH)_2SO_4$ 459.3 mM K_2HPO_4*3 H_2O 35.2% Glycerin (w/v) autoclaved
LB medium, 2x	2% Bacto Tryptone (w/v) 342 mM NaCl 1% yeast extract (w/v) pH 7.2-7.3 (rt), autoclaved

2.1.3.5 ELISA

Assay buffer	1% BSA (w/v) in 1x PBS
OptEIA substrate solution for ELISA	Commercially available; BD Biosciences, Bedford
PBS, 20x	2.74 M NaCl 129.2 mM Na_2HPO_4 * 2 H_2O 54 mM KCl 29.4 mM KH_2PO_4
Wash buffer	0.05% Tween20 (v/v) in 1x PBS

2.1.3.6 Flow assay

Assay buffer	0.5% BSA (w/v) 50 mM HEPES 2 mM $CaCl_2$ + $MgCl_2$ added directly before use in HBSS (with Phenol red, w/o Ca^{2+}/Mg^{2+})

Commercially available buffers:

Bovine serum albumin (BSA), 7.5% solution, cell culture grade	Invitrogen, Carlsbad
Hank´s buffered salt solution (HBSS), with Phenol red, w/o Ca^{2+}/ Mg^{2+}, cell culture grade	Sigma-Aldrich, Taufkirchen
HEPES, 1 M solution, cell culture grade	Invitrogen, Carlsbad

2.1.3.7 Histology and immunohistology

Antigen unmasking solution for paraffin sections, citric acid based	Vector laboratories, Burlingame
Eosin Y solution, alcoholic	Sigma Aldrich, Taufkirchen
Hematoxylin solution, Harris modified	Sigma Aldrich, Taufkirchen
Vectamount mounting medium	Vector laboratories, Burlingame

2.1.3.8 Other buffers and solutions

Buffers and solutions prepared in house:

FACS-buffer	2 mM EDTA 2% FCS (v/v) in 1x PBS (cell culture grade, Invitrogen)
Fixation solution for immunofluorescence	1% PFA (w/v) in 1x PBS (cell culture grade, Invitrogen)

Commercially available solutions:

Biocoll separating solution (Ficoll)	Biochrom AG, Berlin
Hank´s buffered salt solutions (HBSS):	
with Phenol red, with Ca^{2+}, Mg^{2+}	Sigma-Aldrich, Taufkirchen
without Phenol red, with Ca^{2+}, Mg^{2+}	Invitrogen, Carlsbad

2.1.4 Antibodies

Primary antibodies						
Immuno-gen	**Target species**	**Host species**	**Isotype**	**Application**	**Labeling**	**Source**
CD3	human	mouse	IgG1 κ	FACS	FITC	BD Pharmingen, Bedford
CD3	pan	rat	IgG1	IHC	-	AbD Serotec, Langford
c-myc	unspecified	mouse	IgG1 κ	WB, FACS, IF	-	prepared in house
CX3CL1 muc. dom.	human	mouse	IgG1 κ	FACS	-	Abnova, Taipei
CXCL8	human	mouse	IgG2a	WB, FACS	-	prepared in house
CXCL10	human	mouse	IgG2a	WB, FACS	-	BD Biosciences, Bedford
CXCR3	human	mouse	IgG1 κ	FACS	RPE	BD Pharmingen, Bedford
CXCR3	human	mouse	IgG1	FACS	RPE	R&D Systems, Minneapolis
CXCR3	mouse	Armenian hamster	IgG	FACS	APC	Biolegend, San Diego
NKp46	mouse	goat	polyclonal	IHC	-	R&D Systems, Minneapolis
(isotype control)	-	mouse	IgG1 κ	FACS	-	Sigma-Aldrich, Taufkirchen
(isotype control)	-	mouse	IgG2a	FACS	-	Sigma-Aldrich, Taufkirchen
(isotype control)	-	mouse	IgG1	FACS	FITC	Dako, Roskilde
(isotype control)	-	Armenian hamster	IgG	FACS	APC	Biolegend, San Diego
(isotype control)	-	mouse	IgG1	FACS	RPE	BD Pharmingen, Bedford
Secondary antibodies						
IgG	mouse	rabbit		FACS	RPE	Dako, Roskilde
IgG	mouse	rabbit		WB	HRP	Dako, Roskilde
IgG	mouse	rat		IF	Biotin	BD Pharmingen, Bedford
IgG	goat	horse		IHC	Biotin	Vector Laboratories, Burlingame
IgG	rat	rabbit		IHC	Biotin	Vector Laboratories, Burlingame

Abbreviations: IHC = immunohistochemistry; IF = immunofluorescence microscopy; WB = western blotting; FACS = fluorescence activated cell scanning; Other abbreviations: see 5.8 (page 114).

2.1.5 Enzymes

Alkaline phosphatase	Roche, Mannheim
Phosphatidylinositol-specific phospholipase C (PI-PLC)	Invitrogen, Carlsbad
Phusion DNA polymerase	NEB, Frankfurt
Restriction Enzymes: *EcoR*I, *Sal*I, *Xba*I, *Nhe*I, *Mlu*I, *Mfe*I, *Nde*I	NEB, Frankfurt
SuperScript II reverse transcriptase	Invitrogen, Carlsbad
T4 DNA ligase	NEB, Frankfurt
Taq DNA polymerase	NEB, Frankfurt

2.1.6 Recombinant proteins and peptides

Protein	Species	Application	Source
c-myc peptide	unspecified	Protein purification	MBL, Japan
CXCL10	human	*In vitro* and *in vivo* assays	Peprotech, Hamburg
CXCL10	mouse	*In vitro* assays	Peprotech, Hamburg
Streptavidin-HRP	unspecified	ELISA	BD Biosciences, Bedford
Streptavidin-RPE	*S. avidinii*	FACS	Dako, Roskilde

2.1.7 Size standards for electrophoresis

1 kb DNA ladder	Invitrogen, Carlsbad
MagicMark™ *XP* western protein standard	Invitrogen, Carlsbad

2.1.8 Primers

Application	Primer name	Sequence
Amplification of c-myc tag	p2xMycTag_fw	5´- GTTAAGCTGTGTATCTAGAGAACAGAA-3´
	p2xMycTag_rv	5´- CTTCATTGCTAGCCAGGTCCTCCTC-3´
Amplification of CX3CL1 mucin domain	Fra_fw_080901	5´-GAGAATTCATCTAGAAATGGCGGCACCTTCG-3´
	Fra_rv_080901	5´-GGATACAGGTTGTGCTAGCCTGCCTC-3´
Amplification of CXCL8	IL8_fw_1107	5´-GAAGAAACCAATTGAAGGAACCATCTCACTG-3´
	IL8_rv_1107	5´-GAGAATGAATTTCTAGATGAATTCTCAGCCCTCTTC-3´
Amplification of CXCL10	IP10_fw_long	5´-GAGGAACCTGAATTCCCAGTCTCAGCACC-3´
	IP10_rv_long	5´-CCCCTCTGGTGCTAGCAGGAGATCTTTTAG
Amplification of EGFP from pEGFP-N1	EGFP_fw_0408	5´-GATCCACCGACGCGTGCCATGGTGAGC-3´
	EGFP_rv_0408	5´-GAGTCGCGGCCTCTAGACTTGTACAGCTCGTCC-3´
Amplification of GPI signal sequence of DAF	DAFPI_fw	5´-CAAATAAATCTAGAGGAAGTGGAACCACTTC-3´
	DAFPI_rv	5´-CTTTGGGTCGACCTAAGTCAGCAAG-3´
Mut. of pUC-CXCL10-GPI to restore *Nhe*I site	IP10_NheI_320_fw	5´-CTAAAAGATCTCCTGCTAGCGAACAGAAGCTGATCAGC-3´
	IP10_NheI_320_rv	5´-GCTGATCAGCTTCTGTTCGCTAGCAGTAGATCTTTTAG-3´
Mut. of TIMP-1 signal sequence (*Mlu*I site)	SS_mut_fw	5´-GGCTGATAGCCCCCACGCGTGCCTGCACCTGTGTC-3´
	SS_mut_rv	5´-GACACAGGTGCAGGCACGCGTGGGGGCTATCAGCC-3´
Sequencing of inserts in pEF	pEF_Insert_fw	5´-GATCTTGCTTCATTCTCAAGCC-3´
	pEF_Insert_rv	5´-ATACCGGAGTACTAGCCGCC-3´

2.1.9 Plasmids and vectors

Plasmid	Description	Source	Resistance gene	Application
MP71 gp100	Rectroviral vector containing double c-myc tag sequence	Provided by Prof. W. Uckert, MDC Berlin	Ampicillin	Template for amplification of c-myc tag
pEF_{dhfr}	Contains multiple cloning site and dhfr gene separated by internal ribosome binding site under the control of a CMV promoter	Provided by M. Mack, University Regensburg	Ampicillin	Expression vector for stable transfection in CHO cells
pEGFP-N1	Expression vector for EGFP expression in eukaryotic cells	TaKaRa, Kyoto	Kanamycin	Template for amplification of EGFP gene
pUC19	Standard cloning vector	Invitrogen, Carlsbad	Ampicillin	Cloning and mutagenesis

2.1.10 Kits

Avidin/Biotin blocking kit	Vector laboratories, Burlingame
BCA protein Assay kit	Thermo Scientific, Rockford
Bio-Rad protein assay	Bio-Rad, Hercules
DuoSet CXCL8 ELISA development kit	R&D Systems, Minneapolis
DuoSet CXCL10 ELISA development kit	R&D Systems, Minneapolis
Dynabeads® untouched human NK cell isolation kit	Invitrogen, Carlsbad
Endofree Plasmid Maxi kit	Qiagen, Hilden
Fluo-4 NW Calcium assay kit	Invitrogen, Carlsbad
Innuprep Plasmid Mini kit	Analytik Jena, Jena
Innuprep Doublepure kit	Analytik Jena, Jena
PureLink RNA Mini kit	Invitrogen, Carlsbad
Quant-it™ DNA Assay kit, broad range	Invitrogen, Carlsbad
Quant-it™ DNA Assay kit, high sensitivity	Invitrogen, Carlsbad
Quant-it™ RNA Assay kit	Invitrogen, Carlsbad
Quickchange Site-directed mutagenesis kit	Stratagene, Santa Clara
RNase-free DNase set	Qiagen, Hilden
Vectastain ABC kit	Vector laboratories, Burlingame

2.1.11 Protein chromatography equipment

Chromatography machine *ÄktaFPLC*	GE Healthcare, Uppsala
c-myc tagged protein mild purification gel	MBL, Japan
Empty glass column *Tricorn 5/50*	GE Healthcare, Uppsala
HiPrep 26/10 Desalting column	GE Healthcare, Uppsala
HiTrap Desalting column	GE Healthcare, Uppsala
Protein A-HP *HiTrap* column	GE Healthcare, Uppsala
recombinant Protein A FF *HiTrap* column	GE Healthcare, Uppsala

2.1.12 Other laboratory equipment

Automatic tissue processor	Thermo Fisher, Waltham
Developer for autoradiography films	Agfa, Mortsel
E. coli Pulser	Bio-Rad, Hercules
Electroporation device for cell culture	Bio-Rad, Hercules
Fluorescence activated cell scanner *FACSCalibur*	BD Biosciences, San Jose
Fluorescence Microscope *DMRBE*	Leica, Wetzlar
Fluorometer *Qubit*	Invitrogen, Carlsbad
Inverted fluorescence microscope *DMIL*	Leica, Wetzlar
Video Camera for Leica DMIL	Horn Imaging, Aalen
Photo Camera for Leica DMIL	Jenoptik, Jena
Incubation chamber for Leica DMIL	Ibidi, Martinsried
Microtome HM-340-E	Microm, Walldorf
Multiwell plate reader *Genios Plus*	Tecan, Crailsheim
Paraffin embedding machine EC-350-1	Microm, Walldorf
PCR machine *SpeedCycler*	Analytik Jena, Jena
PCR machine *Perkin Elmer*	Perkin Elmer, Waltham
Rolling system for cell culture *CELLROLL*	Integra Biosciences, Fernwald
Scintillation counter *TOPcount*	Canberra Packard, Dreireich
Spinner flask for cell culture *ProCulture*	Corning, Lowell
Syringe Pump for laminar flow assays	WPI, Sarasota

2.1.13 Chemicals

BRIJ 35, 30% w/w solution	Merck, Darmstadt
C12E8 detergent	Merck, Darmstadt
Methotrexate	Sigma Aldrich, Taufkirchen
NaCl, 5 M solution, for chromatography buffers	Sigma-Aldrich, Taufkirchen
n-Dodecyl-β-D-maltoside, *ULTROL* grade	Calbiochem/ Merck, Darmstadt
Nonidet P40 (NP40) detergent, 10% solution	Calbiochem/ Merck, Darmstadt
n-Octyl-β-D-glucopyranoside, *ULTROL grade*	Calbiochem/ Merck, Darmstadt
Paraformaldehyde (PFA)	Merck, Darmstadt
Protease inhibitor cocktail tablets *Complete*	Roche, Mannheim
RNAsin RNase inhibitor	Promega, Madison
Sodium Azide (NaN_3)	Merck, Darmstadt
Triton X-100, hydrogenated (Triton X-100h)	Calbiochem/ Merck, Darmstadt
Water, injection grade (aqua ad injectabilia)	Braun, Melsungen

2.1.14 Disposable and other materials

96-well microtiter plate, round bottom	Greiner, Frickenhausen
96-well microtiter plate for ELISA	Nunc, Roskilde
96-well microtiter plate, flat bottom, black walls	Greiner, Frickenhausen
Amersham *Hyperfilm ECL* autoradiography film	GE Healthcare, Uppsala
Cell culture dishes for immunofluorescence *µ-dish high*	Ibidi, Martinsried
Luer connectors	Ibidi, Martinsried
LumaPlate Scintillant coated 96 well plate	Perkin Elmer, Waltham
Roller bottles for cell culture	Greiner, Frickenhausen
Slides for flow assays *µ-slides 0.4 Luer*	Ibidi, Martinsried
Ultrafiltration devices *Vivaspin 6*	GE Healthcare, Uppsla

2.1.15 Software

Name	Application	Source
CellQuest	Acquisition of FACS data	BD Biosciences, Bedford
FlowJo	Evaluation of FACS data	TreeStar Inc., Ashland
IC Capture	Video acquisition at the Leica DMIL microscope	The Imaging Source, Bremen
Prism 5	Generation of diagrams	GraphPad Software, La Jolla
ProgRes Capture	Image acquisition at the Leica DMIL microscope	Jenoptik, Jena
PyMol	Graphic representations of protein structures	DeLano Scientific, San Francisco
Unicorn	Protein chromatography control and evaluation	GE Healthcare, Uppsala
XFluor	Control of ELISA plate reader	Tecan, Crailsheim

2.1.16 Mice

Female C57/Bl6 mice were purchased from Taconic Farms Inc., Hudson, and used for experiments at 11-21 weeks of age. All mice were housed at the Helmholtz Zentrum Munich under special pathogen free conditions.

2.2 Methods

2.2.1 Cell culture

2.2.1.1 General cell culture

The culture of living cells was performed in a laminar flow hood to prevent contaminations. All reagents were prewarmed to 37°C in a water bath prior to use, except media for primary endothelial cells, which were prewarmed for 30 min in a cell culture incubator set to 37°C and 5% CO_2 to allow for pH adjustment of the media. All cells were incubated at 37°C and 5% CO_2.

For subculturing, adherent cells were washed with PBS and subsequently detached using Trypsin-EDTA solution at rt. The reaction was stopped by adding an equal volume of medium containing 10% FCS (or more if the medium contained less FCS) and the cells were pelleted by centrifugation for 3 min at 220 x g (rt). Subsequently, the cell pellet was resuspended in fresh medium and seeded into the respective cell culture vessel. If surface molecules on the respective cells were analyzed using FACS, western blot or other methods, or the cells were harvested for protein purification, only 6 mM EDTA in PBS at 37°C was used to detach the cells. Suspension cells were resuspended prior to subculturing and subsequently a fraction of the culture medium according to the desired split factor was transferred into a new cell culture flask, which was then filled up with fresh medium to the desired end volume.

For protein production, transfected CHO cells were grown in six 300cm^2 cell culture flasks, detached with EDTA in PBS, washed with PBS and combined to one pellet, which was stored at -80°C. If cell

culture supernatant should be generated from CHO cells transfected with secreted proteins, the cells were grown in 850 cm^2 roller flasks using 30 ml of serum-free MEM alpha medium for each flask. The cells were monitored microscopically for viability and as soon as a decrease in viability was observed (usually after about 4 days), the supernatant was removed, centrifuged for 5 min at 3000 x g (4°C) to remove cell debris, sterile filtered (0.2 µm pore size) and stored at 4°C.

Two hybridoma cell lines were cultured in the current study. The A5.12.14 hybridoma producing an anti CXCL8 antibody was cultured in 150 cm^2 cell culture flasks, each of which could be filled with up to 100 ml of medium. Exponentially growing cells were seeded at 3 x 10^4 cells/ml, and after 7 days the supernatant was harvested, centrifuged for 5 min at 3000 x g (4°C) to remove cell debris, sterile filtered (0.2 µm pore size) and stored at 4°C. The 9E10 hybridoma was cultured in 850 cm^2 roller flasks which could be filled with up to 1 l of medium. For the quantitative production of supernatant, phenol red free RPMI 1640 medium was used and the cells were cultured for 7 days as described for the A5.12.14 hybridoma.

2.2.1.2 Freezing and thawing of cells

All cells, except primary endothelial cells, were frozen in their respective culture medium + 10% DMSO. Primary endothelial cells were frozen in serum free freezing medium (Cryo-SFM). The tubes were cooled to -80°C over 24 h in an isopropanol container prior to transferring them into a liquid nitrogen container. For thawing, the frozen cell suspensions were rapidly thawed in a 37°C water bath and immediately transferred into a cell culture vessel filled with prewarmed medium. The medium was exchanged after 18 h to remove DMSO.

2.2.1.3 Counting cells

To determine the number of cells/ml, an aliquot of the cell suspension was mixed at a 1+1 ratio with Trypan blue solution (0.4%) and pipetted into a Neubauer counting chamber. Dye exclusion was used to differentiate viable from dead cells and the number of cells per ml was calculated from the average number of cells per square x 10^4.

2.2.2 Molecular biology

2.2.2.1 Freezing and thawing of bacteria

For long-term storage of *E. coli* strains, 900 µl of an overnight culture was mixed with 100 µl freezing solution for bacteria (10x) and frozen at -80°C. To establish cultures from frozen cells, a small amount of frozen bacteria was streaked onto an appropriate agar plate and incubated at 37°C over night. Subsequently, a liquid culture was established from a single colony on that plate.

2.2.2.2 Preparation of agar plates

For the preparation of agar plates, 3% Agar was heated in a microwave and mixed with an equal volume of 2x LB medium. When required, appropriate antibiotics were added (Ampicillin: 100 µg/ml final concentration; Kanamycin: 50 µg/ml final concentration) and the solution was poured into petri dishes. Plates were sealed in plastic bags and stored at 4°C.

2.2.2.3 Restriction digestion of DNA

DNA was cut using restriction enzymes. 1 unit restriction enzyme was used to cut 1 µg DNA per hour. In cases when larger amounts of DNA had to be cut, the amount of enzyme and/or the incubation time was increased accordingly. To minimize detrimental effects of glycerol, it was taken care that the volume of enzyme solution did not exceed 1/10 of the total volume. All digestions were performed in a buffer suitable for the respective enzyme (diluted to 1x) at 37°C.

2.2.2.4 Separation of DNA fragments by electrophoresis

Agarose gel electrophoresis was used to separate DNA fragments for analytical or preparative purposes. The concentration of agarose was chosen according to the expected fragment sizes and varied between 0.6% and 2% agarose. Gel solutions were prepared in 0.5x TBE buffer and heated in a microwave to dissolve the agarose. Subsequently, ethidium bromide was added to a final concentration of 100 ng/ml before pouring the gels into appropriate chambers. For electrophoresis, the samples were mixed with loading buffer for agarose gels (6x) to yield a 1x final concentration of loading buffer and loaded into the wells. Electrophoresis was performed in 0.5x TBE buffer at 120 V and the gels were subsequently photographed under UV light for documentation. In the case of preparative gels, the respective bands were cut out of the gel under UV light and DNA was extracted from the gel fragments using a commercial kit (*Innuprep Doublepure kit*) according to the manufacturer´s instructions.

2.2.2.5 Determination of DNA and RNA concentrations

The concentrations of DNA and RNA in solutions were determined fluorometrically using a special fluorometer (*Qubit*) in combination with commercially available reagents (Quant-it^{TM}). All determinations were performed according to the manufacturer´s instructions.

2.2.2.6 Dephosphorylation of DNA ends

In order to prevent religation of linearized vectors, their 5´ DNA ends were dephosphorylated. To this end, 1 unit of alkaline phosphatase per 50 pmol 5´ ends was added to the sample and the mixture was incubated at 37°C for 1 h. The reaction was stopped by the addition of EGTA to a final concentration of 20 mM and a subsequent incubation at 65°C for 10 min. Prior to the next cloning step, the dephosphorylated DNA was purified using a commercially available kit (*Innuprep Doublepure kit*) according to the manufacturer´s instructions.

2.2.2.7 Ligation of DNA fragments

For ligation of vector and insert DNA, separate reactions were prepared using an insert:vector molar ratio of 3:1 and 10:1, respectively. A third reaction containing only vector DNA served as negative control. All reactions were performed in a total volume of 20 µl containing 400 U (1 µl) T4 DNA ligase and 2 µl 10x T4 DNA ligase buffer for 1 h at room temperature.

2.2.2.8 Preparation and transformation of competent *E. coli* DH5α

In order to prepare chemically competent *E. coli*, 4 ml of an overnight liquid culture of *E. coli* DH5α in LB medium was diluted 1:100 into fresh LB medium and incubated at 37°C and 250 rpm until an OD_{600nm} of 0.375 was reached. Subsequently, the suspended bacteria were aliquoted into 50 ml aliquots that were kept on ice for 5 min and afterwards centrifuged for 7 min at 1600 x g (4°C). The supernatant was discarded, each aliquot of bacteria was resuspended in 10 ml ice cold $CaCl_2$ solution and the centrifugation step repeated as above. After that, the supernatant was discarded again, each aliquot of bacteria was resuspended in 10 ml fresh ice cold $CaCl_2$ solution and stored on ice for 30 min. Following another centrifugation as detailed above, the pelleted bacteria were resuspended in 2 ml $CaCl_2$ solution per aliquot, snap frozen in an ethanol/ dry ice bath and stored at -80°C.

For transformation of competent *E. coli* DH5α bacteria using ligation reactions, 1/10 of the entire reaction was used, corresponding to 10-100 ng DNA. The frozen bacteria were rapidly thawed and 50 µl of suspension were added to the DNA. Following an initial incubation on ice for 10 min, the mixture was heated to 42°C for 45 sec and immediately cooled on ice again. The transformed bacteria were suspended in 1 ml LB medium and incubated for 45 min at 37°C and 400 rpm. Subsequently, the suspension was plated onto agar plates containing the appropriate antibiotic for selection of successfully transformed colonies and incubated over night at 37°C. On the next day, single colonies were picked and transferred into liquid cultures in order to prepare plasmid DNA.

2.2.2.9 Isolation and analysis of plasmid DNA from transformed bacteria

Plasmid DNA was isolated from transformed bacteria using commercially available kits (*Innuprep Plasmid Mini kit* for liquid cultures up to 1.5 ml; *Endofree Plasmid Maxi kit* for liquid cultures up to 100 ml) according to the manufacturers´ instructions. Following plasmid DNA isolation, analytical restriction digestions were performed using appropriate restriction enzymes (see 2.2.2.3) and the resulting fragments were analyzed by gel electrophoresis (see 2.2.2.4).

2.2.2.10 Polymerase chain reaction (PCR)

In the current study, several amplifications of genetic material were performed using PCR. The reaction mixtures as well as the cycling parameters for the respective amplifications are summarized below. The primers for each PCR are listed in 2.1.8. Abbreviations: TB = Thermopol buffer; SA2 = Speedamp buffer No. 2; SA3 = Speedamp buffer No. 3; PE = Perkin Elmer cycler; SC = Speed cycler.

	c-myc tag	CXCL10	CXCL8	CX3CL1 mucin dom.	DAF signal sequence
dNTP mix	0.2 mM	0.25 mM	0.2 mM	0.25 mM	0.2 mM
fw-primer	0.4 µM	0.3 µM	0.4 µM	0.3 µM	0.4 µM
rv-primer	0.4 µM	0.3 µM	0.4 µM	0.3 µM	0.4 µM
Taq DNA Polymerase	0.04 U/µl	0.04 U/µl	0.04 U/µl	0.04 U/µl	0.04 U/µl
Buffer	T, 1x	SA3, 1x	T, 1x	SA2, 1x	T, 1x
Target DNA	4 ng/µl	6.6 ng/µl	5.7 ng/µl	6.7 ng/µl	12 ng/µl
H_2O	ad 25 µl	ad 15 µl	ad 35 µl	ad 15 µl	ad 25 µl

	c-myc tag	CXCL10	CXCL8	CX3CL1 mucin dom.	DAF signal sequence
Initial denaturation	94°C 5 min	95°C 2 min	94°C 5 min	95°C 2 min	94°C 5 min
Denaturation	94°C 30 sec	95°C 4 sec	94°C 30 sec	95°C 4 sec	94°C 30 sec
Annealing	64°C 30 sec	57°C 4 sec	56.5°C, 90 sec	58°C 4 sec	58°C 90 sec
Elongation	72°C 30 sec	72°C 20 sec	72°C 2.5 min	72°C 20 sec	72°C 2.5 min
No. of cycles	35	35	30	35	30
Final elongation	72°C 5 min	72°C 50 sec	72°C 7 min	72°C 50 sec	72°C 7 min
Cycler	PE	SC	PE	SC	PE

2.2.2.11 Site-directed mutagenesis

A commercially available kit (*Quickchange*) was used to perform site-directed mutagenesis on plasmids. Primers were designed according to the manufacturer´s instructions and are listed in 2.1.8. The PCR reactions as well as the subsequent transformation steps were performed according to the manufacturer´s instructions.

2.2.2.12 Sequencing of DNA

DNA sequencing was performed by Entelechon, Regensburg or GATC Biotech, Konstanz. The primers that were used for the sequencing of inserts in pEF_{dhfr} are listed in 2.1.8, standard primers were used for other plasmids.

2.2.2.13 Isolation of mRNA and reverse transcription

RNA from cultured cells was isolated using a commercially available kit (*PureLink RNA Mini kit*) according to the manufacturer´s instructions including the optional DNase digestion step. RNA was eluted from the columns using 30 µl RNase free water and the RNA concentration was determined (see 2.2.2.5). 2 µg of RNA were reversely transcribed using the following reaction mixture:

Component	Concentration
RNA	50 ng/µl (total 2 µg)
First strand buffer (5x)	1x
DTT	0.5 mM
RNAsin	0.025 U/µl
Acrylamide	62.5 ng/ml
dNTPs	2 mM
Hexamer nucleotides (10x)	1x
Superscript II reverse transcriptase	0.1 U/µl
RNase free water	ad 40 µl

As a control for contaminations with genomic DNA, a second reaction was prepared using 0.2 µg RNA in which the reverse transcriptase was replaced by RNase free water (RT^{minus} control). The reaction mixtures were incubated for 90 min at 42°C and 400 rpm and subsequently stored at -20°C.

2.2.2.14 Stable transfection of $CHO^{dhfr-/-}$ cells

Dihydrofolate reductase (Dhfr) deficient CHO cells were used to express the membrane-anchored chemokines. This cell line is auxotrophic for hypoxanthine and thymidine, and the deficiency can be complemented by the dhfr gene encoded in the pEF_{dhfr} plasmid. Thus, stably transfected clones could be selected by withdrawal of hypoxanthine and thymidine from the culture medium, which was accomplished by the use of FCS which had been dialyzed against PBS.

Only endotoxin free DNA preparations were used for transfection purposes and to increase the efficiency of genomic integration, all vectors were linearized using *Nde*I prior to transfection. $CHO^{dhfr-/-}$ cells were used in the logarithmic growth phase when 90% confluence was reached. The cells were detached using Trypsin/EDTA and washed twice with PBS. Subsequently, 5×10^6 cells were resuspended in 400 µl PBS, mixed with 30 µg of linearized DNA and incubated on ice for 10 min. After that, electroporation was performed at 960 µF and 260 V, followed by another incubation on ice for 10 min. The transfected cells were transferred into a 75 cm^2 cell culture flask and incubated overnight in complete medium including hypoxanthine/ thymidine supplement. On the next day, the medium was exchanged to selection medium without supplement to allow for the selection of transfected clones.

After this initial selection, some cell lines were additionally treated with methotrexate, an inhibitor of the dihydrofolate reductase, to eliminate cells with a low expression level. The dihydrofolate reductase gene is expressed in the pEF^{dhfr} plasmids together with the transgenes in one mRNA molecule by means of an internal ribosome binding site. Thus, through inhibition of the dihydrofolate reductase by methotrexate, cells with a low expression level of dihydrofolate reductase and consequently also the transgene can be eliminated. Methotrexate was dissolved in 250 mM sodium-bicarbonate buffer, pH 9.4, sterile filtered and stored at 4°C. Initially a concentration of 100 nM was used, which was supplemented to the medium for several passages until resistant clones grew out.

Subsequently the methotrexate concentration was gradually increased up to 200 nM. The expression levels of the recombinant fusion proteins were regularly assessed by FACS staining (see 2.2.5.1.1).

2.2.3 Cloning strategies

2.2.3.1 Cloning of the CXCL10 constructs

2.2.3.1.1 CXCL10-GPI and CXCL10-mucin-GPI

CXCL10-GPI:

The GPI anchor signal sequence of LFA-3 (amino acids 203-232 of the mRNA translation of LFA-3 according to GenBank entry NM_001799.2) had previously been amplified from a human inflamed kidney cDNA sample (Notohamiprodjo et al. 2006). The signal sequence was ligated into a pUC19 plasmid using the *Xba*I (5´) and *Sal*I (3´) restriction enzyme recognition sequences that had been introduced via the PCR primers.

The cloning of the double c-myc epitope tag was performed in collaboration with Dr. N. Rieth. The retroviral vector MP71 containing the double c-myc tag sequence served as template and the c-myc sequence was amplified by PCR using the primers listed in 2.1.8 and the conditions detailed in 2.2.2.10. In this PCR, a 5´ *Xba*I and a 3´ *Nhe*I recognition site were added to the sequence via the primers. These recognition sites were used to ligate the amplicon into the above mentioned pUC19 plasmid which contained the LFA3 GPI anchor signal sequence and had been linearized using *Xba*I. Thus, in the resulting plasmid, the c-myc epitope tag sequence directly preceded the GPI signal sequence and the *Nhe*I restriction site separating the two sequences was lost.

The CXCL10-GPI and CXCL10-mucin-GPI constructs were cloned in collaboration with S. Böcker from our group. A plasmid containing the gene sequence of human CXCL10 had originally been provided by PD Dr. B. Luckow and the gene had previously been subcloned into various plasmids. In the current study, a plasmid containing CXCL10 and a GPI signal sequence but no c-myc tag sequence was used as template to amplify the CXCL10 gene without stop codon. To this end, the primers listed in 2.1.8 were used, which introduced 5´ *Eco*RI and 3´ *Nhe*I restriction sites. These sites were used to ligate the gene into the above mentioned pUC19 vector already containing the c-myc epitope tag and the GPI signal sequence. In the resulting pUC-CXCL10-GPI plasmid, the CXCL10 gene thus preceded the c-myc sequence, which was followed by the GPI signal sequence. Subsequently, the entire construct was subcloned into a pEF_{dhfr} vector for expression in CHO cells using the 5´ *Eco*RI and the 3´ *Sal*I restriction sites.

Additionally, the pUC19-CXCL10-GPI plasmid was mutated by site-directed mutagenesis so that the *Nhe*I restriction site between the CXCL10 gene and the c-myc tag sequence was restored to have greater flexibility for subsequent cloning steps. The primers used for the mutagenesis are listed in 2.1.8 and the resulting plasmid was termed pUC-CXCL10-GPI2.

CXCL10-mucin-GPI:

The mucin domain of CX3CL1 (amino acids 100-341 of the mRNA translation of CX3CL1 according to GeneBank entry BC016164.1) had previously been amplified from a human inflamed kidney cDNA sample and subcloned into various vectors. In the current study, a pEF_{dhfr} plasmid containing (in that order) the CXCL12 gene, the CX3CL1 mucin domain gene, the c-myc tag sequence and the GPI anchor signal sequence from LFA3 was used to generate pEF-CXCL10-mucin-GPI. The CXCL12 gene was cut out by digestion with *Eco*RI and *Xba*I and replaced by the CXCL10 gene that had been cut out of pUC-CXCL10-GPI2 using *Eco*RI and *Nhe*I. The generated plasmid could then directly be used to transfect CHO cells.

2.2.3.1.2 CXCL10-DAFPI and CXCL10-mucin-DAFPI

CXCL10-DAFPI:

A second set of fusion genes was constructed using the GPI anchor signal sequence taken from DAF for comparison purposes. The GPI anchor signal sequence of DAF (referred to as DAFPI; amino acids 348-381 of the mRNA translation of DAF according to GeneBank entry BC001288.1) was amplified by PCR from cDNA of primary human monocytes and umbilical vein endothelial cells (HUVEC) using the primers listed in 2.1.8 and the conditions detailed in 2.2.2.10. *Xba*I (5´) and *Sal*I (3´) restriction sites were added via the PCR primers. The amplicon was ligated into a pEF-sEGFP-GPI plasmid (see below) from which the GPI signal sequence had been removed using *Xba*I and *Sal*I to yield pEF-sEGFP-DAFPi. The sEGFP gene was subsequently removed by digestion with *Eco*RI and *Sal*I and replaced by a cassette containing the CXCL10 gene and the c-myc tag sequence that had been cut out of a second vector using *Eco*RI and *Nhe*I.

CXCL10-mucin-DAFPI:

The same strategy was employed for the cloning of CXCL10-mucin-DAFPI: The sEGFP gene was removed from pEF-sEGFP-DAFPI by digestion with *Eco*RI and *Xba*I and replaced by a cassette consisting of the CXCL10 gene, the CX3CL1 mucin domain gene and the c-myc tag sequence that had been cut out of pEF-CXCL10-mucin-GPI using *Eco*RI and *Nhe*I.

2.2.3.1.3 CXCL10-Stop and CXCL10-mucin-Stop

CXCL10-Stop:

To generate the gene sequence for the secreted protein CXCL10-Stop, the CXCL10 gene was ligated using the *Eco*RI and *Nhe*I restriction sites into a pEF_{dhfr} plasmid containing the c-myc tag sequence and a stop codon to yield pEF-CXCL10-Stop.

CXCL10-mucin-Stop:

The CXCL10-mucin-Stop contruct was generated by first removing the c-myc tag and GPI anchor signal sequences from pUC-CXCL10-GPI2 (see 2.2.3.1.1) by digestion with *Nhe*I and *Sal*I. Subsequently, a cassette consisting of the CX3CL1 mucin domain gene and the c-myc tag sequence

followed by a stop codon was cut out of pEF-CXCL8-mucin-Stop (see 2.2.3.3.2) using *Xba*I and *Sal*I and ligated into the above mentioned plasmid. The resulting CXCL10-mucin-Stop gene was then subcloned into a pEF_{dhfr} vector using *Eco*RI and *Sal*I.

2.2.3.2 Cloning of the sEGFP constructs

2.2.3.2.1 sEGFP-GPI

The sEGFP-GPI construct was generated as a GPI-anchored negative control protein. Since EGFP is an intracellular protein, an N-terminal (5´) secretion signal sequence as well as a C-terminal (3´) GPI anchor signal sequence had to be added to the EGFP gene. The secretion signal sequence was taken from human tissue inhibitor of matrix metalloproteases 1 (TIMP-1; amino acids 1-23 of the mRNA translation of TIMP-1 according to GenBank entry NM_003254.2), and the GPI signal sequence from LFA-3 or DAF as in the other constructs.

As first cloning step, a *Mlu*I restriction site was introduced by site-directed mutagenesis at the 3´ end of the secretion signal sequence of TIMP-1 in pUC-TIMP1-GPI (provided by Dr. N. Rieth). The primers that were used are listed in 2.1.8. The plasmid already contained the GPI anchor signal sequence of LFA-3 at the 5´ end of TIMP-1 and the TIMP-1 gene except the two signal sequences was removed by digestion with *Mlu*I and *Xba*I. In a second step, the EGFP gene was amplified without the stop codon using a pEGFP-N1 plasmid as template. Concomitantly, a *Mlu*I restriction site was introduced at the 5´ end of the gene and an *Xba*I site at the 3´ end that were used to ligate the amplicon into the pUC19 plasmid with the signal sequences (primers are listed in 2.1.8). In order to introduce the c-myc epitope tag sequence, the cassette consisting of the TIMP-1 secretion signal sequence and EGFP was subcloned via *Eco*RI and *Xba*I into a pUC plasmid containing the c-myc epitope tag sequence followed by the GPI signal sequence from LFA-3. The resulting construct was termed sEGFP-GPI (s for secretion signal sequence) and subcloned for expression in CHO cells into a pEF_{dhfr} vector using *Eco*RI and *Sal*I.

2.2.3.2.2 sEGFP-DAFPI

The sEGFP-DAFPI construct containing the GPI anchor signal sequence of DAF instead of the one of LFA-3 was constructed by amplifying the DAF signal sequence from cDNA samples and subsequently ligating it into the pEF-sEGFP-GPI vector, the GPI signal sequence of which had been removed beforehand as detailed above.

2.2.3.3 Cloning of the CXCL8 constructs

2.2.3.3.1 CXCL8-GPI and CXCL8-mucin-GPI

To generate the DNA constructs for the GPI-anchored CXCL8 fusion proteins, the CXCL8 gene without stop codon was amplified from cDNA of HUVEC cells that had been activated over night with 10 ng/ml IL-1β. 5´ *Mfe*I and 3´ *Xba*I restriction sites were added via the primers (see 2.1.8) and used to ligate the amplicon into a pEF_{dhfr} vector already containing the LFA3 GPI signal sequence.

Subsequently, the GPI anchor signal sequence was replaced by a cassette containing the c-myc sequence followed by the LFA3 GPI signal sequence using the *Xba*I and *Sal*I restriction sites. The resulting pEF-CXCL8-GPI plasmid could be transfected into CHO cells.

The CXCL8-mucin-GPI construct was generated by first linearizing pEF-CXCL10-GPI with *Xba*I. Subsequently, the CXC3CL1 mucin domain was amplified using another plasmid containing the mucin domain as template. The corresponding primers are listed in 2.1.8 and introduced a 3´ *Xba*I and a 5´ *Nhe*I site into the amplicon, which were used to ligate the mucin domain gene into the linearized vector.

2.2.3.3.2 CXCL8-Stop and CXCL8-mucin-Stop

The soluble versions of the CXCL8 constructs were created in the same manner as the GPI-anchored versions. CXCL8 was amplified by PCR as described above and ligated into a pEF_{dhfr} vector containing the c-myc tag sequence followed by a stop codon. For CXCL8-mucin-stop, the mucin domain was subsequently inserted as described above for CXCL8-mucin-GPI.

2.2.4 Protein-biochemical methods

2.2.4.1 Protein purification

All protein purifications were performed using an *ÄktaFPLC* fast protein liquid chromatography device. The corresponding *Unicorn* software was used to control and evaluate chromatography runs. All buffers were prepared using pyrogen free components and only pyrogen free disposable materials were used in order to prevent contaminations with pyrogens.

2.2.4.1.1 Purification of the anti c-myc antibody 9E10

The c-myc specific antibody produced by the hybridoma clone 9E10 was used for various purposes in this study. A Protein A (ProtA) Sepharose high performance column (2 x 1 ml columns connected in series, 2 ml total bed volume) was used to purify the antibodies. Conditioned medium was obtained as described in 2.2.1.1. The column was equilibrated using equilibration buffer (see 2.1.3.1) for 5 CV and subsequently the supernatant was loaded with 1 ml/min flow rate. Following a washing step with equilibration buffer for 6 CV, the bound antibodies were eluted from the column using elution buffer and the elution fractions were immediately neutralized using 1 M Tris, pH 8.0. Aliquots of the respective fractions were assayed by reducing SDS-PAGE for the presence of bands corresponding to the heavy and light chains of IgG (about 50 kDa and 25 kDa, respectively). PageBlue protein staining solution was used to stain the gels according to the manufacturer´s instructions. Positively identified fractions were pooled and the buffer was exchanged for PBS using *HiTrap* desalting columns. The protein concentration was determined using the Bradford assay (see 2.2.4.3.3) and aliquots were stored at -20°C.

2.2.4.1.2 Purification of the anti CXCL8 antibody A5.12.14

CXCL8-specific antibodies were isolated from the A5.12.14 hybridoma using a recombinant Protein A Fast Flow column (rProtA FF; 5 ml bed volume). Conditioned medium was obtained as described in 2.2.1.1 and the proteins were transferred into equilibration buffer using a *HiPrep* desalting column. Protein-containing fractions were pooled and loaded onto an equilibrated rProtA FF column with 2 ml/min flow rate. The column was washed with equilibration buffer for 6 CV and the bound proteins were eluted using elution buffer. The subsequent steps were performed as detailed above for the 9E10 antibody. Typically about 14 mg antibody could be isolated from 1 l of conditioned medium.

2.2.4.1.3 Purification of the GPI-anchored fusion proteins

General considerations:

The GPI-anchored fusion proteins (CXCL10-GPI, CXCL10-mucin-GPI, CXCL10-DAFPI, CXCL10-mucin-DAFPI, CXCL8-GPI, CXCL8-mucin-GPI, sEGFP-GPI and sEGFP-DAFPI) were purified using the double c-myc epitope tag that had been integrated into all the constructs preceding the respective GPI anchor signal sequence. This epitope tag enabled affinity-chromatographic isolation of the proteins using a commercially available resin (*c-myc tagged protein mild purification gel*). The resin contained a specially developed antibody directed against the c-myc tag, the affinity of which was designed in a way that allows for efficient binding but also efficient release of the bound proteins using competitive elution with c-myc peptides. Thus, with this resin the fusion proteins could be isolated in a very gentle way avoiding high or low pH elution steps and other denaturing conditions.

Methodology of the c-myc affinity chromatography:

The affinity resins were generally used in *Tricorn 5/50* glass columns. Each column was only used for one fusion protein to avoid cross-contaminations and the columns were stored in 0.1% NaN_3 solution to prevent microbial growth. The resins could be reused up to 10 times. All buffers used during the purification contained hydrogenated Triton X-100 detergent in order to prevent aggregation of the lipophilic fatty acids in the GPI anchors and possibly precipitation of the fusion proteins.

1.5 x 10^8 transfected CHO cells (equivalent to twelve 300cm^2 flasks) were rapidly thawed and resuspended in 10 ml extraction buffer. The extraction buffer contained n-Dodecyl-β-D-maltoside, which had been identified as the most efficient detergent for solubilizing the fusion proteins from the cell membranes (see 2.2.4.3.2). The cell suspensions were rotated for 1 h at 4°C and subsequently centrifuged at 16,000 x g for 20 min (4°C) to remove cell debris and non-solubilized proteins. The supernatant was filtered through at 0.2 µm filter prior to chromatography.

The respective c-myc affinity column was washed with PBS and equilibrated in equilibration buffer for 5 CV. Afterwards, the cell extract was applied to the column with 0.01 ml/min flow rate, followed by a washing step for 2 CV with equilibration buffer at 0.1 ml/min. In order to elute non-specifically

bound proteins, 3 CV of high-salt washing buffer which contained 280 mM NaCl were perfused through the column at 0.1 ml/min. Following another washing step with equilibration buffer to normalize the salt concentration, the proteins were eluted by injecting 5 ml of elution buffer containing 0.01 mg/ml c-myc peptide. The column was subsequently regenerated using regeneration buffer, immediately flushed with PBS and stored in storage buffer.

Analysis of the chromatography fractions:

All fractions collected over the course of the chromatography were assayed for their content of the respective fusion proteins by western blotting. In the case of the sEGFP fusion proteins, the fluorescence (485 nm excitation, 535 nm emission) in the respective fractions was measured instead of western blotting. Elution fractions containing the highest amount of fusion protein were pooled and the elution pool was concentrated using ultrafiltration devices with a molecular size cutoff of 5 kDa to obtain higher concentrations of fusion protein. The specific concentrations of the chemokine fusion proteins were determined using commercially available CXCL8 or CXCL10 ELISA kits according to the manufacturer´s instructions. Protein purity was assessed using SDS-PAGE and silver staining as well as a comparison between the specific protein content (ELISA) and the total protein content (BCA Assay).

2.2.4.1.4 Purification of the soluble chemokine fusion proteins

The soluble chemokine fusion proteins were purified from conditioned media that were obtained as described in 2.2.1.1 and could be applied directly to the affinity column. Chromatography was performed as described above for the membrane-anchored proteins with the only differences being that loading was performed at 0.05 ml/min and all buffers were prepared without Triton X-100h.

2.2.4.2 SDS-PAGE, western blot and silver staining

2.2.4.2.1 SDS-PAGE

Preparation of SDS gels:

SDS PAGE was performed as described by Laemmli (Laemmli 1970). The percentage of Acrylamide/Bis-Acrylamide in the gels was chosen according to the expected size of the proteins of interest. Separation gels with a final volume of 20 ml were prepared as summarized below:

Percentage	Acrylamide/Bis-Acrylamide mix, 30% (ml)	H_2O (ml)	Other components (for all gel percentages)
8%	5.3	9.3	5 ml 1.5 M Tris, pH 8.0
10%	6.7	7.9	200 µl 10% SDS
15%	10.0	4.6	200 µl 10% Ammoniumpersulfate (APS)
16%	10.6	4.0	20 µl Tetramethylethylendiamine (TEMED)

Following polymerization, a 5% stacking gel was poured on top of the separation gels, composed of 1.7 ml Acrylamide/ Bisacrylamide mix, 1.25 ml Tris (1 M, pH 6.8), 6.8 ml H_2O, 100 µl 10% SDS, 100 µl 10% APS and 10 µl TEMED. Gels were stored in humidified atmosphere at 4°C for no longer than one week.

Electrophoresis:

For electrophoresis, the protein samples were mixed with the respective sample buffer (either Laemmli buffer for reducing or LDS sample buffer for non-reducing chromatography; see below for each antibody) to yield a 1 x sample buffer concentration. Afterwards, the samples were incubated at 95°C for 5 min, centrifuged shortly and loaded onto a gel. 0.5-1.5 µl MagicMark size standard were loaded in a separate well for molecular weight estimation. All gels were run in electrophoresis buffer first at 80 V until the samples had entered the stacking gel and subsequently at 120 V.

2.2.4.2.2 Western blotting

Western blotting was performed analogous to (Towbin et al. 1979). Proteins were transferred from the gels onto polyvinylidene fluoride (PVDF) membranes electrophoretically using the wet blot technique in *NuPage* transfer buffer at 30 V for 1 h. Subsequently, the membranes were blocked in blocking solution for 1-3 h at room temperature or over night at 4°C, washed twice with water, and incubated with the respective primary antibody for 1-3 h at room temperature or over night at 4°C. The diluents and conditions for each primary antibody are summarized below.

Antibody	SDS-PAGE type	Diluent	Concentration
anti c-myc 9E10	reducing	blocking buffer	1 µg/ml
anti CXCL10	non-reducing	*WesternBreeze* blocking solution	0.75 µg/ml
anti CXCL8 A5.12.14	non-reducing	*WesternBreeze* blocking solution	2 µg/ml

Following incubation with the primary antibody, the membranes were washed 4 times with TBST and incubated for 1 h at room temperature with the secondary antibody anti mouse IgG which was coupled to horse radish peroxidase (HRP) and diluted in blocking buffer to a concentration of 0.26 µg/ml. The washing steps were repeated as after incubation with the primary antibody with two additional washing steps in TBS for 5 min and the membrane was immersed in 4 ml ECL substrate solution for 1 min. Excess substrate was dabbed off and an autoradiography film (*Amersham Hyperfilm ECL*) was exposed to the membrane. The film was subsequently developed using a developing machine.

2.2.4.2.3 Coomassie staining

To stain protein bands in SDS gels, Coomassie was performed using *PageBlue* protein staining solution according to the manufacturer´s instructions.

2.2.4.3 Protein quantification methods

2.2.4.3.1 ELISA for the quantification of CXCL8 and CXCL10 fusion proteins

The concentrations of the recombinant chemokine fusion proteins were quantified using commercially available sandwich ELISA development kits (*DuoSet*). Samples were diluted in assay buffer (see 2.1.3.5) and each measurement was done in duplicates. Additionally, concentrations of at least 3 different dilutions of each sample were measured. All other procedures were performed according to the manufacturer´s instructions. OptEIA substrate solution was used for the chromogenic development.

2.2.4.3.2 Modified ELISA for determination of solubilization efficiencies

A modified ELISA was established in order to test the solubilization efficiency of various detergents with regards to the recombinant fusion proteins. The protocol was modified from Bumgarner et al. (Bumgarner et al. 2005) and essentially was based on the following principle: First, the proteins were labeled with specific antibodies on the cell surface of the CHO cells. Then, the labeled cells were incubated with various detergents to solubilize the proteins. The extracts were divided into one sample that was centrifuged to remove non-solubilized proteins and one sample that was left uncentrifuged. The specific signal strengths in the centrifuge supernatant and the uncentrifuged sample were subsequently obtained, compared to each other and expressed as percent solubilization.

A frozen CHO cell pellet was thawed and 10^6 cells were transferred into each well of a 96 well round bottom plate. The plate was centrifuged for 2 min at 755 x g (4°C), the supernatant was discarded and the cells were resuspended in 100 µl primary antibody solution per well (10 µg/ml in MEM alpha medium; anti CXCL8 for CXCL8 constructs, anti c-myc for CXCL10 constructs). The plate was incubated at 4°C for 30 min, centrifuged as above, and the cells were resuspended in 150 µl PBS per well. Following another centrifugation, the cells were resuspended in 100 µl secondary antibody solution per well (1.3 µg/ml anti mouse IgG, in MEM alpha medium) and incubated at 4°C for 30 min. Subsequently, the cells were washed twice with PBS as described above, resuspended in 100 µl of the respective lysis buffer per well (duplicates were taken for each lysis buffer) and incubated for 1 h at 4°C and 200 rpm shaking. The lysis buffers generally contained 50 mM Tris/HCl, pH 7.5 and the respective detergent in different concentrations. Only nonionic detergents were tested and only such that were available in very high purity (*ULTROL* grade or similar). Following solubilization, the samples were mixed by pipetting and 10 µl of each sample were transferred into a 96 well flat bottom plate (non-centrifuged control = 100% value). The rest of each sample was transferred into test tubes and centrifuged at 16.000 x g for 30 min (4°C) to remove non-solubilized proteins and debris. 10 µl of the supernatant were transferred into the 96 well flat bottom plate, and 100 µl OptEIA ELISA substrate was added to all samples. The reaction was stopped by adding 50 µl 1 M

H_2SO_4 and absorption readings of each well were taken at 450 nm in a microplate reader. The percentage of solubilization was subsequently calculated as:

$$Solubilization\ [\%] = \left(\frac{Absorption\ in\ centrifuge\ supernatant}{Absorption\ in\ uncentrifuged\ sample}\right) * 100$$

2.2.4.3.3 Bradford and BCA assays

Total protein concentrations were determined using either the Bradford (Bradford 1976) or the bicinchonic acid (BCA) method (Smith et al. 1985). The Bradford assay was used only for samples that did not contain detergents as these cause precipitation of the Coomassie dye. Consequently, the BCA assay was used for samples containing detergents. The Coomassie assay was performed as follows: A standard curve was prepared using serial dilutions of BSA as well as several dilutions of the samples. 200 µl of each sample were mixed in a 96 well flat bottom plate with 50 µl of *Bio-Rad protein assay reagent* and the absorption at 590 nm was taken using a microplate reader. Subsequently, a standard curve was generated, to which the readings of the samples were correlated. The BCA assay was performed with a commercially available kit using the microplate procedure described by the manufacturer.

2.2.4.4 Edman sequencing

A correct N-terminal amino acid sequence is essential for the function of chemokines. In order to verify correct N-terminal processing of the CHO-cell expressed chemokine fusion proteins, Edman sequencing was performed (Edman 1949). Sequencing was done using purified protein samples that had been prepared as detailed in 2.2.4.1.4. An SDS-PAGE was performed where 1 µl of the sample was applied to one lane in order to perform western blotting and 45 µl were applied to another lane for Coomassie staining and the actual Edman sequencing. Laemmli buffer was chosen as sample buffer in all cases. Following SDS-PAGE, the proteins were transferred onto a PVDF membrane and the membrane was cut in half for western blotting (see 2.2.4.2.2) and Coomassie staining. Western blotting was carried out using anti c-myc antibodies. For Coomassie staning, the membrane was washed with H_2O and submerged in Coomassie staining solution (see 2.1.3.2), followed by several washes in H_2O once the staining was strong enough. The membrane was air-dried, and the respective bands were identified by comparison with the western blot and cut out. The Edman sequencing reaction as well as data acquisition and analysis were performed by R. Mentele, Max Planck Institute for Neurobiology, Martinsried.

2.2.5 *In vitro* experiments

2.2.5.1 Fluorescence activated cell scanning (FACS) analyses

2.2.5.1.1 Detection of the recombinant fusion proteins

FACS was used to detect the recombinant fusion proteins on cell surfaces either after expression in CHO cells or after incorporation in various cells. For the analysis of protein expression, the cells were detached using EDTA, resuspended in FACS buffer and transferred into a 96 well round bottom plate (1 x 10^6 cells per well). If incorporation of the purified proteins into cell membranes should be analyzed, the cells were pretreated with the proteins as detailed in the next section. In both cases, the cells were washed with FACS buffer, the plate was centrifuged for 2 min at 755 x g (4°C) and the supernatant was discarded. After that, the cells were resuspended in 100 µl FACS buffer per well containing the primary antibody (10 µg/ml for antibodies against the c-myc tag, CXCL8 or CXCL10, 5 µg/ml for antibodies specific for the CX3CL1 mucin domain) or isotype-matched control antibodies at the same concentration. Following an incubation for 45 min at 4°C, the cells were washed with FACS buffer. To this end, the plate was centrifuged at 755 x g for 2 min (4°C), the supernatant was removed and the cells were resuspended in 175 µl of FACS buffer followed by another centrifugation at 755 x g for 2 min (4°C) and removal of the supernatant. The cells were resuspended in 100 µl FACS buffer per well containing RPE or FITC labeled secondary antibodies at a concentration of 10 µg/ml and 4 µg/ml 7-AAD for the identification of dead cells. After 30 min incubation at 4°C, the cells were washed again as detailed above and resuspended in 200 µl FACS buffer for analysis.

Compensation was performed using single-stained samples to ensure that measurements in the single fluorescence channels did not interfere with each other and only living cells based on 7-AAD exclusion were evaluated.

2.2.5.1.2 Incorporation of the recombinant fusion proteins

The ability of the purified recombinant fusion proteins to incorporate into cell membranes was assessed by FACS staining. CHO or endothelial cells were detached using Trypsin/EDTA and resuspended in prewarmed serum-free medium (the medium that was used for the respective cell line without addition of serum or other supplements; compare 2.1.1.1). 1 x 10^6 CHO cells or 5 x 10^5 endothelial cells per well were transferred into a sterile 96 well round bottom plate. The plate was centrifuged for 3 min at 220 x g (rt) and the supernatants were removed. Subsequently, the cells were resuspended in 100 µl of prewarmed serum-free medium containing defined concentrations of purified recombinant fusion proteins or a buffer control. The volume of recombinant fusion proteins in chromatography buffer (or the buffer control) was not allowed to exceed 17.5% of the total volume and it was taken care that all samples contained the same percentage of buffer. The

resuspended cells were incubated at 37°C and 5% CO_2 for 1-1.5 h, and the following staining procedures were performed as detailed in 2.2.5.1.1.

2.2.5.1.3 Cleavage of the GPI anchor using PI-PLC

GPI anchors can be cleaved by phosphatidylinositol-specific phospholipase C (PI-PLC), and this property was used to test if the recombinant fusion proteins were GPI-anchored and if the incorporation process was dependent on the GPI anchor. 5 x 10^5 HMEC cells per well were treated with the proteins as detailed in 2.2.5.1.2., but following incubation with the proteins, the cells were washed with PBS instead of FACS buffer and subsequently resuspended in 100 µl DMEM medium per well which contained 0.1 unit of PI-PLC (or DMEM only as control). The cells were incubated at 37°C and 5% CO_2 for 1 h, washed with PBS again and subsequently stained for the presence of the recombinant fusion proteins using anti c-myc antibodies as detailed in 2.2.5.1.1.

2.2.5.1.4 CXCR3 expression and internalization assays

CXCR3 expression analysis:

To determine the expression of CXCR3 in murine 291 lymphoma cells or murine T cells, 1-1.25 x 10^6 cells were suspended in 50 µl FACS buffer. APC-labeled, CXCR3-specific antibodies or an identically labeled isotype control were added at a final concentration of 20 µg/ml, as well as 5 µl Propidiumiodide (PI). All samples were incubated for 45 min at 4°C. Subsequently, the cells were washed twice with FACS buffer and suspended in 200 µl FACS buffer for analysis. Approporiate compensation was performed, and dead cells were identified in the FL-3 channel and excluded from analysis.

CXCR3 internalization on human cells:

CXCR3 internalization was used as readout for receptor activation by the recombinant fusion proteins. To this end, coincubations of JB4 T cells and transfected CHO cells were performed. CHO cells were detached using EDTA, washed using serum free RPMI 1640 medium, and 6 x 10^5 cells in 25 µl RPMI 1640 per well were transferred into a 96 well round bottom plate. 25 µl recombinant human CXCL10 at concentrations of 1.5 µg/ml or 200 ng/ml in RPMI 1640 was added to other wells of the same plate as positive control, and 25 µl RPMI 1640 only as negative control. All samples were prepared in duplicates to allow for staining with CXCR3-specific antibodies and an isotype control. JB4 cells were washed in RPMI 1640 and 2 x 10^5 cells in 25 µl RPMI 1640 were subsequently added to each well that had been prepared as described above. The plate was incubated at 37°C and 5% CO_2 for 30 min, and after this time, 150 µl ice cold FACS buffer was added to each well. All following steps were performed on ice using precooled buffers. The cells were washed using FACS buffer and resuspended in 75 µl FACS buffer per well. Subsequently, 7-AAD at a final concentration of 4 µg/ml and 4 µl of FITC-labeled CD3-specific antibodies (original concentration not disclosed by the manufacturer) were added to all samples. Among each pair of duplicates, one sample additionally

received 3 µl of RPE-labeled, CXCR3 specific antibodies (BD Pharmingen¸ original concentration not disclosed by the manufacturer), while the other one received the same volume of RPE-labeled isotype control. The plate was incubated at 4°C for 45 min, and following another wash with FACS buffer, the cells were resuspended in 200 µl FACS buffer and measured.

Compensation was performed using single-stained samples to ensure that measurements in the single fluorescence channels did not interfere with each other and gating was performed as follows: First, JB4 cells were roughly identified in a FSC-H/ SSC-H dot plot by their smaller size and lower granularity compared to the CHO cells. Among this population, FL-3 positive dead cells were excluded. Within that population again, CD3-positive cells were identified in the FL-1 channel and subjected to analysis. The strength of CXCR3 signal in the FL-2 channel was determined for each sample as the geometric mean of FL-2H. The mean fluorescence intensity (MFI) was determined as the difference between the respective isotype-stained sample and the one stained with specific antibodies. Subsequently, the MFIs of the sample containing non-transfected CHO cells (for the coincubation samples) or the sample containing RPMI 1640 only (for the samples with recombinant CXCL10) were defined as 100% expression and the other samples were related to them.

As additional controls, either the cells were coincubated at 4°C instead of 37°C to slow down cellular metabolism, or RPE-labeled CXCR3-specific antibodies from a different supplier (R&D Systems) were utilized, of which 10 µl were used.

CXCR3 internalization on murine cells:

CXCR3 internalization was also used as readout to assess the cross-reactivity of human CXCL10 with murine T cells. This assay was performed essentially as described above for human cells, with the following deviations: 3.75 x 10^5 T cells per well were used, and the assay was performed entirely in HBSS (phenol red free, +Mg^{2+}, +Ca^{2+}; Invitrogen) supplemented with 20 mM HEPES. For the staining, 4 µl of APC-labeled CXCR3-specific antibodies and 4 µl PI were used per 50 µl and comparisons were done against cells stained only with PI. Human and murine CXCL10 were tested only at a concentration of 660 ng/ml.

2.2.5.2 Calcium mobilization assays

2.2.5.2.1 Calcium mobilization assays using recombinant proteins

Calcium is released from the endoplasmatic reticulum as an essential step in the signaling cascade triggered by chemokine receptors. The resulting transient rise in cytoplasmatic calcium concentration was used as another readout for receptor activation in order to assess the cross-reactivity of human CXCL10 with murine T cells.

Murine $CD4^+$ T cells were loaded with the calcium-sensitive fluorescent dye Fluo-4 using a commercially available kit essentially according to the manufacturer´s instructions. However, the following modifications were made to the protocol: Loading was performed in 15 ml tubes, and

15 min before the end of the loading time, 7-AAD was added to the cells at a final concentration of 4 µg/ml. After 15 min, the cells were centrifuged and resuspended in fresh assay buffer to a concentration of 1.7 x 10^6 cells/ml. Using a FACS machine, the development of the fluorescence of living (as determined by 7-AAD exclusion) cells in the FL-1 channel was monitored in each sample over time. After 30 sec, recombinant chemokines at a final concentration of 1 µg/ml or buffer were added to the samples and the fluorescence was monitored for an additional 3 min.

2.2.5.2.2 Calcium mobilization assays using transfected CHO cells

Intracellular calcium mobilization was also measured in T cells interacting with transfected CHO cells. To this end, cells of the human T cell line DS4 were loaded with Fluo-4 using the same kit as mentioned above. Loading was performed according to the manufacturer´s instructions, but treatment was performed in 15 ml tubes and after the incubation in loading solution, cells were centrifuged and resuspended in fresh assay buffer to yield 5 x 10^6 cells/ml. 50 µl of this suspension were transferred into each well of a special 96 well flat bottom plate with black side walls and ultra-thin bottom. As a control for CHO cell autofluorescence, the same number of wells as those that now contained DS4 cells was filled with 50 µl of assay buffer only. Subsequently, non-transfected CHO cells or cells transfected with the recombinant fusion proteins were detached using EDTA, washed and resuspended in assay buffer to yield a concentration of 1 x 10^7 cells/ml. Using a multichannel pipette, 50 µl of the CHO cell suspensions were added simultaneously to wells containing labeled DS4 cells or assay buffer. Immediately after the addition of the CHO cells, measurements were started using 485 nm excitation wavelength and 535 nm emission wavelength, and additional measurements were taken every 20 sec over a period of 40 min, during which the plate was kept heated to 37°C. All samples were run in duplicates. For data evaluation, averages were calculated from the two replicates for every sample and time point. To compensate for CHO cell autofluorescence, readings that had been taken in the samples in which the respective CHO cells had been “coincubated” with assay buffer only were subtracted for each time point from the readings that had been taken in samples in which the respective CHO cells had been coincubated with DS4 cells. Finally, to compensate for T cells settling to the bottom of the well, thereby steadily increasing the background fluorescence, the calculated values with non-transfected CHO cells were subtracted from those obtained with transfected cells to obtain Δ fluorescence values against non-transfected CHO.

As additional positive and negative controls, four wells with labeled DS4 cells were treated with 1 µg/ml (final concentration) recombinant human CXCL10 or assay buffer only (duplicates each) and the resulting fluorescence values were evaluated directly.

2.2.5.3 Immunofluorescence microscopy of cells

Immunofluorescent staining was performed to microscopically detect the GPI-anchored proteins on cell surfaces and to determine their subcellular localization. Identical experiments were done using

either transfected CHO cells or primary microvascular endothelial cells (HDBEC) that had been pretreated ("painted") with the purified proteins. In both cases, the cells were grown in special cell culture dishes until they reached 90% confluence. If the cells should be treated with purified proteins, they were at this point washed with PBS and incubated for 1.5 h at 37°C and 5% CO_2 with the respective proteins that had been diluted in serum-free culture medium. In both cases again, the cells were washed with PBS and fixed for 20 min using 1% paraformaldehyde in PBS at room temperature. All subsequent steps were performed at room temperature and all antibodies as well as streptavidin-RPE were diluted in HBSS (with phenol red, with Ca^{2+}, Mg^{2+}). After two washes in PBS, the cells were incubated for 50 min in 10 µg/ml anti c-myc antibodies. The cells were washed twice with PBS and subsequently incubated for 50 min in 5 µg/ml biotin-conjugated secondary antibodies. Following another two washes with PBS, 6 µg/ml streptavidin-RPE was used to stain the cells for 40 min in the dark. The cells were subjected to two last washing steps in PBS, and covered using 350 µl PBS and appropriately sized cover slips. Microscopic images were taken with an inverted-stage microscope and appropriate fluorescence filters.

2.2.5.4 Laminar flow assays

2.2.5.4.1 Background and general considerations

Laminar flow assays were performed to assess the effect of the recombinant fusion proteins on the adherence of leukocytes to endothelial cells or CHO cells. Such assays mimic the conditions found in blood vessels in terms of shear stress and are typically performed using channels with rectangular geometry. Endothelial cells are grown within the channel, pretreated according to the respective experiment, and subsequently leukocytes are perfused through the channel over the endothelial cell monolayer and the interactions are monitored by video microscopy. In the current study, flow chambers consisting of disposable microscope slides that contained a 5 mm wide, 0.4 mm tall and 5 cm long channel (*µ-slide I* 0,4) were used. In these slides, the shear stress at the bottom of the channel is constant for any point that is further than 500 µm away from the side walls of the channel ("observation area"). In all experiments, HBSS was used in the assay buffer, the viscosity of which has been demonstrated to be 0.01 dyn x sec/cm^{-2} (Donahue et al. 2003). This allowed the direct adaptation of the shear stress calculations, which the manufacturer of the flow channels used in the current study had made assuming a viscosity of 0.01 dyn x sec/cm^{-2}.

2.2.5.4.2 Experimental details

For experiments involving endothelial cells, the cells were grown to 80% confluence in tissue culture flasks. 24 hours prior to the experiment, the cells were seeded into the microscope slides. To this end, all media and the slides were prewarmed to 37°C in a cell culture incubator to prevent the formation of bubbles within the slides. The cells were detached using Trypsin/EDTA (diluted 1:5 in PBS), centrifuged and resuspended in culture medium (100 µl/slide) so that the cells were split at an

area ratio of 1 : 0.8 into the slides. The slides were precoated with Collagen G for 30 min at 37°C and 5% CO_2 using 100 µl of 12 µg/ml Collagen G in PBS. After washing with PBS, the slides were immediately filled with cell suspension and incubated for 24 h. If the endothelial cells should be "painted" with purified GPI-anchored proteins, the different slides were treated with the proteins for exactly 1 h prior to the analysis of the respective slide. For the treatment, the channel was washed with 100 µl purified proteins diluted in serum-free culture medium and the washing medium was subsequently replaced with 100 µl fresh protein dilution. Each protein mixture including all buffer and recombinant protein controls contained 17.5% v/v chromatography buffer.

For experiments assessing adhesion to transfected CHO cells, the cells were grown to 90% confluence. On the day before the assay, the cells were detached using EDTA and seeded at a ratio of 1:1 into the slides. All solutions were warmed to 37°C in a cell culture incubator prior to their use, and the slides were not precoated.

The assay buffer was prepared as indicated in 2.1.3.6 excluding $CaCl_2$ and $MgCl_2$ and prewarmed to 37°C. Directly before use, $CaCl_2$ and $MgCl_2$ were added to a final concentration of 2 mM. Leukocytes were counted and stored at 37°C and 5% CO_2 in aliquots, each of which contained sufficient cells for the analysis of two samples, so that the cell suspension was renewed in every other sample. Before the analysis, leukocytes were centrifuged for 5 min at 250 x g (rt) and resuspended in assay buffer to yield a concentration of 2×10^5, 2.6×10^5 or 3×10^5 cells/ml for DS4 cells, YT cells and murine NK cells, respectively. Subsequently, the cells were transferred into a water bath to keep the cell suspension at 37°C throughout the experiment. The respective slide was transferred to an incubation chamber which was kept at 37°C and which could be mounted on the stage of an inverted phase contrast microscope equipped with a digital video camera. Pyrogen-free perfusion tubing was used to connect the flow channel on one side with the cell suspension or assay buffer (using a 3-way stop cock) and on the other side with a 50 ml syringe that was operated by a programmable syringe pump, so that fluid could be drawn through the slide at a defined flow rate. Each slide was first flushed with assay buffer at 1 ml/min for about 1 min until all cell debris had been removed. To allow comparisons between the slides, observation areas in all slides were determined to be at least 1 cm away from the inlet and outlet of the channel and as close as possible to the diagonal middle of the slide (at least 0.5 mm away from the channel´s side walls). Subsequently, the medium was switched to cell suspension using the 3-way stop cock and the cells were flushed into the slide until it appeared homogenously perfused. Afterwards, the flow rate was lowered to the rate that would yield the desired shear stress (indicated in each figure) and the interactions were recorded for 5 min. Before the next slide was mounted, the system was flushed with assay buffer.

2.2.5.4.3 Data evaluation

The recorded videos were used to determine the number of leukocytes in the respective field of view displaying rolling or tight adhesion. The analysis was performed manually by splitting the field of view into eight sections and assessing the events in each of the sections. For the analysis, the following rules were applied:

- Tight adhesion was defined as an event where the leukocyte did not move further than one cell diameter within 30 sec.
- Rolling adhesion was defined as an event where the leukocyte was abruptly stopped from the flow, but did not reach tight adhesion or detached again from the substrate.
- Each cell that passed the entire field of view was counted only once.
- Each cell was counted either as rollingly or tightly adherent. If the cell displayed both forms of adhesion, it was counted as tightly adherent.
- Only such cells were counted that were stopped from the flow within the observation period, not such that were already adherent to the substrate at the beginning of the observation.

The obtained numbers were subsequently converted into adhesive events per 5 min per mm^2.

2.2.5.4.4 Contributions

Laminar flow assays involving primary microvascular endothelial cells in combination with YT cells or primary murine NK cells were performed in collaboration with R. Djafarzadeh. She performed seeding of the endothelial cells into the microscope slides as well as treatment of the endothelial cells with the various proteins, while N. Münchmeier performed the adhesion experiments and evaluated the data. Primary murine NK cells were provided by J. Pötzl (Helmholtz Zentrum Munich), who isolated them freshly for each assay from spleens of C57/Bl6 mice using magnetic beads.

2.2.5.5 Chromium release assays

The effect of CXCL10-mucin-GPI on target cell lysis by human NK cells was evaluated using chromium release assays.

2.2.5.5.1 Preparation of target cells:

Two different target cell lines were tested: RCC26, a human renal cell carcinoma line and K562, an erythroleukemia line (both provided freshly for each experiment by Prof. Noessner, Helmholtz Zentrum Munich). The target cells were harvested, washed with PBS and resuspended in 100 µl FCS. Cells were labeled with 50 µCi $Na_2{}^{51}CrO_4$ for 1.5 h at 37°C and 5% CO_2. Subsequently, the cells were washed once with RPMI 1640 medium + 15% FCS and once with RPMI 1640, counted and resuspended at 4 x 10^6 cells/ml in CXCL10-mucin-GPI protein that had been diluted in RPMI 1640 to 240 pM. As controls, additional aliquots of labeled cells were resuspended in RPMI 1640 medium containing either 14 nM recombinant CXCL10 or chromatography buffer only. All mixtures contained

25% v/v chromatography buffer to exclude buffer artifacts. The cells were incubated for 1 h at 37°C and 5% CO_2, washed twice with RPMI 1640 + 15% FCS and counted again. Afterwards, the prepared target cells were resuspended in RPMI 1640 + 15% FCS (4 x 10^4 cells/ml) and 50 µl cell suspension per well (2000 cells) were added to the effector cells (see below). To assess the maximal possible signal (100% lysis), 50 µl of the differently treated target cells were pipetted directly onto the 96 well Scintillant coated plate.

2.2.5.5.2 Preparation of effector NK cells:

Human NK cells were isolated from peripheral blood mononuclear cells (PBMCs). Peripheral blood (heparinized) was mixed with an equal volume of RPMI 1640 and 15 ml aliquots were layered above 35 ml Ficoll solution. The mixture was centrifuged for 20 min at 840 x g (rt) and the interphase containing mononuclear cells was collected. For washing, the cells were mixed with RPMI 1640 and centrifuged for 12 min at 758 x g (rt), and the supernatant was removed. The washing step was repeated with a 5 min centrifugation step at 302 x g (rt). To remove thrombocytes, the cells were resuspended in isolation buffer from the kit mentioned below, centrifuged for 12 min at 210 x g (4°C) and the supernatant was removed. This step was repeated once. NK cells were subsequently isolated from the PBMCs using a commercially available kit that allowed untouched isolation of the cells with magnetic beads. The kit was used according to the manufacturer´s instructions.

Experiments were done either with freshly isolated NK cells or NK cells that had been activated over night in AIM-V medium containing 10% human serum and 500 U/ml recombinant human IL-2. In both cases, the NK cells were resuspended in RPMI 1640 + 15% FCS and 50 µl of the suspension were diluted in 1:2 steps in a V-bottom 96 well plate to yield various effector:target ratios (the amount of target cells per well was kept constant at 2000 cells/well). Effector:target ratios of 10:1 to 0.3125:1 were used for K562 and ratios of 40:1 to 1.25:1 for RCC26 target cells. All samples were run in duplicates. To assess spontaneous release of ^{51}Cr from the target cells, 2 additional wells for each target were prepared that contained only RPMI 1640 + 15% FCS and no effector cells. Afterwards, the labeled target cells were added (see above).

2.2.5.5.3 Killing assay:

After the target and effector cells had been mixed, the plate was incubated for 4 h at 37°C and 5% CO_2. Subsequently, 50 µl of the supernatant of each well were pipetted onto a 96 well Scintillant coated plate, which was dried in a fume hood over night. The plate was sealed with adhesive foil and the radiation in each well was measured in a Scintillation counter. For data evaluation, first the counts per minute (cpm) of the wells where the target cells had directly been pipetted into the Scintillant coated plate were divided by 2 to allow comparison with the other wells where the target cells had always been diluted 1:2 with effector cells. This yielded the value for maximum release (100% lysis). The cpm of the wells in which target cells had been mixed with medium only

(spontaneous release = 0% lysis) were subtracted from the cpm of every other well to compensate for spontaneous release of ^{51}Cr. The percentage of lysis could then be calculated by dividing the values of each well by the value for maximum release. The calculation is summarized in the formula below:

$$Lysis\ [\%] = \frac{(specific\ release\ in\ the\ respective\ sample) - (spontaneous\ release)}{(maximum\ release) - (spontaneous\ release)} * 100$$

2.2.6 *In vivo* experiments

In order to test if CXCL10-mucin-GPI is able to recruit leukocytes in a physiologic setting, *in vivo* experiments were performed using subcutaneously implantable tumors in C57/Bl6 mice. These experiments were performed in collaboration with the group of Prof. Mocikat, Helmholtz Zentrum Munich. Culturing and injection of tumor cells as well as protein injections and resection of tumors was performed by L. Bankel from this group. The experiments were conducted in accordance with animal protection regulations and approved by the responsible authorities.

2.2.6.1 The 291 tumor model and protein injection protocols

2.2.6.1.1 Background

Because of the relative ease and speed, a subcutaneous tumor model was chosen for proof-of-concept experiments. Murine 291 cells were used to implant tumors. These B cell lymphoma cells had previously been isolated from a C57/Bl6 mouse carrying the c-myc oncogene under the control of the Igλ promoter. Such mice spontaneously develop B cell lymphomas (Kovalchuk et al. 2000).

2.2.6.1.2 Experimental details

Only female mice at an age between 11 and 21 weeks were used for experiments. The experiment presented in 3.7 was performed with 11 weeks old mice. 10^7 291 cells in 150 µl PBS were injected subcutaneously into each flank of the mice, each mouse thus receiving 2 tumor injections. Tumor growth was monitored by palpation and the experiments were conducted once the tumors had reached a diameter of about 8 mm. Purified GPI-anchored proteins or respective controls diluted in PBS + 0.025% Triton X-100h were prepared and 50 µl were injected into the center of each tumor. Three separate tumors were treated with each protein or control. It was taken care that the different samples were equally distributed over larger and smaller tumors. After 4 h, mice were sacrificed and the tumors were removed. For analysis, the tumors were cut in half, and one half was subjected to FACS analysis, while the other half was fixed for 24 h in 10% neutral buffered formalin for histology.

2.2.6.2 FACS analysis of the tumors

To analyze infiltrating leukocytes, FACS analysis was performed using CD3, CD4, CD8, NK1.1 and CXCR3 specific antibodies. To this end, the tumors were mechanically minced, washed in PBS, filtered through a nylon mesh and subjected to FACS analysis, which was performed by L. Bankel.

2.2.6.3 Histology of tumor sections

Fixed tumors were dehydrated with an automatic tissue-processor using a series of 70% ethanol for 5 h, 96% ethanol for 2 h, 100% ethanol for 3.5 h, xylene for 2.5 h and paraffin for 4 h. Paraffin blocks were prepared using liquid paraffin. After cooling, 2 µm sections were cut from these blocks using a microtome and mounted on glass slides. Deparaffinisation and rehydration was performed by incubating the slides 3 x 5 min in xylene, 3 x in 100%, 2 x in 96%, and once in 70% ethanol (3 min each).

2.2.6.3.1 Immunohistochemistry

Immunohistochemical staining was performed to detect $CD3^+$ and $NKp46^+$ cells in the tumors. Before the first and in between all incubation steps, the slides were washed with PBS. Endogenous peroxidase activity was blocked by incubating the slides in 3% hydrogen peroxide in methanol for 20 min in the dark. Antigen retrieval was performed using antigen unmasking solution in an autoclave oven for 20 min (CD3 staining) or 50 µg/ml proteinase K for 10 min at room temperature (NKp46 staining).

Endogenous biotin was blocked using a commercially available Avidin/Biotin blocking kit. Subsequently, the slides were incubated with CD3-specific antibodies (10 µg/ml, diluted in PBS, for 1 h at rt), NKp46-specific antibodies (10 µg/ml, diluted in 10% skimmed milk powder in PBS, for 1 h at rt) or respective controls. Following incubation with biotinylated secondary antibodies (5 µg/ml in PBS) for 30 min, a commercially available kit was used to detect bound antibodies (*Vectastain*) according to the manufacturer´s instructions. 3,3´-Diaminobenzidine (3 mM) was used as substrate diluted in Tris/HCl, pH 7.7 in combination with $NiCl_2$ (1.7 mM) and H_2O_2 (0.075 ‰) resulting in a black coloured staining. Slides were counter stained using methyl green and washed using 2 x 96% and 3 x 100% ethanol followed by xylol. *Vectamount* mounting medium was used to mount the slides.

2.2.6.3.2 Hematoxylin/ Eosin Y (H/E) staining

H/E staining was performed to assess the general morphology of the tumor tissue. Following deparaffinisation, the slides were washed using distilled water, stained for 5 min in Harris modified hematoxylin solution, washed for 5 min in tab water for bluing, incubated in 70% ethanol for 2 min and in eosin Y solution for 30 sec. Subsequently, the slides were washed once in 70%, twice in 96% and 3 times in 100% ethanol, followed by xylol and mounted using *Vectamount* mounting medium.

3 Results

3.1 Cloning and expression of the recombinant fusion proteins

A novel class of protein reagents designed to modulate tissue micromilieus was developed in this study. The work focused primarily on one example as proof of concept: CXCL10-mucin-GPI – a fusion protein consisting of a CXCL10 chemokine head, fused to the mucin domain taken from CX3CL1, and a C-terminal GPI anchor signal sequence substituting for the transmembrane domain of CX3CL1. Based on the biology of CXCL10, this reagent should allow the selective recruitment of cytotoxic $CXCR3^+$ leukocytes into solid tumors. In parallel, a series of constructs were generated to act as controls: CXCL10-GPI, identical to CXCL10-mucin-GPI but lacking the mucin domain, should serve as a control for effects mediated by this domain. A membrane-bound, GPI-anchored EGFP protein was constructed to act as a GPI-anchored negative control protein lacking any obvious function in leukocyte recruitment. In addition, soluble versions of both CXCL10 fusion proteins (CXCL10-Stop and CXCL10-mucin-Stop) were designed as controls for the GPI anchor.

3.1.1 Cloning of the recombinant fusion genes

The fusion constructs were cloned as described in 2.2.3 and the respective compositions are summarized in Figure 9 A. Briefly, the GPI anchor signal sequence from LFA-3 had been previously cloned from a human inflamed kidney cDNA sample and inserted into a pUC19 plasmid (Notohamiprodjo et al. 2006). The DNA sequence encoding the double c-myc epitope tag that was used to facilitate purification and detection strategies was amplified by PCR from the MP71 gp100 vector and inserted into the pUC19 plasmid, 5´ of the GPI signal sequence. Subsequently, the coding sequence of human CXCL10 was ligated in-frame into the plasmid, 5´ of the double c-myc tag and the GPI anchor signal sequence. The resulting construct termed CXCL10-GPI was subcloned into a pEF_{dhfr} vector for expression in dihydrofolate reductase deficient Chinese hamster ovary ($CHO^{dhfr-/-}$) cells.

The CXCL10 gene was then further subcloned into a pEF_{dhfr} plasmid containing the mucin domain of CX3CL1, which had been amplified from a human inflamed kidney cDNA sample, a double c-myc tag and the GPI signal sequence from LFA-3. In the resulting construct termed CXCL10-mucin-GPI, the CXCL10 gene thus directly preceded the mucin domain sequence, followed by the c-myc tag and the GPI anchor signal sequence.

In addition to the genes for the surface anchored proteins, constructs were generated in which the GPI signal sequence was replaced by a stop codon. The resulting CXCL10-Stop and CXCL10-mucin-Stop proteins were expected to be secreted into the supernatant and should serve as non-anchored control proteins.

Finally, the sEGFP-GPI construct was created to act as a GPI-anchored control protein. It was generated by fusing the secretion signal sequence of human TIMP-1 N-terminally (5´) to the gene sequence of EGFP followed by a double c-myc tag and the GPI signal sequence from LFA-3. Figure 9 shows a schematic overview of the various recombinant genes (A) as well as an electrophoretic analysis of the respective plasmids (B). For this analysis, all pEF-plasmids were digested with *Eco*RI and *Sal*I and the resulting fragments were separated in a 1% agarose gel.

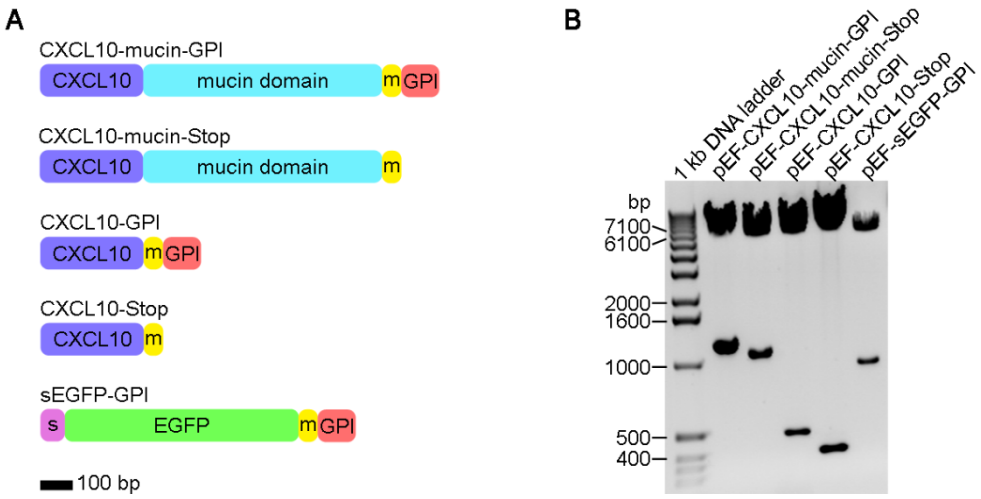

Figure 9: The recombinant CXCL10 and EGFP fusion genes display the anticipated lengths. A: Schematic overview of the different recombinant genes that were cloned in the present study. The scale indicates a length of 100 bp. Abbreviations: s = secretion signal sequence of TIMP-1; m = double c-myc epitope tag. **B:** Electrophoretic analysis of the various recombinant genes. 200 ng of pEF-CXCL10-mucin-GPI, pEF-CXCL10-mucin-Stop, pEF-CXCL10-GPI, pEF-sEGFP-GPI or 600 ng of pEF-CXCL10-Stop were digested with *Eco*RI and *Sal*I to cut out the entire coding sequences and the fragments were separated in a 1% agarose gel. DNA bands were visualized under UV light using ethidium bromide staining. An inverted image of the resulting gel is shown to visualize the different sizes of the recombinant constructs.

As seen in the electrophoretic analysis, the CXCL10-GPI construct was 500 bp long, 317 of which constituted the CXCL10 chemokine domain at the 5´ end. The c-myc tag accounted for the following 66 bp, and the GPI anchor signal sequence for the last 117 bp. CXCL10-mucin-GPI had a total length of 1235 bp with the mucin domain, located between CXCL10 and the c-myc tag, accounting for the additional 735 bp (245 amino acids) compared to CXCL10-GPI and thus forming the biggest part of the resulting protein. The soluble constructs CXCL10-Stop and CXCL10-mucin-Stop were both 112 bp shorter than their GPI-anchored counterparts due to the lack of the GPI-anchor signal sequence resulting in total lengths of 388 and 1123 bp, respectively. The sEGFP-GPI gene sequence had a total length of 978 bp. The first 75 bp of the gene encoded the secretion signal sequence of TIMP-1, followed by the 720 bp long EGFP sequence and again 66 bp for the c-myc tag and 117 bp for the GPI anchor sequence. The exact DNA sequences of all constructs can be found in 5.7.

3.1.2 Expression and detection of the recombinant fusion proteins

Chinese hamster ovary (CHO) cells were chosen for the expression of the recombinant proteins for two reasons: First, only eukaryotic cells are capable of attaching GPI anchors to proteins, which precluded the use of bacterial expression systems. Second, a mammalian cell line was chosen in order to keep the glycosylation pattern of the mucin domain similar to that found on human proteins. All plasmids were linearized prior to transfection and dihydrofolate reductase (dhfr)-deficient CHO cells that are auxotrophic for hypoxanthine and thymidine were transfected by electroporation as described in 2.2.2.14. The dhfr gene in the pEF_{dhfr} plasmids enabled the selection of successfully transfected cells on the basis of its ability to complement the auxotrophy of $CHO^{dhfr-/-}$ cells. Dialyzed serum devoid of nucleotides was therefore used in the medium to generate selective pressure. The transfected CHO-CXCL10-GPI and CHO-CXCL10-mucin-GPI cells were subsequently additionally treated with methotrexate, an inhibitor of the dihydrofolate reductase, to eliminate cells with a low expression level as described in 2.2.2.14. By means of this treatment, cells with a low expression level of the transgenes could be eliminated, as evidenced by the loss of a moderately positive population in FACS staining (data not shown).

3.1.2.1 Subunits of the GPI-anchored fusion proteins can be detected on transfected CHO cells

FACS staining was performed to evaluate the expression of the recombinant fusion proteins in transfected CHO cells. To this end, the cells were stained with antibodies specific for the c-myc epitope tag, the CX3CL1 mucin domain or CXCL10 and subsequently analyzed by flow cytometry as described in 2.2.5.1.1. Figure 10 shows the results of a representative FACS staining.

As shown in the figure, the GPI-anchored CXCL10 fusion proteins could readily be detected on the surface of the transfected cells. As expected, both CHO-CXCL10-GPI and CHO-CXCL10-mucin-GPI cells stained positively for the c-myc epitope tag and the CXCL10 chemokine head, while only CHO-CXCL10-mucin-GPI cells stained positively also for the mucin domain. The cells that had been transfected with the soluble CXCL10-mucin-Stop construct could not be stained with any of the antibodies, indicating that this fusion protein was (due to the lack of a GPI anchor) secreted into the medium, where it could also be detected by western blotting (data not shown). The same was found for CXCL10-Stop transfected cells, suggesting that fusion proteins lacking a GPI anchor did not bind nonspecifically to the CHO cells (data not shown). On CHO-sEGFP-GPI cells, the c-myc epitope tag could be detected as well as the fluorescence of the EGFP protein, indicating that the protein structure of EGFP was not compromised by the membrane-associated expression.

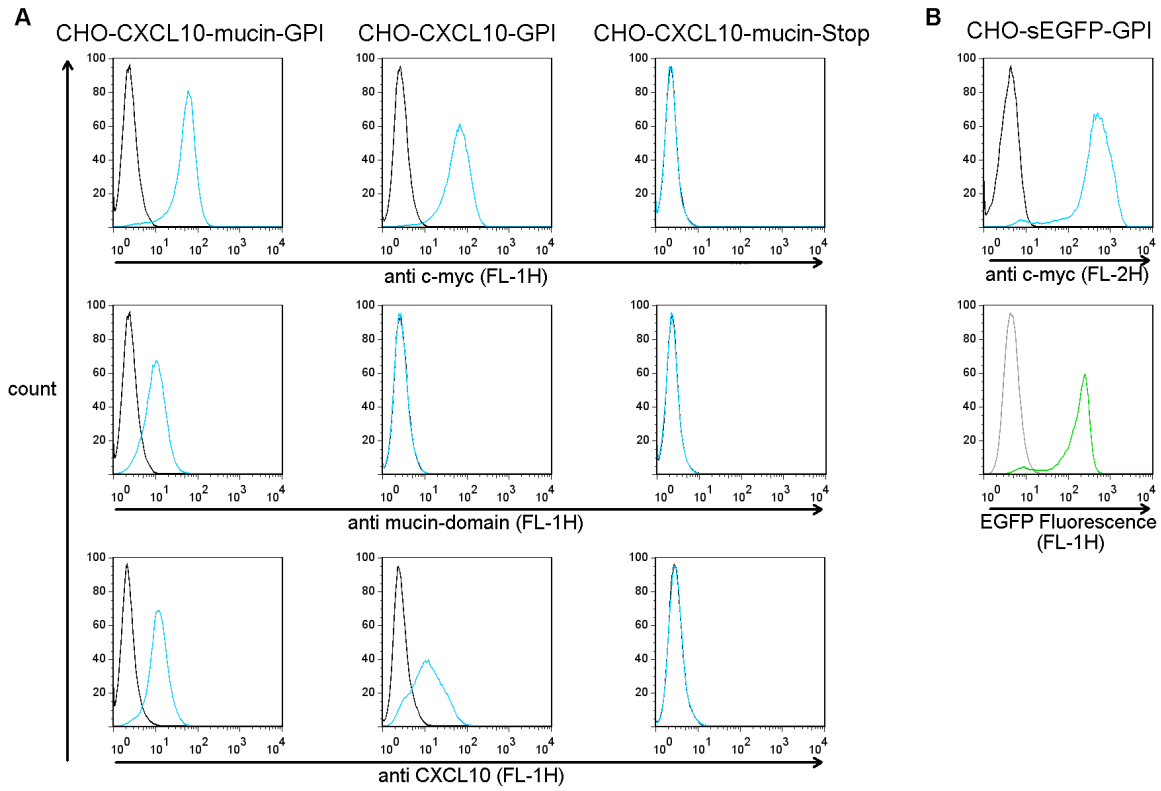

Figure 10: Subunits of the recombinant GPI-anchored proteins can be detected on the surface of transfected CHO cells. A: Stably transfected CHO cells were incubated with antibodies against the c-myc epitope tag, the mucin domain, the CXCL10 chemokine head or matching isotype controls. Bound antibodies were detected by staining with FITC-conjugated secondary antibodies and the fluorescence intensity was measured by FACS (FL-1H). Black lines indicate staining with the isotype controls, blue lines indicate staining with the specific antibodies. **B:** In the case of sEGFP-GPI transfected CHO cells, RPE-conjugated secondary antibodies were used to detect the c-myc epitope tag (anti c-myc antibodies: blue line, isotype control: black line) while the fluorescence by the EGFP-protein was measured in the FL-1 channel (FL1-H; green line) and compared to non-transfected CHO cells (grey line). All histograms are gated on viable cells identified by 7-AAD exclusion.

3.1.2.2 The GPI-anchored fusion proteins are targeted to the cell membranes of transfected cells

The FACS analysis described above demonstrated surface expression of the recombinant fusion proteins. As an additional verification of correct targeting of the proteins to the cell membrane, immunofluorescence microscopy was performed as detailed in 2.2.5.3, because this approach is able to more precisely identify the subcellular localization of the detected proteins. To this end, the cells were grown in special dishes developed for fluorescence microscopy, fixed, and subsequently stained with c-myc specific antibodies. A combination of biotinylated secondary antibodies and RPE-labeled streptavidin was used to detect bound antibodies. Figure 11 shows representative images acquired on an inverted fluorescence microscope.

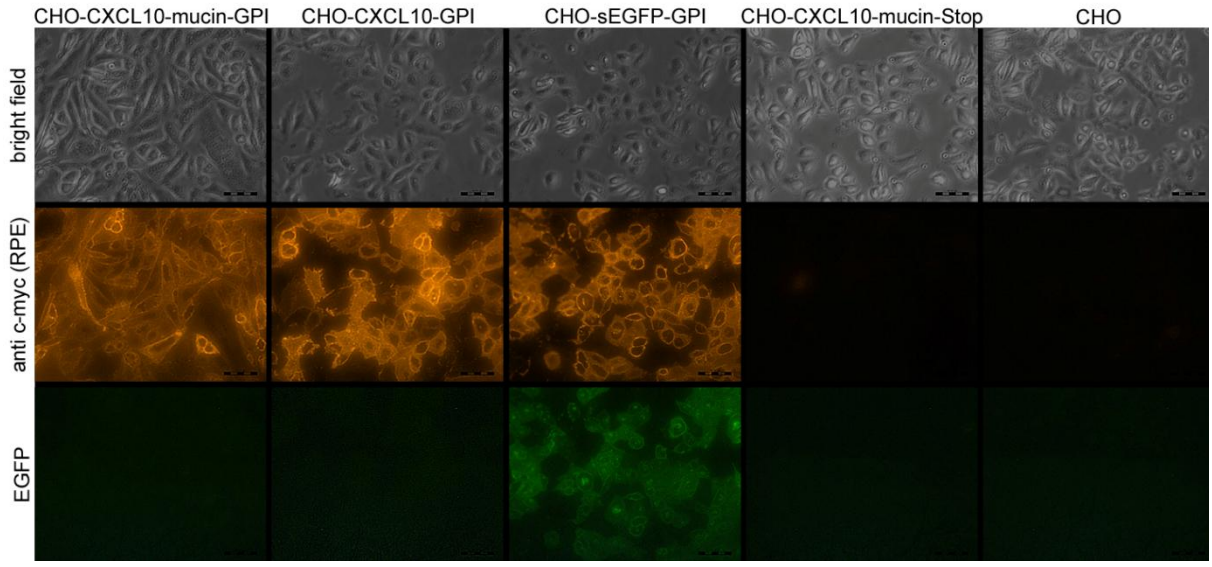

Figure 11: The recombinant GPI-anchored proteins are expressed in a membrane-associated manner. The indicated stably transfected CHO cell lines or non-transfected CHO cells (CHO) were grown in special fluorescence microscopy dishes, fixed and subsequently stained with anti c-myc primary and biotin-conjugated secondary antibodies followed by RPE-labeled streptavidin. In the case of CHO-sEGFP-GPI, the fluorescence of the EGFP protein was additionally detected using appropriate filters. All images within each horizontal row were acquired using the same exposure time. The bars in each image indicate a length of 50 µm.

For all cells transfected with GPI-anchored fusion proteins, a strong staining by the c-myc specific antibodies was observed. The signal was most pronounced at the periphery of each cell, indicating that the fusion proteins were expressed in a membrane-associated manner. In contrast, the cells transfected with the soluble CXCL10-mucin-Stop construct did not stain positively. This finding was expected as the lack of a GPI anchor in CXCL10-mucin-Stop lead to secretion of the expressed protein into the medium. An absence of surface staining was also found for non-transfected cells, showing that the signal obtained with the anti c-myc antibodies was specific. In the case of sEGFP-GPI transfected cells, the fluorescence by EGFP was additionally detected at the cell surface. In summary, these results showed that the GPI-anchored proteins had successfully been targeted to the cell membrane by the addition of a GPI anchor signal sequence.

3.1.2.3 The N-termini of the CXCL10 fusion proteins are correctly processed

The N-terminus of chemokines is vitally important for their function. Changes in the amino acid composition of the N-terminus can lead to dramatic changes in the physiologic activity of the respective chemokine. For that reason, the N-terminal amino acid sequence of one of the CHO-cell-expressed CXCL10 fusion proteins was exemplarily determined using Edman sequencing. CXCL10-mucin-Stop was analyzed because for the soluble protein it was possible to obtain protein amounts sufficient for Edman sequencing from cell culture supernatants. The analyses were conducted in collaboration with R. Mentele from the Max-Planck Institute for Biochemistry in Martinsried. CXCL10-

mucin-Stop protein purified from cell culture supernatants as detailed in 2.2.4.1.4 was subjected to SDS-PAGE and subsequently transferred onto a PVDF membrane. As control, commercially available recombinant CXCL10 that had been demonstrated to be bioactive by the manufacturer and also in our own assays (see below) was identically treated. The membrane was stained and protein bands displaying the expected sizes were cut out and subjected to the sequencing procedure.

The results showed that both recombinant conventional CXCL10 and CXCL10-mucin-Stop comprised a mixture of proteins with either the sequence V-P-L or P-L-S at the N-terminus. The V-P-L sequence corresponds to the mature N-terminus of the well-documented, naturally occurring 77 amino acid form of CXCL10, while P-L-S would correspond to a 76 amino acid form. The latter form could have originated either from imprecise cleavage of the signal sequence during the secretion process, or from post-translational proteolytic modification which might also occur during the electrophoretic procedure. Because the mixture occurred in both protein samples, with the commercial protein having been demonstrated to be bioactive, the N-terminus of CXCL10-mucin-Stop was considered to be correctly processed by the CHO cells. As all CXCL10 fusion proteins were expressed in the same cell type from the same vector and the same CXCL10 gene sequence, it was assumed that the signal sequence was also correctly cleaved in the other fusion proteins. This consideration was complemented by several bioactivity experiments that were performed later on with the GPI-anchored proteins (see 3.2, 3.6 and 3.7).

3.2 Verification of the bioactivity of the fusion proteins

The fusion of different proteins can lead to changes in their respective secondary and tertiary structures. In the case of the CXCL10 fusion proteins, such changes might alter the structure of the CXCL10 chemokine head, leading to diminished binding to CXCR3 or even to an antagonistic effect where the receptor is occupied but no intracellular signal in the target cell is elicited. To exclude these possibilities, three different tests were performed to verify CXCR3-stimulatory activity.

3.2.1 The GPI-anchored CXCL10 fusion proteins stimulate CXCR3 internalization

Following activation by a chemokine ligand, the CXCR3 receptor is rapidly internalized, degraded and later on replenished on the cell surface by *de novo* synthesis (Meiser et al. 2008). Receptor internalization also occurs with other chemokine receptors [reviewed in (Borroni et al. 2010)] and is an established assay to verify bioactivity of chemokines (Proudfoot et al. 2001; Colvin et al. 2004). To assess if the CXCL10 fusion proteins could still induce CXCR3 internalization in a surface-bound context, the $CXCR3^+$ human T cell line JB4 was incubated for 30 min with stably transfected CHO cells or soluble CXCL10 as positive control. The CXCR3 surface signal on the T cells was then determined by FACS analysis and the degree of internalization was calculated. The signal intensities found after coincubation with non-transfected CHO cells or medium were set as 100%, and the levels found in

the other samples related to them. Figure 12 depicts the relative intensities of the CXCR3 signal in the various samples.

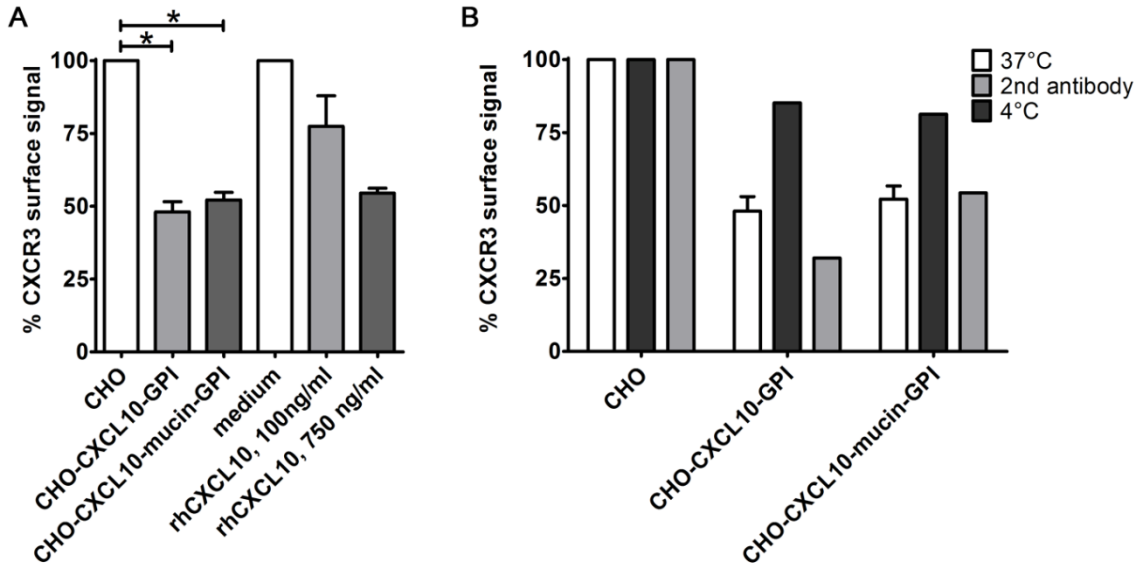

Figure 12: CXCR3 on human T cells is internalized after coincubation with cells expressing CXCL10-GPI or CXCL10-mucin-GPI. A: Human JB4 T cells were incubated for 30 min at 37°C with stably transfected CHO cells at threefold excess or commercially available soluble CXCL10 (rhCXCL10) at the indicated concentrations. The CXCR3 signal on the T cells was subsequently determined by FACS and related to the CXCR3 signal on T cells incubated with non-transfected CHO cells or medium without chemokine, respectively. Bars represent averages of two (CHO-CXCL10-GPI and 100 ng/ml rhCXCL10) or three (all other conditions) independent experiments +/- standard deviations. Statistical significance was calculated using the Kruskal-Wallis test (P = 0.0167), followed by Dunn´s post test; * = P<0.05. 100 ng/ml rhCXCL10 = 11 nM; 750 ng/ml rhCXCL10 = 86 nM. **B:** As additional controls, either the coincubation was performed at 4°C (black bars) in order to slow down cellular metabolism or different CXCR3-specific antibodies from a second supplier (R&D Systems; grey bars) were used for the CXCR3 detection. Control experiments were performed once.

A significant decrease of CXCR3 surface staining was found on the T cells after coincubation with CHO-CXCL10-GPI or CHO-CXCL10-mucin-GPI cells as seen in panel A. The signal was reduced to about 50% of the values found after coincubation with non-transfected CHO cells. A similar degree of internalization was observed when the T cells were incubated with 750 ng/ml (86 nM) commercially available soluble CXCL10. This finding indicated that the surface-bound GPI-anchored CXCL10 fusion proteins could induce internalization of CXCR3. To exclude the possibility that the decrease in signal intensity was due to occupation of CXCR3 by CXCL10 leading to decreased accessibility of the epitope for the detection antibody, additional experiments were performed as depicted in panel B. First, the coincubation was performed at 4°C instead of 37°C in order to slow down cellular activity. This lead to a much attenuated CXCR3 internalization, consistent with the observation that receptor internalization is an active process that is slowed with decreasing temperature. Second, different antibodies were used for the detection of CXCR3, which yielded the same results as the first antibodies.

Interestingly, pertussis toxin, a bacterial toxin that is often used to inhibit the signaling of G-protein coupled receptors, was not able to inhibit the internalization process (data not shown) – a finding that has also been reported in other studies (Sauty et al. 2001) and will be discussed in 4.2 in more detail.

Taken together, the experiments demonstrated that the GPI-anchored CXCL10 fusion proteins were able to induce internalization of the CXCR3 receptor, which served as the first indication that the proteins are bioactive.

3.2.2 The GPI-anchored CXCL10 fusion proteins induce calcium mobilization

The signaling cascade triggered by activated chemokine receptors also includes the release of calcium from the endoplasmatic reticulum (ER) as a reaction to the second messenger inositol 1,4,5-trisphosphate (IP3). A transient rise in the cytoplasmic calcium concentration is frequently used to monitor chemokine receptor activation and the initiation of downstream signaling (Proudfoot et al. 2001). To test if the GPI-anchored CXCL10 fusion proteins could trigger calcium mobilization in $CXCR3^+$ cells, additional coincubation experiments were performed. Cells of the human T cell line JB4 were loaded with Fluo-4, a dye that exhibits a strongly increased fluorescence in the calcium-bound state as compared to the unbound state. The “loaded” cells were then incubated with a twofold excess of stably transfected CHO cells at 37°C in a multiwell plate and fluorescence readings were taken at regular intervals. For normalization against the background fluorescence, readings obtained from coincubation with non-transfected CHO cells were subtracted from the readings obtained with the transfected cells. Commercially available soluble CXCL10 was used in separate wells as positive control for the loading procedure and the function of the Fluo-4 dye (data not shown). Before the experiment, the transfected CHO cells were assayed for the expression levels of the recombinant fusion proteins by FACS analysis and found to express the proteins at similar levels (data not shown). Figure 13 shows a representative example of the development of the normalized fluorescence intensities over time.

During the coincubation time of 40 min, a transient increase of the fluorescence intensities could be observed. This increase was presumably due to calcium being released from the ER in the T cells as a result of chemokine receptor triggering. The relatively long period of 40 min, over the course of which the increased fluorescence was observed, may have resulted from single contacts between T cells and CHO cells - each resulting in short-lived calcium mobilizations - until eventually all T cells had been desensitized for CXCL10. Interestingly, CHO cells transfected with CXCL10-mucin-GPI induced a much faster and stronger calcium response than cells transfected with CXCL10-GPI. It is possible that the mucin domain facilitated the interaction of the chemokine head with CXCR3 on T cells by presenting the chemokine domain away from the cell surface. This facilitated interaction may then have lead to a faster and stronger response in the cell population as will be discussed in 4.2.

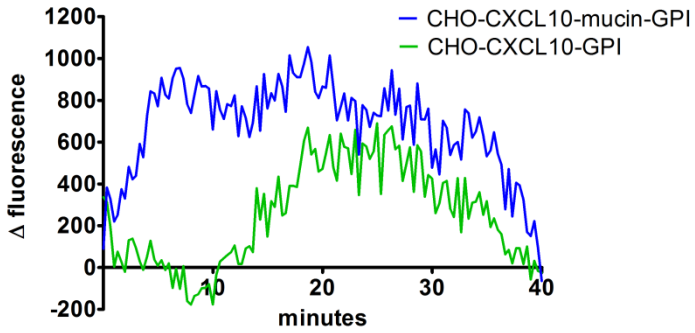

Figure 13: Coincubation with CHO cells expressing CXCL10-GPI or CXCL10-mucin-GPI leads to calcium mobilization in CXCR3$^+$ T cells. JB4 T cells were loaded with the cytoplasmic calcium-sensitive fluorescent dye Fluo-4, which displays a much increased fluorescence in the calcium-bound state. Subsequently, the cells were coincubated with a twofold excess of transfected CHO cells at 37°C and the fluorescence was measured. The curves show the fluorescence (arbitrary units) in the samples incubated with the indicated CHO cell lines, each normalized against the fluorescence values obtained from coincubation with non-transfected CHO cells. Data represent averages of duplicates.

In summary the data showed that the GPI-anchored CXCL10 fusion proteins were able to induce calcium mobilization in CXCR3$^+$ T cells, supporting the conclusion that the proteins were bioactive.

3.2.3 The GPI-anchored CXCL10 fusion proteins stimulate T cell adhesion

One of the central functions of chemokines is the regulation of leukocyte adhesion in the process of recruitment. Here, chemokines bound to glycosaminoglycan molecules are presented to leukocytes rolling along the vessel wall. Recognition of those chemokines via chemokine receptors leads to a so called inside-out signaling cascade which results in activation of the leukocyte´s integrin molecules. This leads to an enhanced ability of the respective leukocyte to adhere to its substrate, e.g. the endothelium of a blood vessel. This type of adhesion can be monitored and quantified *in vitro* by laminar flow assays that allow the application of precisely defined shear stresses on the adhering leukocytes (see 2.2.5.4 and 3.6 for more details). In this study, assessing the effect of the recombinant GPI-anchored CXCL10 fusion proteins on the ability of CXCR3$^+$ T cells to adhere to a cell monolayer should serve as a third indicator of bioactivity. Transfected CHO cells were grown to confluence in channels with defined geometry. Subsequently, cells of the CXCR3$^+$ human T cell line DS4 were drawn into the channel and left to adhere for 5 min under static conditions. Afterwards, the cells were subjected to a physiologic shear stress (1 dyn/cm^2). The detachment of the T cells was monitored by video microscopy and cells that were still adherent after 2 min of flow were counted. Figure 14 shows the averaged results of three independent experiments.

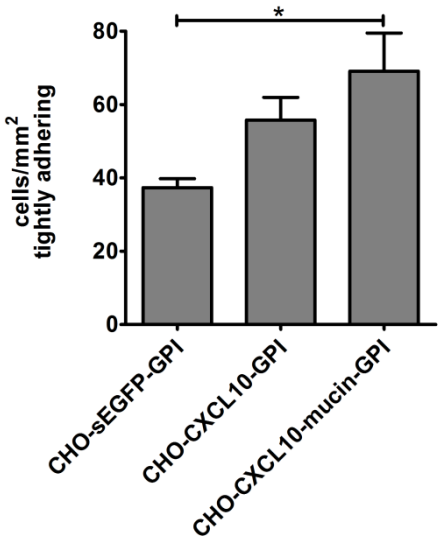

Figure 14: Adhesion of CXCR3$^+$ T cells is stimulated by contact with the GPI-anchored CXCL10 fusion proteins. CHO cells transfected with CXCL10-GPI, CXCL10-mucin-GPI or sEGFP-GPI as control were grown to confluence in channels with defined geometry. On the day of the assay, DS4 T cells were drawn into the channel, left to adhere for 5 min under static conditions and subsequently subjected to a shear stress of 1 dyn/cm^2. T cells that were still adherent after 2 min of flow were counted and the results were expressed as cells/mm^2. The bars represent averages from three independent experiments +/- standard deviations. Statistical significance was calculated using the Kruskal-Wallis-test (P = 0.039) followed by Dunn´s post test; * = P<0.05.

Significantly more T cells adhered in a shear-resistant manner to CHO cells expressing CXCL10-mucin-GPI (on average 69 cells/mm^2) than to CHO-sEGFP-GPI cells that were used as negative control (on average 37 cells/mm^2). Thus, the recombinant CXCL10-mucin-GPI protein expressed on the CHO cells enabled the T cells to more efficiently adhere to the CHO cell monolayer. On average 56 cells/mm^2 remained adherent to CHO cells expressing CXCL10-GPI. This observation indicated a positive trend also for the protein lacking the mucin domain, which was however not statistically significant.

The mucin domain of CX3CL1 has been demonstrated to mediate capture of leukocytes under flow conditions. Thus, it was hypothesized that CXCL10-mucin-GPI could, in contrast to CXCL10-GPI, be able to bind freely flowing T cells under conditions of continuous flow. To test for this hypothesis, DS4 T cells were continuously drawn over the CHO cell monolayer at a subphysiologic shear stress (0.5 dyn/cm^2) and the number of cells that adhered tightly was quantified using video microscopy. Figure 15 summarizes the averaged results of three independent experiments. The results indicated a trend towards the CHO cells carrying CXCL10-mucin-GPI on their surface being able to recruit more T cells (on average 13 cells/cm^2) under flow conditions than the CHO cells expressing either CXCL10-GPI or sEGFP-GPI (on average 8 cells/mm^2 for both proteins).

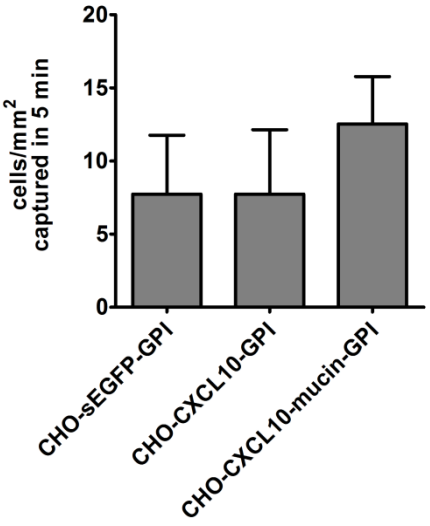

Figure 15: CXCL10-mucin-GPI expressed on CHO cells shows a trend towards being able to bind CXCR3$^+$ T cells under flow. CHO cells were grown in channels with defined geometry as detailed in the legend of Figure 14. Subsequently, DS4 T cells were perfused over the CHO cell monolayer at 0.5 dyn/cm^2 and the interactions were monitored by video microscopy over the course of 5 min. Only such T cells were counted that tightly adhered to the CHO cell monolayer for at least 30 sec. The bars represent averages from three independent experiments +/- standard deviations. Differences between the mean ranks of different samples were not statistically significant as assessed by the Kruskal-Wallis test.

These results contrast those of the assay depicted in Figure 14 where the T cells were allowed to adhere under static conditions, and in which also CXCL10-GPI showed a positive trend. This discrepancy might indicate an important role for the mucin domain in mediating adhesion under conditions of flow. However, the differences observed in this experiment were not statistically significant, and the cell numbers were generally relatively low, therefore not allowing definitive interpretations. On the other hand, the transfer of these results to the context of leukocyte recruitment in a blood vessel is very difficult as the experiments were performed using CHO cells. The extracellular composition of these cells including integrin ligands is presumably profoundly different from endothelial cells, with the latter cell type being designed to allow efficient recruitment of leukocytes from the blood stream.

Taken together, the conclusion that could be drawn from the experiments detailed above was that the recombinant GPI-anchored CXCL10 fusion proteins were able to activate CXCR3$^+$ T cells leading to enhanced adhesion to cell monolayers. This again indicated that the proteins were bioactive. Thus, having demonstrated bioactivity, a purification protocol for the recombinant proteins had to be established in order to be able to test their bioactivity in the intended setting of “painted” primary endothelial cells, which will be detailed below.

3.3 Dodecyl-maltoside can efficiently solubilize the GPI-anchored fusion proteins

Prior to their purification, the recombinant GPI-anchored proteins had to be solubilized from the cell membranes of transfected CHO cells. In the process of solubilization, the cell membrane lipids are replaced with detergent molecules resulting in the membrane proteins being embedded with their hydrophobic parts in detergent micelles. These micelle-bound proteins can then be purified using conventional methods. The choice of detergent plays an important role in the purification process as a too strong detergent may disrupt the protein´s secondary or tertiary structure, while using too weak a detergent could result in incomplete solubilization and thereby loss of protein.

A panel of different detergents was established based on two characteristics: The detergents had to be available in ultra-pure form to avoid contaminations, e.g. with pyrogens, and only nonionic detergents known to be “gentle”, i.e. to solubilize proteins in their native state, were included. To test the different detergents, a modified ELISA protocol was established [based on (Bumgarner et al. 2005)] as described in 2.2.4.3.2. Briefly, the proteins were labeled with anti c-myc primary and horse radish peroxidase (HRP)-conjugated secondary antibodies prior to solubilization. Subsequently, the cells were treated with lysis buffers containing the various detergents. An aliquot of each cell lysate was centrifuged to remove debris and non-solubilized proteins. The HRP signal in the supernatant was then related to the signal in the uncentrifuged sample and expressed as percent solubilization. Figure 16 shows the averaged results of at least two independent experiments for CXCL10-GPI and CXCL10-mucin-GPI.

The experiments showed that n-Dodecyl-β-D-maltoside (DDM) was most potent at solubilizing the CXCL10 fusion proteins. With this detergent, solubilization rates of over 90% at the given cell concentration of 10^7 cells/ml could be reached. The efficiency of DDM ranged between 86% and (calculatively) 101% solubilization for CXCL10-GPI and between 92% and 104% for CXCL10-mucin-GPI, depending on the respective detergent concentration. A related detergent, n-Octyl-β-D-glucopyranoside, was found to be the second best at solubilizing the proteins with maximum efficiencies of 84% for CXCL10-GPI and 91% for CXCL10-mucin-GPI. The efficiencies of all other detergents under study ranged below 75% solubilization. Of note, DDM was efficient over a relatively wide range of concentrations. This was in contrast to n-Octyl-β-D-glucopyranoside, the efficiency of which dropped drastically already at 15 mM to 36% for CXCL10-GPI and 51% for CXCL10-mucin-GPI. Thus, DDM appeared to be a robust reagent for the intended purpose.

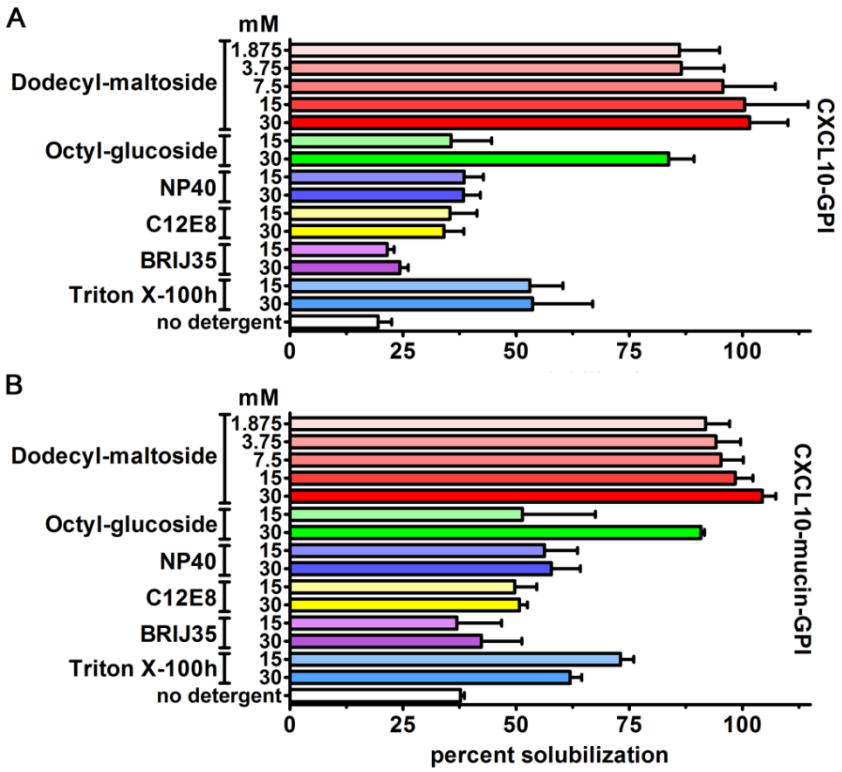

Figure 16: N-Dodecyl-β-D-maltoside is most efficient for the solubilization of the GPI-anchored CXCL10 fusion proteins. A modified ELISA variant was used to determine solubilization efficiencies of various detergents. CHO-CXCL10-GPI (**A**) or CHO-CXCL10-mucin-GPI (**B**) cells were labeled with anti c-myc primary and HRP-conjugated secondary antibodies and treated with different detergents at the indicated concentrations for 1 h. An aliquot of each extract was centrifuged to remove unsolubilized proteins and debris and the HRP signal in the supernatants was related to the signal in uncentrifuged samples. Bars represent the average values of three (CXCL10-GPI) or two (CXCL10-mucin-GPI) independent experiments +/- standard deviations. Abbreviations: Dodecyl-maltoside = n-Dodecyl-β-D-maltoside; Octyl-glucoside = n-Octyl-β-D-glucopyranoside; NP40 = Nonidet P40; C12E8 = octaethylene glycol monododecyl ether; BRIJ35 = tricosaethylene glycol ether; Triton X-100h = Triton X-100, hydrogenated.

Similar experiments were performed for the sEGFP-GPI protein by measuring the EGFP fluorescence in cell extracts and comparing the values to the fluorescence in uncentrifuged samples (data not shown). These experiments lead to virtually the same results with solubilization rates of up to 95% using DDM. This detergent was therefore found to be best suited for the solubilization of the GPI-anchored fusion proteins and was consequently used in the following experiments.

3.4 Purification of the recombinant fusion proteins by affinity chromatography

Once solubilized, the GPI-anchored proteins had to be purified in order to test their efficiency of insertion into cell membranes. Attempts to isolate the proteins by cation exchange, anion exchange, size exclusion or heparin affinity chromatography yielded unsatisfactory results as discussed in 4.3.

To help address this problem, the double c-myc epitope tag was included into all constructs directly adjacent to the GPI anchor. This tag allowed isolation of the fusion proteins from cell extracts by

affinity chromatography using a commercially available resin that contained a specially designed antibody directed against the c-myc tag.

The GPI-anchored proteins CXCL10-GPI, CXCL10-mucin-GPI or sEGFP-GPI were solubilized (see above), and non-solubilized proteins and debris were removed by centrifugation. The samples were sterile filtered and applied to the c-myc affinity resin. In cases when soluble proteins were isolated from cell culture supernatants, the supernatants were directly applied to the affinity resin. A slow flow rate was used to allow quantitative binding of the proteins. After a washing step with PBS + 145 mM NaCl to remove nonspecifically bound contaminants, the proteins were eluted using c-myc peptides in equilibration buffer. Following chromatography, all fractions were assayed for their specific protein content by western blotting and the fractions containing the highest amounts of protein were pooled. Figure 17 shows exemplary chromatograms and matching western blots for the isolation of CXCL10-GPI and CXCL10-mucin-GPI. Similar chromatograms were obtained from purifications of sEGFP-GPI.

In the western blot analysis, CXCL10-GPI appeared as a prominent band at about 10-15 kDa (see Figure 17 A). The observed band matches the molecular weight of CXCL10 plus the c-myc tag as derived from the amino acid sequence (11.6 kDa). Predicting the contribution of the GPI anchor to the apparent molecular weight is difficult as the GPI anchor structure interacts with SDS in a way much different from protein structures. (Azzouz and Capdeville 1992; Walmsley et al. 2001; O'Connor et al. 2005). Sometimes an additional band at around 20 kDa was seen for CXCL10-GPI, suggesting dimerization of the protein. Also additional bands at 30 to 40 kDa were occasionally observed (as seen in the cell extract and the flow through), which presumably contained protein oligomers. Oligomers that do not break up in SDS-PAGE are a phenomenon frequently found for chemokines in general and in particular for CXCL10 (Luster et al. 1995).

CXCL10-mucin-GPI appeared in western blots predominantly as a band at around 45-50 kDa (see Figure 17 B). The molecular weight of the CXCL10 part plus the mucin domain and the c-myc tag predicted from the amino acid sequence is 36.8 kDa. The difference between the predicted and the observed size was due to glycosylations in the mucin domain, as this domain has been demonstrated to contain around 10-20 kDa of glycosylations (Fong et al. 2000). It was therefore assumed that the 45-50 kDa band contained monomeric glycosylated CXCL10-mucin-GPI protein. A second band was often observed at around 90 kDa, which most likely contained protein dimers.

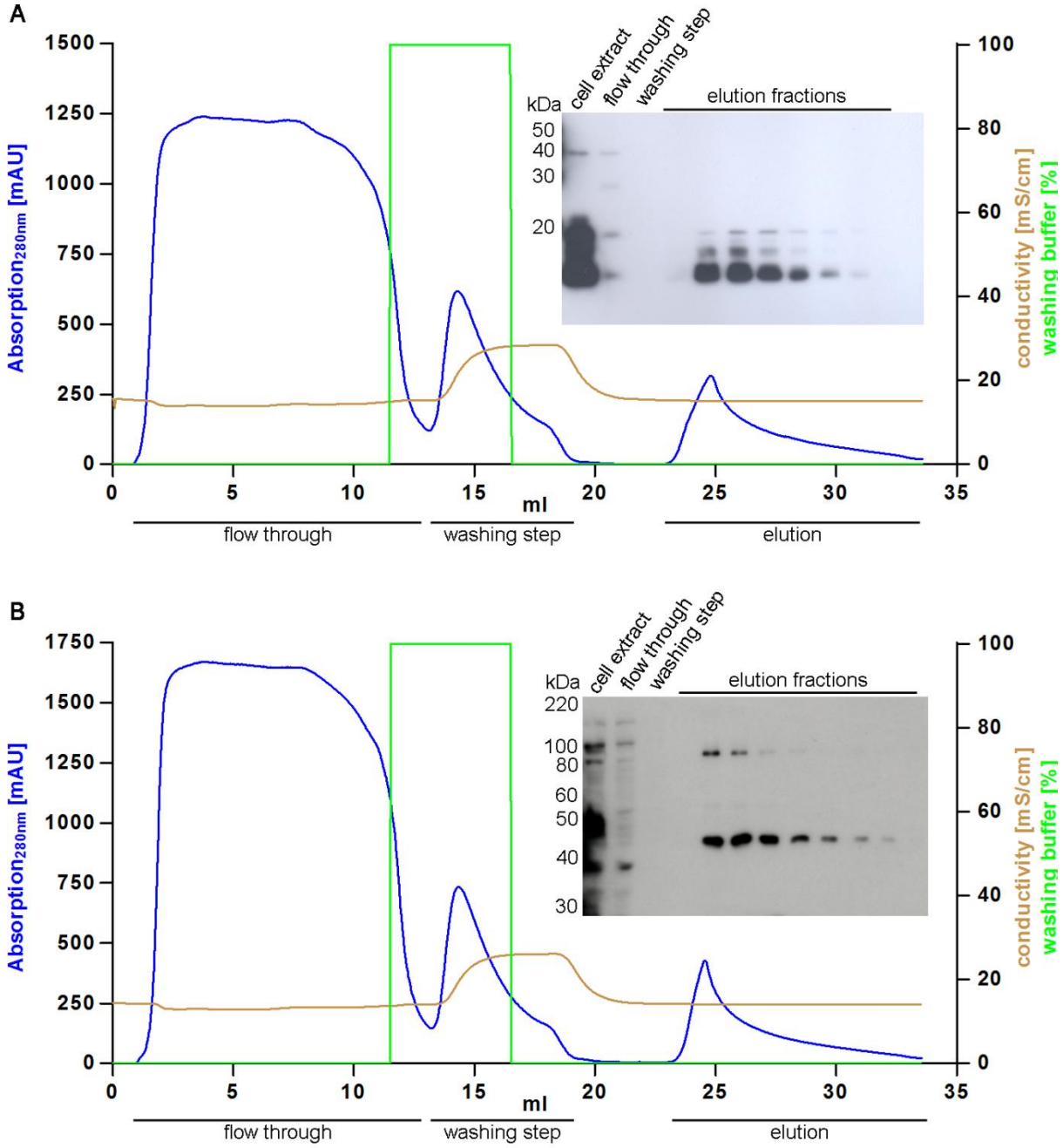

Figure 17: Solubilized CXCL10-GPI and CXCL10-mucin-GPI proteins can be purified by anti c-myc affinity chromatography. Transfected CHO cells were lysed in extraction buffer containing n-Dodecyl-β-D-maltoside. Non-solubilized proteins and debris were removed by centrifugation and the extract was applied to a commercially available resin containing immobilized anti c-myc antibodies. Representative chromatograms and matching western blots for the purifications of CXCL10-GPI (**A**) or CXCL10-mucin-GPI (**B**) are shown. The UV absorption at 280 nm (blue line) as a measure of protein concentration and the conductivity (brown line) as a measure of the salt concentration are plotted against the total volume passing through the column. The green line indicates the percentage of washing buffer being applied to the column. Following a washing step at high salt concentration, proteins were competitively eluted using c-myc peptides. Fractions were collected and assayed by western blotting for their specific protein content.

Observing the chromatograms for both CXCL10 fusion proteins, it was evident that large amounts of proteins passed through the columns without binding (flow through), while the western blots showed that the respective fractions contained only minimal amounts of CXCL10 fusion proteins. Thus, many contaminating proteins could be removed during this step. The same was true for the washing step, where significant amounts of contaminants were eluted, but no CXCL10 fusion proteins. In the elution step, a distinct protein peak was generated, the fractions of which contained the majority of the CXCL10 fusion proteins.

A commercially available CXCL10-specific sandwich ELISA was used to determine specific protein concentrations. The total protein content was additionally determined and compared to the ELISA values. On average, the percentage of the CXCL10 fusion proteins among the total proteins was about 45 times higher in the elution fractions than in the cell extracts, indicating that the respective proteins had been significantly enriched. For the sEGFP-GPI proteins, the fluorescence in the respective fractions (which correlates linearly to the EGFP concentration) was compared to the total protein content. The ratio of these values was also much increased in the elution fractions, in the same order of magnitude as found for the CXCL10 fusion proteins using the ELISA measurements. This degree of specificity and purification efficiency could in our hands not be reached with any other purification chemistry. Nevertheless, the GPI-anchored fusion proteins were not purified to homogeneity. For that reason, the sEGFP-GPI protein was used as control in functional assays, as it contained the same type and amount of contaminants as the CXCL10 fusion proteins, which was also verified using silver staining (data not shown).

In summary, sufficiently pure preparations of the GPI-anchored proteins could be obtained by c-myc affinity chromatography, which allowed further experiments assessing the functionality of the purified proteins.

3.5 Purified GPI-anchored fusion proteins incorporate into cell membranes

The GPI anchor at the C-terminus of the recombinant fusion proteins should enable them to integrate into the cell membranes of virtually any cell type when added exogenously. Experiments were performed to test this hypothesis and characterize the incorporation process using purified proteins which had been prepared as detailed above.

3.5.1 The GPI-anchored fusion proteins can be detected on the surface of treated cells

FACS staining was used to determine the presence of incorporated GPI-anchored proteins on the surface of cells that had been treated with the purified proteins. Non-transfected CHO cells were routinely used as target cells. As detailed in 2.2.5.1.2, the cells were incubated for 1 h with 0.9 nM of purified CXCL10-GPI or CXCL10-mucin-GPI or with sEGFP-GPI that had been identically purified and diluted in MEMα medium. As control for the GPI anchor, purified CXCL10-mucin-Stop protein was

used, which lacked the GPI anchor. It was applied at a higher concentration than the GPI-anchored proteins (3.9 nM) to allow potential detection of non-specific binding occuring at low affinity. Two additional samples were treated with elution buffer from the chromatographic purification of the fusion proteins, or MEM alpha medium as controls. All samples (except the medium control) contained the same percentage of chromatography buffer and detergent to exclude buffer artifacts. Following treatment, the cells were washed and subsequently stained using c-myc specific primary and RPE-labeled secondary antibodies as detailed in 2.2.5.1.1. Dead cells were identified by 7-AAD staining and excluded from the analysis. Figure 18 shows the results of a representative FACS staining.

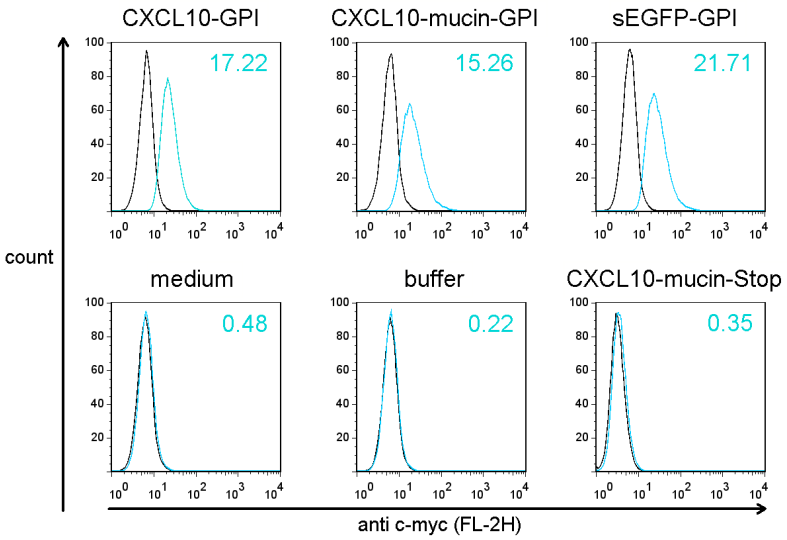

Figure 18: Purified GPI-anchored proteins incorporate into cell membranes. In order to test the capacity of the purified GPI-anchored fusion proteins to incorporate into cell membranes, non-transfected CHO cells were incubated with the proteins for 1 h at 37°C. As controls, two samples were treated either with identically diluted chromatography buffer (buffer) or MEM alpha medium (medium). The soluble CXCL10-mucin-Stop protein served as additional control because it lacked the GPI anchor and should therefore not be able to integrate into cell membranes. All samples except the medium control contained the same percentage of chromatography buffer and detergent. Following incubation, the cells were washed and tested for the presence of the proteins on their surface by FACS staining using anti c-myc primary and RPE-labeled secondary antibodies. Dead cells were identified by 7-AAD staining and the histograms shown are gated on viable cells. The black lines indicate staining with isotype-matched control antibodies, blue lines staining with anti c-myc antibodies. Mean fluorescence intensities (MFIs; geometric mean of c-myc stained sample – geometric mean of isotype control) are given for each sample.

As evident from the histograms, only the CXCL10-GPI, CXCL10-mucin-GPI and sEGFP-GPI proteins could successfully be detected on the surface of the treated CHO cells, whereas the soluble CXCL10-mucin-Stop protein could not be detected. The buffer and medium controls did not result in a fluorescence signal demonstrating specificity of the staining protocol. These observations indicated

that the GPI-anchored proteins incorporated spontaneously into the cell membranes of the target cells.

Similar results were obtained using primary or immortalized microvascular endothelial cells (HDBEC or HMEC, respectively; see 3.5.2, 3.5.3 and data not shown) or primary endothelial cells isolated from umbilical veins (HUVEC; data not shown). Thus, a variety of different cells could be "painted" with the purified proteins, which indicated that the exact extracellular composition of the target cells was of minor importance for the incorporation process. The staining intensities were found to correlate with the general concentration of recombinant proteins used in the respective experiment (compare the MFIs in the experiments described in 3.5.3 and 5.6, which were performed with lower protein concentrations and data not shown). The technique of cell painting thus allowed the transfer of defined amounts of proteins onto target cell surfaces by varying the protein concentrations used for cell painting. Furthermore, this observation also indicated that it might be possible to generate a stable gradient of recombinant proteins if they were injected into a tissue. Here, diffusion in combination with incorporation of a fraction of the proteins at each point should gradually lower the concentration of available proteins, leading to lower degrees of painting with increasing distance from the injection site. However, this assumption is largely hypothetical.

3.5.2 Incorporated GPI-anchored fusion proteins associate with the cell membranes of treated cells

Having shown that the purified GPI-anchored fusion proteins could integrate spontaneously into cell membranes, the exact subcellular localization of the incorporated proteins was assessed in more detail using immunofluorescence microscopy.

In order to mimic the situation found in a blood vessel as closely as possible, primary microvascular endothelial cells (HDBEC) were used as target cells. Furthermore, the cells were treated with the purified proteins in an adherent state to exclude changes to the incorporation process when the cells are detached from their substrate for treatment. In this adherent setting, it was expected to find a membrane-associated incorporation pattern of the recombinant proteins. Of note, the experimental conditions used in this experiment were virtually identical to the painting of endothelial cells for the laminar flow assays described in 3.6, allowing conclusions also for these assays.

Primary microvascular endothelial cells were grown in special culture dishes with high fluorescence permeability as described in 2.2.5.3. Subsequently, the cells were washed and incubated for 1.5 h with purified CXCL10-GPI (1.8 nM), CXCL10-mucin-GPI (0.8 nM) or a buffer control, all diluted in culture medium and all containing the same percentage of buffer to exclude artifacts. Different protein concentrations were used in this experiment as a comparison of staining intensities was not the primary objective, but rather the maximal available amount of the respective proteins (which depended on the yield in the respective protein purification) should be transferred onto the cells to

enable precise localization of the incorporated proteins. Following treatment, the cells were washed and fixed with paraformaldehyde to exactly preserve the situation found after the incorporation process. Incorporated proteins were then detected using anti c-myc primary and biotinylated secondary antibodies in combination with RPE-labeled streptavidin. Figure 19 shows representative fluorescence images and corresponding bright field images acquired on an inverted fluorescence microscope.

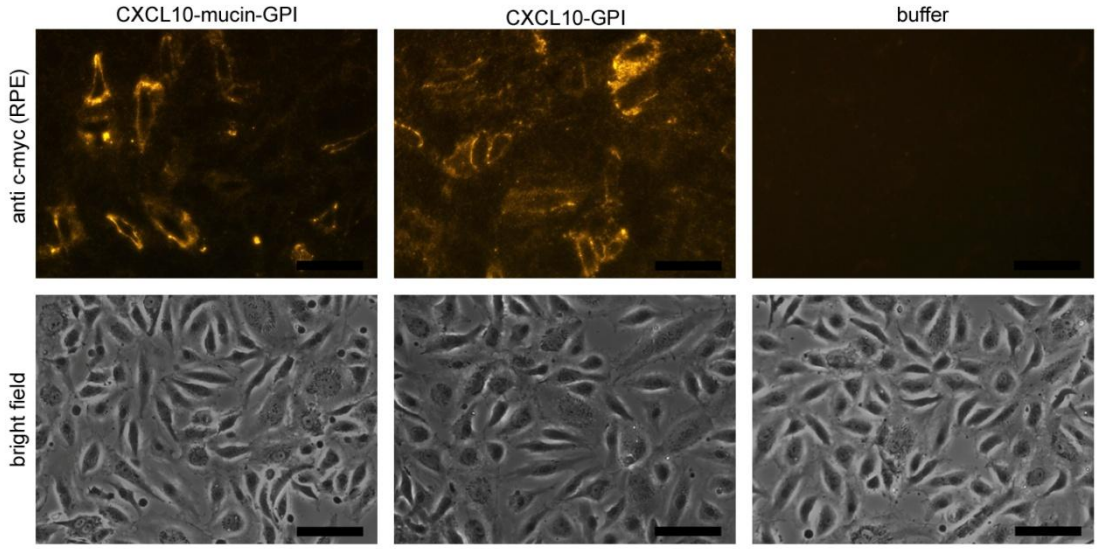

Figure 19: The GPI-anchored CXCL10 fusion proteins can be detected on the cell membranes of primary microvascular endothelial cells following treatment with purified proteins. In order to identify the subcellular localization of the incorporated proteins, immunofluorescence microscopy was performed. Primary microvascular endothelial cells were treated with 1.8 nM purified CXCL10-GPI, 0.8 nM CXCL10-mucin-GPI or a buffer control, with all samples containing the same percentage of buffer to exclude artifacts. Primary cells were used and the cells were treated in an adherent state to mimic the situation found in a blood vessel. Following treatment, the cells were fixed and incorporated proteins were detected using anti c-myc primary and biotinylated secondary antibodies followed by RPE-labeled streptavidin. Representative fluorescence images and corresponding bright field images are shown. All images within each row were acquired using the same exposure time. The black bars represent a length of 50 µm.

The images showed pronounced fluorescence signals in both samples treated with the GPI-anchored CXCL10 fusion proteins, but not in the buffer control, indicating specificity of the staining. The strongest signals were found at the periphery of the cells, a staining pattern which is commonly associated with membrane-bound targets. For the sample treated with CXCL10-GPI, a stronger overall fluorescence was found, which was due to the higher protein concentration used in this sample. In summary, it can be stated that the purified GPI-anchored CXCL10 fusion proteins incorporated spontaneously into the cell membranes of primary microvascular endothelial cells. Furthermore, the incorporated proteins could be detected in a membrane-associated manner, indicating correct targeting to the cell membrane.

3.5.3 The incorporation process is dependent on the presence of a GPI anchor

Additional experiments were performed to more directly show that the GPI anchor was responsible for anchoring the purified proteins to the cell membranes of target cells after incorporation. To this end, microvascular endothelial cells were treated with purified CXCL10-GPI (0.5 nM) or CXCL10-mucin-GPI (0.6 nM) or a buffer control and then treated with 0.1 U phosphatidylinositol-specific phospholipase C (PI-PLC) for 1 h. PI-PLC specifically cleaves GPI anchors, thereby releasing the proteins for the cell surface. Thus, if the proteins were anchored via GPI structures, this treatment should lead to a reduction in surface staining. Following treatment with PI-PLC, the cells were stained with anti c-myc primary and RPE-labeled secondary antibodies and staining intensities were assessed by FACS. Figure 20 depicts the results of a representative experiment.

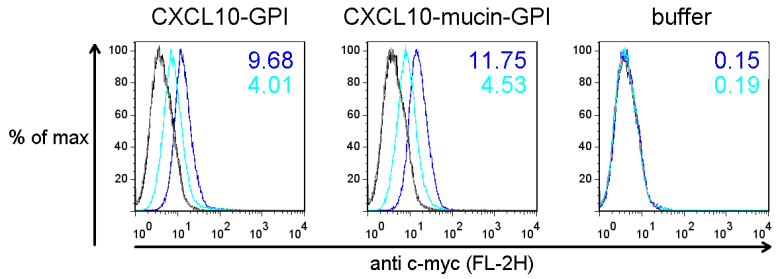

Figure 20: Phosphatidylinositol-specific phospholipase C (PI-PLC) treatment releases the GPI-anchored CXCL10 fusion proteins from the cell surface following incorporation. Microvascular endothelial cells were treated with 0.5 nM CXCL10-GPI, 0.6 nM CXCL10-mucin-GPI or a buffer control with all samples containing the same percentage of chromatography buffer. Subsequently, the samples were aliquoted and incubated with 0.1 U PI-PLC or medium as control. FACS staining was performed using anti c-myc primary and RPE-labeled secondary antibodies. Chromatograms are gated on viable cells identified by 7-AAD exclusion. The light blue lines indicate cells treated with PI-PLC (matching isotype control: grey lines) while the dark blue lines indicate the medium control (matching isotype control: black lines). The MFIs (geometric mean of c-myc stained sample – geometric mean of isotype control) are given for every treatment condition. In order to better visualize the differences in fluorescence intensity, the histograms are displayed using a relative scale on the Y axis (% of max), where the number of events is related for each particular fluorescence intensity to the number of events in the largest group of cells with the same fluorescence intensity.

Treatment with PI-PLC lead to a pronounced reduction in surface staining of the GPI-anchored protein treated cells (light blue lines). The MFIs of these samples were reduced by about 60% compared to the respective medium controls (dark blue lines). This marked reduction in surface staining verified that the proteins were anchored to the cell membrane via GPI anchor structures.

3.6 CXCL10-mucin-GPI can enhance leukocyte recruitment *in vitro* under conditions of physiologic flow

Based on our initial hypothesis, CXCL10-mucin-GPI should be able to recruit leukocytes in the absence of an inflammatory reaction, thereby overcoming endothelial cell anergy within tumor

tissues. Once anchored into the cell membranes of endothelial cells via the GPI anchor, the mucin domain together with the chemokine head should concertedly induce rolling and tight adhesion of leukocytes, followed by diapedesis into the tumor tissue. Two major types of leukocytes were envisioned as targets of CXCL10-mucin-GPI as both types express the CXCR3 receptor: cytotoxic T cells and NK cells. Therefore, the effect of CXCL10-mucin-GPI on the recruitment of these cell types was assessed *in vitro* using laminar flow assays. These assays mimic conditions found in blood vessels in terms of shear stress, and are typically performed using channels with rectangular geometry. Endothelial cells are grown within these channels, pretreated according to the respective experiment, and leukocytes are then perfused through the channel over the endothelial cell monolayer. The subsequent interactions between leukocytes and endothelial cells are monitored by video microscopy. The rectangular geometry of the channel allows a precise calculation of the shear stress occurring between the channel walls (or the endothelial cells) and adhering leukocytes. The local flow velocity at any given point within the channel can be calculated from the dimensions of the channel, the viscosity of the medium, and the pressure change within the channel, which is dependent on the volumetric flow rate (Cornish 1928). The local flow velocity is then used to calculate the shear stress at any given point, which is again dependent on the viscosity of the medium. Most experiments presented here were performed at a shear stress of 1 dyn/cm^2, which resembles the shear stress found in postcapillary venules, where leukocyte recruitment predominantly occurs (Lawrence et al. 1987; Lawrence and Springer 1991; DiVietro et al. 2001). Primary microvascular endothelial cells from blood vessels (HDBEC) were used in the experiments to as closely as possible mimic the capillary vasculature (for details see 2.2.5.4).

3.6.1 CXCL10-mucin-GPI mediates enhanced adhesion of NK cells to primary microvascular endothelial cells

In order to gain initial insights into the function of the GPI-anchored fusion proteins, a series of laminar flow assays were performed using the human NK cell line YT. A low expression of CXCR3 was detected in these cells by reverse transcriptase real-time PCR (2^{dCt} vs. 16S rRNA = 1.37 x 10^{-6}) as well as in FACS analyses (data not shown). The assays were conducted using resting primary micro-vascular endothelial cells. These cells normally do not support adhesion of leukocytes under conditions of physiologic flow due to the absence of selectin molecules, which are only upregulated in response to pro-inflammatory stimuli and are not present on resting cells (Haraldsen et al. 1996). Also in our hands, E-selectin was not detected on resting endothelial cells by FACS analysis (data not shown).

For the experiments, endothelial cells were grown in microscope slides containing a channel of defined geometry. On the day of the assay, the cells were incubated for 1 h in 0.34 nM of purified GPI-anchored CXCL10 fusion proteins diluted in endothelial cell growth medium, or with identically

purified and diluted sEGFP-GPI protein. As an additional control, parallel slides were incubated with commercially available recombinant CXCL10 at 1000 fold higher concentration (340 nM), to allow detection of even small effects mediated by conventional CXCL10. All samples contained the same percentage of chromatography buffer and detergent to exclude buffer artifacts. Following treatment of the endothelial cells, NK cells were suspended in assay buffer and perfused over the endothelial cells with a shear rate of 1 dyn/cm^2 for 5 min. The interactions were monitored by video microscopy and the number of NK cells that accumulated on the endothelial cells within the respective field of view was counted and expressed as cells/mm^2. Figure 21 summarizes the results of at least three independent experiments that were performed using independent protein preparations with each symbol representing one independent slide and horizontal bars representing the overall average.

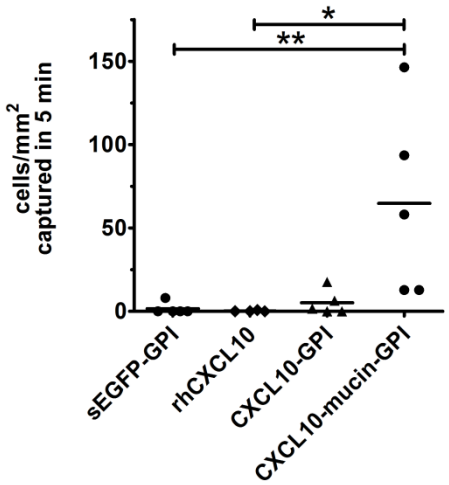

Figure 21: Human NK cells accumulate on primary microvascular endothelial cells treated with purified CXCL10-mucin-GPI. Laminar flow assays were performed to test if resting primary microvascular endothelial cells that had been treated with the GPI-anchored CXCL10 fusion proteins were able to recruit freely flowing NK cells under conditions of physiologic flow. Resting endothelial cells were treated with 0.34 nM of GPI-anchored CXCL10 fusion proteins or with identically diluted sEGFP-GPI protein for 1 h. Other slides were treated with commercially available CXCL10 at 1000 fold higher concentration as additional control (rhCXCL10). All samples contained the same percentage of chromatography buffer and detergent. Subsequently, YT cells (a human NK cell line) were perfused over the endothelial cells with 1 dyn/cm^2 and the number of cells that had accumulated on the endothelial cells after 5 min was counted. Data shown here are derived from three (controls) or four (CXCL10 fusion proteins) independent experiments that were performed using independent protein preparations. Each symbol represents one independent slide, horizontal bars the average. Statistical significance was calculated using the Kruskal-Wallis test (P = 0.0084) followed by Dunn´s post test; * = P<0.05, ** = P<0.01.

In these experiments, on average 65 NK cells/mm^2 were found to have adhered to endothelial cells that had been incubated with CXCL10-mucin-GPI. Despite this large average number of cells, the outcomes of single experiments varied considerably, resulting in a large standard error of the mean (SEM) of 25 cells/mm^2. These variations are thought to reflect the series of variables that underlie

laminar flow experiments, although extensive efforts were taken to minimize these variables. Nevertheless, on average only 2 cells/mm^2 adhered to the samples treated with the GPI-anchored negative control protein sEGFP-GPI, and the difference between this protein and CXCL10-mucin-GPI was highly significant. This indicated that the incorporation process itself, or the presence of a GPI-anchored protein on the cell surface, did not activate the endothelial cells and cause the adhesion events observed with CXCL10-mucin-GPI.

CXCL10-GPI lacking the mucin domain failed to recruit significantly more cells than the two controls (5 cells/mm^2 on average), suggesting that the presence of the mucin domain is a prerequisite for efficient function of the fusion proteins in NK cell recruitment.

A significant difference was also observed between CXCL10-mucin-GPI treated cells and cells treated with commercially available CXCL10 (0 cells/mm^2 on average), although the latter protein was used at 1000 fold higher concentration than the GPI-anchored proteins. This observation made it unlikely that the effects seen in the experiments were based upon an interaction of the CXCL10 chemokine domain with the endothelial cells. The fact that chemokines alone were insufficient to induce leukocyte recruitment on resting endothelial cells has also been demonstrated in other publications (Kukreti et al. 1997; Peled et al. 1999; Manes et al. 2006).

These experiments described the first proof of principle that a fusion protein containing a chemokine head, the mucin domain of CX3CL1 and a GPI anchor can incorporate spontaneously into endothelial cell membranes, and once incorporated, bind leukocytes that are moving at physiologic flow rates. The recruitment occurred in the absence of inflammatory stimulation of the endothelial cells, which is an important finding because the upregulation of adhesion molecules by inflammatory cytokines is often defective in tumor endothelia (see 1.1.3). Efficient recruitment of NK cells would however require not only binding, but also that the cells undergo tight adhesion, which represents an important step in the extravasation cascade and was evaluated as described below.

3.6.2 CXCL10-mucin-GPI induces both rolling and tight adhesion of NK cells

In the recruitment cascade, rolling adhesion is first initiated by endothelial-expressed selectin molecules. Subsequently, tight adhesion is triggered in rolling leukocytes via chemokine receptor stimulation leading to activation of the leukocyte´s integrins (Jones et al. 1994; Laudanna and Alon 2005). This tight adhesion to the endothelium is required for leukocyte extravasation from blood vessels into the tissue. To more precisely analyze if CXCL10-mucin-GPI also induced tight adhesion of the captured NK cells, the adherent cells in the experiments described above were further subgrouped. Cells that displayed tight adhesion, defined as an event in which the respective NK cell did not move further than one cell diameter within 30 sec, were differentiated from those that displayed rolling adhesion, defined as an event in which the leukocyte was abruptly stopped from the flow, but did not reach tight adhesion or detached again. The exact evaluation criteria that were

applied can be found in 2.2.5.4.3. Figure 22 shows the results of a representative experiment, each bar representing the average of two independent slides.

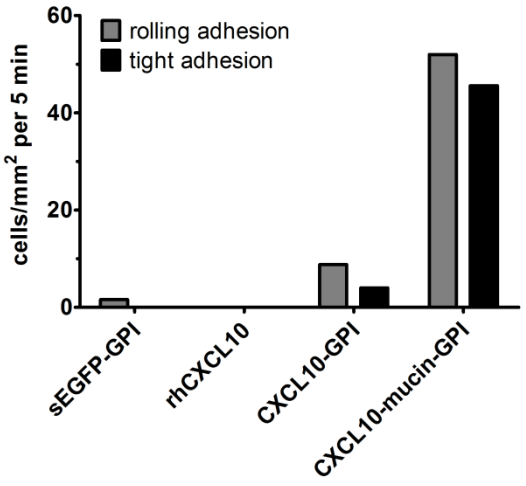

Figure 22: CXCL10-mucin-GPI induces both rolling and tight adhesion under conditions of physiologic flow. Primary microvascular endothelial cells were treated with the GPI-anchored fusion proteins or commercially available CXCL10 (rhCXCL10) as described in the legend of Figure 21. Subsequently, NK cells of the YT cell line were perfused over the endothelial cells with a shear rate of 1 dyn/cm^2 and interactions were monitored by video microscopy. Tight adhesion was defined as an event in which the particular NK cell did not move further than one cell diameter within 30 sec, while rolling adhesion was defined as an event in which the cell was abruptly stopped but did not reach tight adhesion or detached again. Cells displaying both types of adhesion were counted as tightly adherent. Each bar represents averaged values from two independent slides.

The evaluation showed that endothelial cells incubated with 0.34 nM CXCL10-mucin-GPI induced both rolling and tight adhesion of the NK cells. On average 52 cells/mm^2 displayed rolling adhesion, while 46 cells/mm^2 adhered tightly to the endothelial cells. CXCL10-GPI lacking the mucin domain could only induce 9 events of rolling adhesion and 4 tight adhesions/mm^2. Virtually no adhesion was seen with endothelial cells incubated with the sEGFP-GPI control protein or commercially available CXCL10 (340 nM), again indicating that the incorporation process or the CXCL10 chemokine domain alone did not activate the endothelial cells.

In summary, primary microvascular endothelial cells treated with CXCL10-mucin-GPI acquired the ability to recruit NK cells at physiologic flow in the absence of inflammatory stimulation. The recruitment process involved the induction of both rolling and tight adhesion, indicating robust binding of the leukocytes and thus laying the ground for subsequent extravasation.

Since following the *in vitro* proof of concept also *in vivo* trials should be performed, further experiments were carried out to examine the activity of the CXCL10 proteins with murine cells, which will be described in the next sections.

3.6.3 CXCL10-mucin-GPI can recruit also primary murine NK cells

The experiments described in the last sections were all performed with human cells and the GPI-anchored CXCL10 fusion proteins contained a human CXCL10 domain. Human and murine CXCL10 share the same three-dimensional structure and display 83% amino acid homology (Jabeen et al. 2008). Nevertheless, with respect to the *in vivo* experiments that should be performed later on, it was tested if the CXCL10 fusion proteins were active with murine cells. Soluble human CXCL10 was shown in calcium mobilization and receptor internalization assays to crossreact with murine CXCR3 using a murine T cell line (see 5.2). Here, murine and human CXCL10 elicited virtually identical signals. In the following experiment, the effects of the GPI-anchored proteins on murine NK cells were tested in terms of the induction of adhesion under flow.

Primary murine NK cells were kindly provided by J. Pötzl from the Helmholtz Zentrum Munich and isolated freshly on the day of each assay from the spleens of wildtype C57/Bl6 mice. Magnetic beads were used for the isolation and the purity of the preparation was routinely assessed by FACS staining. In the experiment presented here, the cell population comprised 94% NK cells. High CXCR3 expression was found on 43% of the murine splenic NK cells (data not shown). Primary human microvascular endothelial cells were used in the experiments as primary murine microvascular endothelial cells were not commercially available. It was though assumed that the general cell surface composition of human endothelial cells was largely compatible with murine leukocytes.

The experiment was performed as described in 2.2.5.4. Resting endothelial cells grown in microscope slides were treated with 0.2 nM of CXCL10-GPI or CXCL10-mucin-GPI or commercially available CXCL10 at much higher concentration (115 nM) to allow detection of small effects mediated by the soluble protein. All samples were diluted in culture medium and contained the same percentage of buffer and detergent. Partly also a medium control with completely untreated endothelial cells was included. Subsequently, murine NK cells were perfused over the endothelial cells with a shear rate of either 0.4 or 1 dyn/cm^2. The subphysiologic shear rate of 0.4 dyn/cm^2 was included to allow a more precise characterization of the effects of the proteins. The interactions were monitored for 5 min and adherent NK cells were counted. Cells with rolling adhesion were differentiated from tightly adherent cells as described above and in more detail in 2.2.5.4.3. Figure 23 shows the results of the experiment, with panel A summarizing cell counts at 0.4 dyn/cm^2 and panel B at 1 dyn/cm^2.

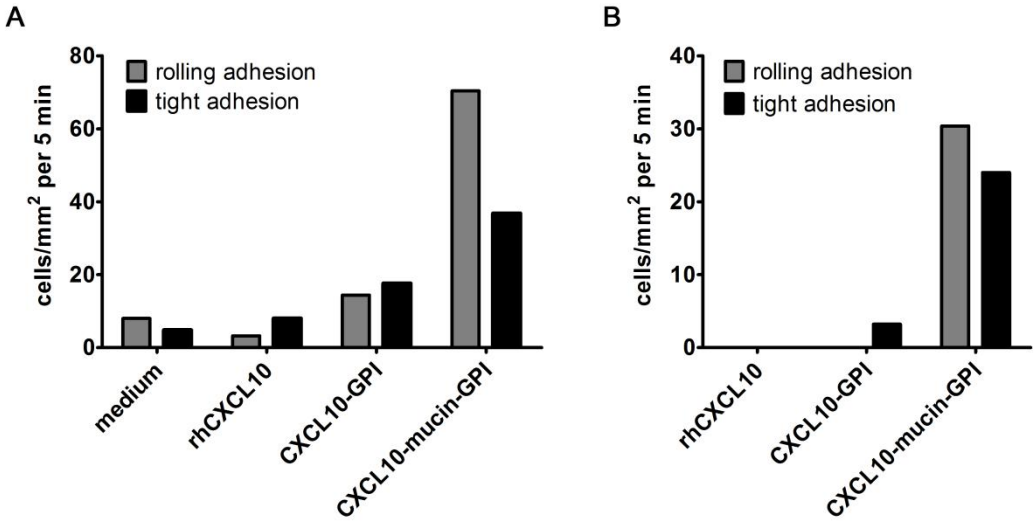

Figure 23: CXCL10-mucin-GPI efficiently recruits murine NK cells and induces both rolling and tight adhesion under conditions of physiologic flow. Experiments were performed to assess the applicability of the GPI-anchored fusion proteins in the murine system. Primary microvascular endothelial cells were incubated for 1 h with 0.2 nM of CXCL10-GPI or CXCL10-mucin-GPI or commercially available CXCL10 (rhCXCL10) at much higher concentration (115 nM) to allow detection of even minor effects. All samples except the medium control contained the same percentage of buffer and detergent. Primary murine NK cells were then perfused over the endothelial cells with 0.4 (**A**) or 1 (**B**) dyn/cm^2 and adherent cells were counted. Cells with rolling adhesion were differentiated from such that adhered tightly to the endothelium as described in the legend of Figure 22.

At the subphysiologic flow rate of 0.4 dyn/cm^2, 70 events of rolling adhesion and 37 tightly adhering NK cells/mm^2 were observed on endothelial cells treated with CXCL10-mucin-GPI. For the CXCL10-GPI protein, 14 rolling and 18 tight adhesions/mm^2 were found, indicating that 20% of the rolling adhesions and about half of the tight adhesions seen with CXCL10-mucin-GPI also took place in the absence of the mucin domain. While some adherence (up to 8 events/mm^2) was seen with soluble CXCL10, this was also true for the medium control, indicating that the events observed with soluble CXCL10 were based only on the low flow rate. This background adherence was completely abrogated when the physiologic shear rate of 1 dyn/cm^2 was employed as shown in panel B. At this shear rate also the difference between the two CXCL10 fusion proteins was more pronounced. Endothelial cells treated with CXCL10-GPI triggered tight adhesion of 3 NK cells/mm^2, while endothelial cells incubated with CXCL10-mucin-GPI recruited 24 tightly adhering cells/mm^2. Thus, 8 x more cells were tightly bound by the protein containing the mucin domain, opposed to a twofold difference observed at 0.4 dyn/cm^2. In addition, also the differences in the induction of rolling adhesion were more pronounced at the more physiologic shear rate: No events were observed in the sample with CXCL10-GPI, while CXCL10-mucin-GPI was able to induce 30 rolling adhesions/mm^2.

These results showed that CXCL10-mucin-GPI is able to recruit murine NK cells in the same range of efficiency as seen with human NK cells and underlined the importance of the mucin domain for

recruitment at physiologic shear stress. Having demonstrated activity of CXCL10-mucin-GPI on NK cells, further experiments were performed to test the efficacy in terms of recruitment also with T cells.

3.6.4 CXCL10-mucin-GPI has no significant effect on T cell recruitment

In the experiments described above, CXCL10-mucin-GPI was shown to be highly active in recruiting NK cells under conditions of physiologic flow. The activity of the recombinant protein in T cell recruitment was tested analogous to the assays described above for NK cells. Primary microvascular endothelial cells were treated with 0.23 nM CXCL10-mucin-GPI, identically diluted sEGFP-GPI or commercially available CXCL10 at either the same concentration as the GPI-anchored CXCL10 protein or at a much higher one in order to detect even small effects of the soluble protein. Subsequently, cells of the human $CD8^+$ T cell line DS4, which had been demonstrated to be highly CXCR3-positive by FACS analysis (see 3.2.1 and data not shown), were perfused over the endothelial cells with the physiologic shear rate of 1 dyn/cm^2. In these experiments, however, no significant adhesion to the endothelial cells could be detected (data not shown). For this reason, the shear rate was lowered to 0.4 dyn/cm^2, as it had been shown earlier (e.g. see 3.6.3) that this subphysiologic shear rate can considerably increase the numbers of adhering cells and should therefore allow to detect even small effects. Figure 24 summarizes the results of two independent experiments performed at 0.4 dyn/cm^2, with each dot representing one individual sample.

The figure shows background adhesion of approximately 10 cells/mm^2 in all treatment conditions, which could be attributed to the subphysiologic flow rate. However, CXCL10-mucin-GPI was not superior to the other proteins in the recruitment of T cells. In fact, none of the treatments was able to significantly augment cell adhesions. This finding was in contrast to the results presented in 3.2.3, where CXCL10-mucin-GPI expressed on CHO cells had shown at least a trend towards being able to recruit freely flowing T cells of the same cell line as the one used in the experiment described here.

The explanation for this divergence may possibly be found in the surface levels of CXCL10-mucin-GPI. Clearly the levels of the protein were much lower on “painted” endothelial cells than on CHO cells expressing the construct. Thus, the amount of protein present on treated endothelial cells may have been too low to induce T cell adhesion, although it was able to efficiently induce NK cell adhesion.

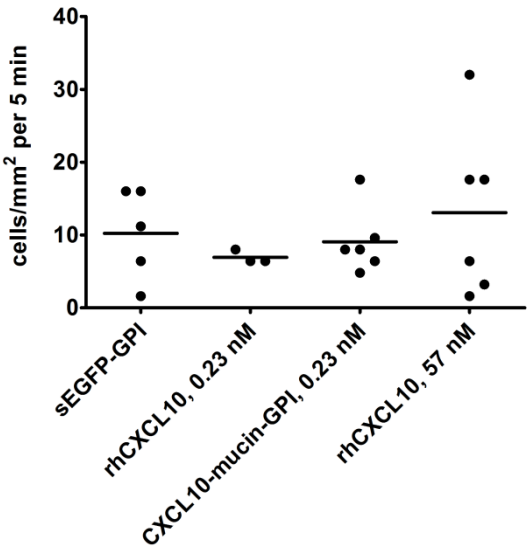

Figure 24: CXCL10-mucin-GPI fails to recruit T cells under conditions of flow. Primary microvascular endothelial cells were incubated with 0.23 nM CXCL10-mucin-GPI or sEGFP-GPI which had been identically diluted in culture medium. Additional samples were treated with commercially available soluble CXCL10 (rhCXCL10), either at the same or at 250 x higher concentration. All samples contained the same percentage of chromatography buffer. Subsequently cells of the human T cell line DS4 were perfused over the endothelial cells with a shear rate of 0.4 dyn/cm^2 and tightly adherent cells were counted. Data are presented from two independent experiments, each dot representing one independent slide and horizontal bars the average values.

The assumption that T cells required relatively high degrees of chemokine stimulation were further corroborated by another experiment, where human umbilical vein endothelial cells (HUVEC) were used. Manes et al. demonstrated that CXCL10 can induce rapid transendothelial migration (TEM) of T cells through a monolayer of TNFα-stimulated HUVEC using a similar system of physiologic flow (Manes et al. 2006). Thus, although directed at a different step of leukocyte recruitment, the advantage of this assay was that a direct positive control (commercially available CXCL10) was available. In this assay, only high concentrations of commercially available CXCL10 (115 nM) were in our hands efficient in increasing TEM, while concentrations identical to that of CXCL10-mucin-GPI used in the experiments (0.92 nM) were not. The same was true for CXCL10-mucin-GPI itself (data not shown). It was therefore concluded that either CXCL10-mucin-GPI was ineffective with regards to T cell recruitment or (rather) the amounts of CXCL10-mucin-GPI protein that could be transferred onto endothelial cells *in vitro* using the available purification methods were not sufficient to induce a significant effect in T cells. Possible ways to overcome this problem will be discussed in 4.5 and 5.5.

3.7 CXCL10-mucin-GPI can enhance intratumoral leukocyte recruitment *in vivo*

A model based on subcutaneously transplantable tumors was used to study the effects of CXCL10-mucin-GPI after intratumoral injection *in vivo*. The experiments were performed in collaboration with L. Bankel from the Helmholtz Zentrum Munich. Cells of the 291 B cell lymphoma line were used as a

model system, which have been isolated from a transgenic C57/Bl6 mouse carrying the c-myc oncogene under the control of the Igλ promoter. The tumor cells were demonstrated to be negative for CXCR3 by FACS and reverse transcriptase real-time PCR (data not shown). This was a prerequisite for their use as model system for the CXCL10 fusion proteins as binding of the proteins to tumor cell chemokine receptors should be avoided. The cells were injected into the flanks of wildtype C57/Bl6 mice. Wildtype mice were used as recipients to ensure a normal immune response, despite the general artificiality of a transplantable tumor model. In pilot experiments, it was found that 10^7 tumor cells were required to induce robust tumor growth, allowing to conduct experiments approximately 10 days after tumor injection. For a general characterization of the tumor tissue, tumors were excised and subjected to hematoxylin/eosin staining (H/E) or immunohistology for CD3 and NKp46 as described in 2.2.6.3. Representative images are shown in Figure 25.

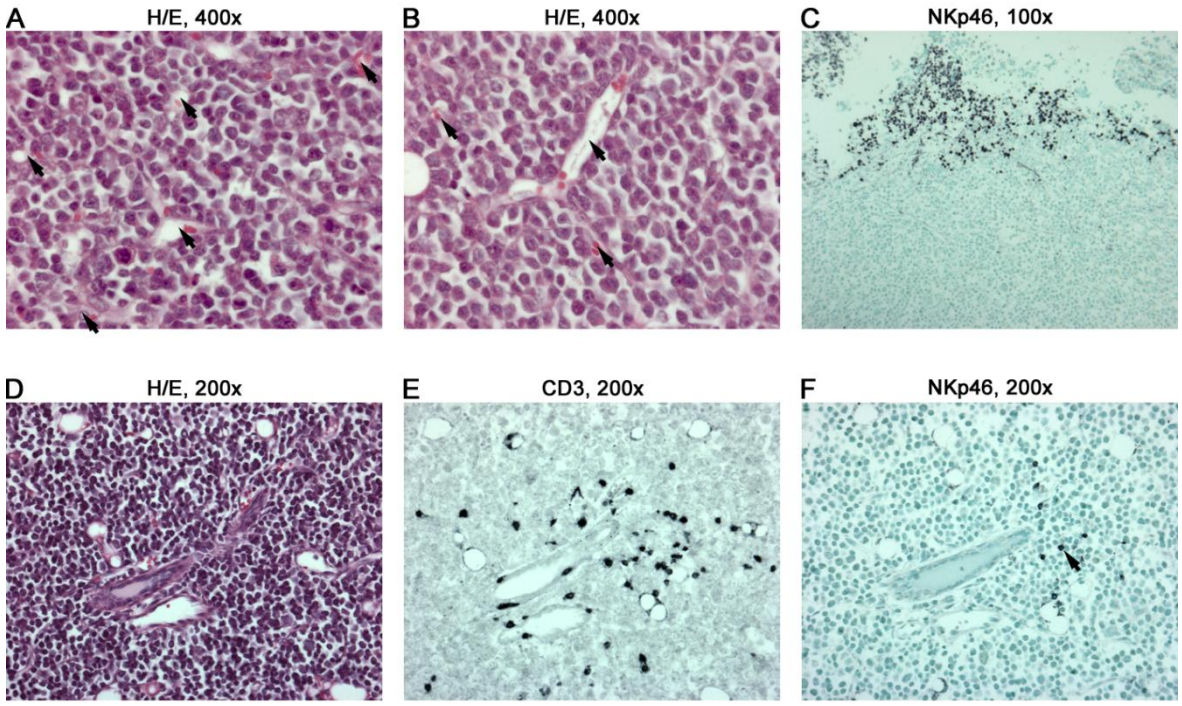

Figure 25: Subcutaneously implanted tumors of the 291 cell line are well vascularized and show a pronounced infiltration with T cells. Tumor cells (10^7 cells) were injected subcutaneously into the flanks of wildtype C57/Bl6 mice. Grown tumors were excised, fixed and analyzed by hematoxylin/eosin (H/E) staining or immunohistology using antibodies against CD3 or NKp46. The respective magnifications are indicated at the top of each image. Panels **A** and **B** show the presence of numerous blood vessels (arrows) throughout the tumors in H/E staining. Panels **D**, **E** and **F** represent serial sections of the same position within a tumor. Various blood vessels are visible in H/E staining and the CD3 staining shows infiltration of the tumor with $CD3^+$ cells (dark grey/ black staining). Less $NKp46^+$ cells could be detected in the respective staining of the same position (dark grey/ black staining; one cell is marked by an arrow). Panel **C** depicts a cluster of $NKp46^+$ cells, which could sometimes be found at the margins of tumors (margin: upper part of the picture).

The tumors were mostly well vascularized with a relatively high number of blood vessels visible in H/E staining as depicted in panels A and B and usually displayed little signs of necrosis such as loss of nuclear staining. Panels D, E and F represent serial sections of a position near the tumor center. Various blood vessels could be seen, and CD3 staining showed marked infiltration of the tumor mass with T cells in the vicinity of the blood vessels. NKp46 staining of the same position revealed a much lower infiltration with NK cells compared to $CD3^+$ cells. This finding was true for all untreated tumors, where a much more pronounced infiltration of the tumor with $CD3^+$ than $NKp46^+$ cells was seen. At the tumor margins, however, occasionally clusters of $NKp46^+$ cells could be found, as exemplified in panel C. These clusters contained only few $CD3^+$ cells (data not shown). In summary, $CD3^+$ cells were found relatively equally distributed throughout the tumors, while $NKp46^+$ cells sometimes displayed a highly unequal distribution. For this reason, it was chosen to analyze the infiltration of the tumors by NK cells with FACS analysis in order to avoid skewing of the results by biased image acquisition in histology, while infiltration with $CD3^+$ cells could be assessed by immunohistological staining of tumor sections.

3.7.1 Injection of CXCL10-mucin-GPI moderately increases T cell infiltration

Protein injections were performed to analyze the effect of CXCL10-mucin-GPI on the infiltration of tumors with T cells and NK cells. Once the tumors had grown to a size that technically allowed injection of the proteins (about 5 mm in diameter), 0.23 pmol of CXCL10-mucin-GPI or the same molar amount of commercially available CXCL10 were injected into the center of the tumors in a volume of 50 µl. As controls, equally purified sEGFP-GPI protein or a 500 x higher molar amount of commercially available CXCL10 (115 pmol) were injected also in a volume of 50 µl. All proteins were diluted in PBS + 0.025% Triton X-100h to exclude buffer artifacts. It was taken care that the various treatment conditions were equally distributed over larger and smaller tumors. Four hours after the injections, the animals were sacrificed and the tumors excised. This time point was selected as it had been found to be the one where injection of commercially available CXCL10 had the most potent effect (data not shown). Half of each tumor was subjected to FACS analysis, the results of which will be shown in 3.7.2, and the other half was fixed in formalin for immunohistology. All tumors were embedded in the same orientation and sections were made perpendicular to the surface where the tumors had been bisected, so that center and margin of each tumor could easily be identified. The sections were stained immunohistologically to identify $CD3^+$ cells and three low-power images (100 x magnification) of each section were taken at the tumor center, the margin and in between these two positions. The numbers of $CD3^+$ cells in each image were counted by an observer blinded to the experimental conditions and averages were calculated for each tumor. The results are presented in Figure 26, with each symbol representing the averaged values of one tumor.

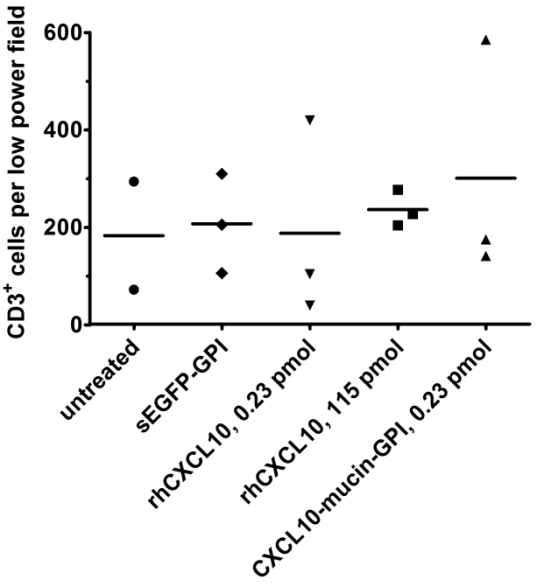

Figure 26: Injection of CXCL10-mucin-GPI tends to moderately increase T cell infiltration of subcutaneous tumors. Purified CXCL10-mucin-GPI (0.23 pmol) was injected into subcutaneously implanted 291 tumors. As controls, either the same or a 500 x higher molar quantity (115 pmol) of commercially available human CXCL10 (rhCXCL10) were injected. Additional controls included completely untreated tumors and injection of the same volume of identically purified sEGFP-GPI. All injections were done using the same volume and the same buffer. The animals were sacrificed 4 h after injection and tumor sections were stained immunohistologically to detect $CD3^+$ cells. The numbers of cells in three low power fields per tumor were counted by an observer blinded to the experimental conditions and averaged. Each symbol represents averaged values for one tumor.

The cell counts showed no pronounced differences between the single treatments, which had already been anticipated from the *in vitro* results presented in 3.6.4. Moreover, a high basal level of infiltration was found already in completely untreated tumors (on average 183 cells per low power field; also compare the high power microscopic image depicted in 3.7), indicating a preexisting strong stimulus for T cell infiltration. This pronounced basal infiltration of course made it more difficult to assess potential interventional strategies to further enhance T cell infiltration. Nevertheless, tumors treated with CXCL10-mucin-GPI showed a small trend towards higher infiltration (on average 301 cells per low power field), which could not be reached by commercially available CXCL10 even at 500 x higher molar quantities (on average 237 cells per low power field). The cell counts in tumors treated with 0.23 pmol commercially available CXCL10 or sEGFP-GPI (188 and 207 cells per low power field, respectively) were similar to the counts in untreated tumors. Of note, the data presented here are of preliminary nature and further experiments with larger sample sizes will be needed to draw definitive conclusions.

In many tumor sections secondary lymphoid organs were observed at the tumor margins, which had been resected together with the tumors. These organs naturally contain large numbers of $CD3^+$ cells and were omitted in the cell counts presented above. However, the presence of these organs

rendered the analysis of T cell infiltrations generated by FACS uninformative, which is why these results are not presented here. In order to assess the influence of this finding on the analysis of NK cell infiltrations by FACS, tumor sections containing the described organs were stained for the presence of NKp46$^+$ cells. This revealed that only very few NKp46$^+$ cells were present in these structures, which should therefore not interfere with FACS analysis (see 5.3).

3.7.2 Injection of CXCL10-mucin-GPI leads to NK cell accumulation

In order to analyze infiltration by NK cells, half of each tumor treated as described above was analyzed by FACS (performed by L. Bankel, Helmholtz Zentrum Munich). NK cells were defined as CD3$^-$ NK1.1$^+$ cells and the percentage of NK cells among the total number of cells was used for evaluation rather than absolute values in order to compensate for the slightly different sizes of the tumors. Figure 27 summarizes the results for the various treatment conditions, with each symbol representing one individual tumor and horizontal bars the average values.

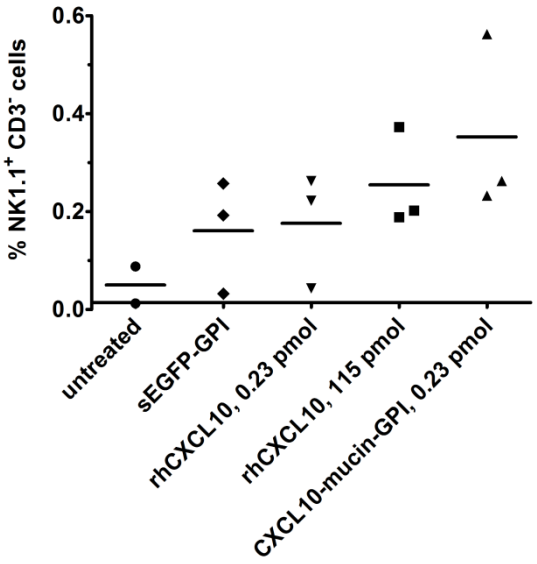

Figure 27: Injection of CXCL10-mucin-GPI increases NK cell infiltration of subcutaneous tumors. Subcutaneous tumors were implanted and treated as described in the legend of Figure 26. Following resection, infiltration of the tumors was assessed by FACS analysis. The figure shows the percentage of CD3$^-$ NK1.1$^+$ cells among the total cell count with each symbol representing one individual tumor and horizontal bars the average values. Statistical significance was calculated using the Kruskal-Wallis-test (P = 0.19) followed by Dunn´s post test.

The analysis revealed the presence of NK cells in the tumors at ratios ranging from 0% to 0.55%. The Kruskal-Wallis test showed that the mean ranks of all treatment groups did not differ significantly from each other (P = 0.19), although Dunn´s post test indicated a significant difference between untreated tumors and such treated with CXCL10-mucin-GPI. Nevertheless, clear trends were evident despite the lack of statistical significance. Based on the average values, tumors treated with CXCL10-mucin-GPI harbored higher numbers of NK cells (0.34%) than tumors that had received any of the

other treatments. Tumors injected with the same molar amount of commercially available CXCL10 contained on average only half as many NK cells (0.16%) as CXCL10-mucin-GPI treated tumors. Also 500 x higher molar amounts of commercially available CXCL10 were on average less efficient (0.24%) than CXCL10-mucin-GPI.

In summary, CXCL10-mucin-GPI was much more efficient in recruiting NK cells into tumors *in vivo* than commercially available CXCL10 or the GPI-anchored negative control protein sEGFP-GPI. The differences between the differently treated tumors were also much higher for NK cells than for T cells, which might be based on the lower background degree of infiltration by NK cells or on the higher chemokine signal strength required for T cell recruitment as detailed in 3.6. In order to generate statistically significant conclusions, however, further experiments with higher sample sizes will be performed in future studies.

Taken together, CXCL10-mucin-GPI showed a modest trend towards being able to recruit T cells after intratumoral injection, and a much stronger trend with regards to NK cells. The average efficiency of CXCL10-mucin-GPI was orders of magnitude higher than the efficiency of the soluble natural CXCL10 chemokine based on the concentrations required to generate a robust infiltration. Thus, the CXCL10-mucin-GPI agent developed in this study might be used to strengthen the infiltration of tumors with NK cells, potentially also in an adjuvant setting to adoptive NK cell therapy.

4 Discussion

Chemokines are a family of chemotactic cytokines that direct the migration of cells. Since cellular migration plays a central role in many human diseases, therapeutic tools to modify chemokine signaling networks have been studied by many researchers, mostly with the aim of suppressing recruitment of select cell types (Mackay 2008; Proudfoot et al. 2010). In the present study, a novel approach to modify tissue micromilieus was developed that in contrast allowed selective recruitment of cells carrying specific chemokine receptors. The approach was based on fusion proteins consisting of an N-terminal chemokine head, linked to the mucin-like domain taken from CX3CL1, with a C-terminal GPI anchor replacing the CX3CL1 transmembrane domain. According to the underlying hypothesis, the recombinant proteins should integrate by means of their GPI anchor into virtually any cell membrane when injected into a tissue (Medof et al. 1996). On cell membranes of endothelial cells, the mucin domain in combination with the chemokine should assist in the recruitment of cells carrying the receptor for the respective chemokine from the blood stream. In the tissue itself, the proteins would generate a stable haptotactic gradient that could be used by recruited cells to migrate towards the injection site. This novel type of reagents has diverse potential applications ranging from regenerative medicine, e.g. in the context of myocardial infarction where endothelial progenitor cells need to be recruited, to cancer therapy, where tumor infiltration with anti-neoplastic effector cells needs to be enhanced.

In the present study, first examples of fusion proteins were designed and tested in order to investigate the feasibility of this approach. The proteins were designed for an application in cancer therapy, especially as adjuvants to adoptive cell transfer. This adoptive transfer of immune effector cells (T cells or NK cells) has proven efficacy under some circumstances and thus holds promise for the development of future cancer therapies [reviewed in (June 2007) and (Levy et al. 2011)]. However, one of the major hurdles for a broader application of this treatment modality lies in insufficient infiltration of the tumors by the adoptively transferred cells (Pockaj et al. 1994; Griffioen et al. 1999; Mukai et al. 1999; Dirkx et al. 2003; Shrimali et al. 2010). The fusion proteins described in the present study were designed to help overcome this hurdle through selective modification of the tumor micromilieu. To this end, a CXCL10 chemokine head was used in the proteins (the primary protein thus being termed CXCL10-mucin-GPI) because this chemokine acts on cytotoxic effector cells like $CD8^+$ T cells and NK cells that express the CXCR3 receptor. A second set of proteins containing the CXCL8 chemokine, specific for a subset of highly cytotoxic $CD8^+$ T cells and neutrophils, was additionally generated and characterized as described in 5.1. Thereby, the applicability of the general concept to a broader perspective should be assessed, at least with regards to technical issues.

4.1 The recombinant fusion proteins can be expressed in eukaryotic cells

Expression of the recombinant fusion proteins represented an important step because bioactivity, especially of the chemokine fusion proteins, could only be assured if the proteins were correctly processed. In addition to correct three-dimensional folding of the proteins, necessary processing steps involved glycosylation of the mucin domain, cleavage of the N- and C-terminal signal sequences at the correct positions, and subsequent transfer of the proteins to a preformed GPI anchor. The latter step precluded the use of a prokaryotic expression system and among the many eukaryotic expression systems, Chinese hamster ovary (CHO) cells were chosen for several reasons. First, as they are derived from a mammalian host, CHO cells display a glycosylation pattern similar to that of human cells (Hossler et al. 2009), which might be important for the architecture and stability of the mucin domain. Second, CHO cells are already being used for the production of many protein-based drugs in large scale, which could facilitate the transfer of the approach described here to clinical studies (Wurm 2008).

Following transfection, the recombinant GPI-anchored fusion proteins were detected on the CHO cell surfaces by FACS staining. Monoclonal antibodies against various subunits of the proteins (chemokine head, mucin domain and c-myc epitope tag) were used in order to ensure that all parts were correctly expressed. For the sEGFP-GPI control protein, the protein´s autofluorescence could easily be detected, implicating that the addition of a GPI anchor did not compromise the architecture of the protein. The subcellular localization of the expressed proteins was determined by immuno-fluorescence microscopy and a membrane-associated staining pattern could be observed. These findings indicated that the proteins had been correctly targeted to the cell membrane by the addition of a GPI anchor signal sequence.

In addition to proper anchoring of the proteins, another concern was the correct cleavage of the N-terminal secretion signal sequence. This sequence is normally cleaved from the nascent proteins during synthesis in the ER, thereby generating the mature N-terminus of the respective protein. Cleavage of the chemokine heads had to occur at precisely the correct site as the N-terminal amino acid sequence is vitally important for the physiologic activity of chemokines (Proudfoot et al. 1996). Therefore, the N-terminal amino acid sequence of one of the CHO-cell expressed chemokine fusion proteins was verified by Edman sequencing. This analysis revealed that the N-terminus was identical to that of commercially available CXCL10 which had been proven to be bioactive. This finding was complemented by several experiments, which at later stages showed bioactivity of the GPI-anchored proteins. Thus, it was assumed that the N-termini of all of the recombinant CXCL10 fusion proteins were correctly processed by the CHO cells.

4.2 The GPI-anchored CXCL10 fusion proteins are bioactive as they can trigger CXCR3

Prior to their purification, the bioactivity of the expressed proteins was tested as described in 3.2. Due to the lack of direct assays assessing the bioactivity of the mucin domain, the activity of this domain could only be tested indirectly at later stages of the project by comparisons between the protein containing the mucin domain and the one that did not. However, a series of experiments were performed to investigate the bioactivity of the chemokine heads of CXCL10-GPI and CXCL10-mucin-GPI as the three-dimensional arrangement of various parts of the CXCL10 structure is required for efficient receptor binding. Interactions of CXCL10 with the CXCR3 receptor are mediated by amino acids at or near the N-terminus, in the N-loop preceding the first beta-sheet, in the 30s loop between the first and the second beta-sheet and within the second beta-sheet, and all these amino acids have to be in the correct three-dimensional arrangement (Booth et al. 2002). In contrast, the mucin domain can be completely replaced by non-related protein modules without impairing CX3CL1 function (Fong et al. 2000). Of note, amino acids at similar positions were found to be involved in receptor binding by the similarly structured CX3CL1 chemokine domain, underlining from a molecular standpoint the possibility to functionally replace the CX3CL1 chemokine head with a CXCL10 head (Mizoue et al. 1999).

Internalization of the CXCR3 receptor upon chemokine triggering was assessed as a first readout of bioactivity. Most chemokine receptors are internalized after triggering (Borroni et al. 2010), and subsequently either recycled to the cell membrane as is seen with CCR5 (Signoret et al. 2000), or degraded in the lysosomal pathway as it is the case for CXCR3 (Meiser et al. 2008). Because the proteins designed here are surface bound, a modified assay was developed to measure potential internalization of CXCR3. In this assay, CHO cells expressing the GPI-anchored CXCL10 fusion proteins were coincubated with CXCR3-positive human T cells. The presence of CXCR3 on the T cells was subsequently tested by FACS, where a pronounced reduction of the CXCR3 surface levels was observed. Normal soluble CXCL10, which was used as positive control, lead to identical results, while incubation at 4°C instead of 37°C much attenuated internalization, indicating an active process. CXCR3 internalization could not be inhibited by pertussis toxin, an inhibitor of signal transduction by G protein coupled receptors. The fact that pertussis toxin can inhibit CXCR3-mediated chemotaxis and calcium mobilization, but not internalization has been previously published (Sauty et al. 2001). Mutagenesis analyses have shown that the amino acids in CXCR3 required for internalization differ from the ones required for calcium mobilization and chemotaxis (Colvin et al. 2004). Thus, independent signaling pathways are thought to mediate these effects.

The question arises how CXCR3 could be internalized when it was bound to a construct anchored to the cell membrane of a neighboring cell. CXCR3 has however been shown to be internalized after

contact with CXCL10 immobilized on glycosaminoglycan (GAG) molecules (Sauty et al. 2001). Importantly, the internalization observed in the present study indicated that the physical connection between the T cells and the CHO cells could be dissociated. This might be beneficial as in the context of facilitated recruitment of leukocytes by the fusion proteins, efficient binding of the leukocytes would be as important as their subsequent release, because the latter would allow diapedesis and migration of recruited leukocytes.

Cytoplasmic calcium mobilization in T cells was used as a second means of verification of bioactivity. As detailed above, this signaling is thought to be mediated by a second set of signal transduction pathways. Here, chemokine receptor triggering leads to activation of phospholipase C-β, which in turn generates diacyl glycerol and inositol 1,4,5-trisphosphate. The latter then acts on ligand-gated calcium channels in the ER, inducing release of calcium into the cytosol (Wu et al. 2000). To assess the activation of this signaling cascade, T cells were loaded with a calcium-sensitive fluorescent dye and coincubated with CHO cells expressing the GPI-anchored CXCL10 fusion proteins. The fluorescence was continuously measured and normalized against a sample with non-transfected CHO cells. A transient rise in the fluorescence signal over the course of 40 min was found.

The observed curves presumably represent transient activation of single T cells within the total cell population, each resulting in a short-lived fluorescence signal until eventually all T cells had been desensitized for CXCL10. The cell-cell contact required for this signaling resulted in a time course kinetic differing from that seen with soluble proteins. The fluorescence signals occurred earlier and slightly stronger when T cells were coincubated with CHO cells expressing CXCL10-mucin-GPI as compared to the CXCL10-GPI transfected cells. Thus, the mucin domain appears to have enhanced the interaction of the chemokine domain with the CXCR3 receptor. Interestingly, a second, smaller fluorescence peak was observed for both CXCL10 fusion proteins from 40 min to about 60 min (data not shown). This second peak may represent replenishment of surface CXCR3 in the T cells triggered at the beginning of the incubation time.

Chemokine receptor signaling in leukocytes also leads to the activation of integrin molecules. The activated high-affinity integrins then allow the leukocyte to more efficiently adhere to immuno-globulin superfamily molecules such as ICAM-1 or VCAM-1 [reviewed in (Laudanna and Alon 2005)]. In studies by Piali and coworkers, IL-2 activated T cells were left to adhere in the presence of CXCL10 to immobilized ICAM-1 or VCAM-1 under static conditions and CXCL10 was shown to increase T cell adherence, with maximal activation occurring after 3-10 min (Piali et al. 1998).

Similar experiments were performed as a third assay of bioactivity. T cells were left to adhere under static conditions to monolayers of transfected CHO cells. Non-adherent or loosely adherent cells were washed away using a physiologic shear rate of 1 dyn/cm^2. Significantly more T cells remained adherent to CXCL10-mucin-GPI transfected CHO cells than to cells expressing the negative control

protein sEGFP-GPI. CXCL10-GPI transfected cells showed a clear positive trend, but were less efficient than cells expressing CXCL10-mucin-GPI. The presence of the mucin domain thus played a role in the adhesion process, as T cell counts were higher on cells expressing the CXCL10 fusion protein containing this domain as compared to cells expressing only membrane-anchored CXCL10. Based on the calcium mobilization experiments, it appeared that the CXCR3 receptor was more efficiently triggered by the CXCL10 protein presented by the mucin domain. In subsequent laminar flow assays however, CXCL10-mucin-GPI was also found to directly enhance leukocyte binding under flow (see below). Thus, adherence to CXCL10-mucin-GPI transfected CHO cells may in part have been mediated by this effect. In future studies, antibodies able to detect activated integrins or block their activity can be used to dissect the effects of leukocyte activation from direct binding to CXCL10-mucin-GPI.

In summary, the described *in vitro* experiments showed on multiple levels that the GPI-anchored CXCL10 fusion proteins were able to efficiently induce CXCR3 signaling. Thus, the structure of the chemokine domain was not compromised by fusing it to the mucin domain of CX3CL1, an important prerequisite for the applicability of the proteins.

4.3 The recombinant fusion proteins can be purified by affinity chromatography

In the next phase of the study, the recombinant proteins were purified from CHO cell extracts. Since the proteins were anchored to the cell membranes via a hydrophobic GPI anchor structure, detergents had to be used to allow solubilization of the proteins. An assay was established based on works by Bumgarner and colleagues that allowed direct quantification of the relative amounts of solubilized and non-solubilized proteins following the application of different detergents (Bumgarner et al. 2005). In these experiments, n-Dodecyl-β-D-maltoside (DDM) proved to be most efficient in solubilizing all GPI-anchored proteins under study. The fact that other commonly used detergents such as Triton X-100 were less efficient is not surprising as GPI-anchored proteins are known to associate with cholesterol-rich microdomains within the cell membrane, which may cause resistance to solubilization with weak detergents such as Triton X-100 (Cerneus et al. 1993; Schroeder et al. 1998). In addition, DDM is a gentle detergent commonly used for solubilizing membrane proteins in their native state, both for crystallization and functional studies (Wiener 2004; Reisinger and Eichacker 2008). Notably, identical results were also obtained with proteins containing a CXCL8 chemokine head (see 5.1), suggesting that DDM may be generally applied for the solubilization of this novel class of reagents. This might facilitate broader application of the technique.

Considerable efforts were made to develop robust purification protocols for the GPI-anchored chemokine fusion proteins without the use of an affinity tag. As chemokines bind strongly to GAG molecules, heparin affinity chromatography was applied, as well as anion and cation exchange chromatography. However, no combination of these methods yielded pure enough protein

preparations for cell painting. Purification factors were generally too low, and enhanced aggregation phenomena were observed that were associated with the changes in salt concentration used during the various elution steps. In addition, attempts to generate custom-built affinity resins using antibodies against the chemokine domain (e.g. for the CXCL8 fusion proteins) failed because the proteins bound too strongly to the antibodies, resulting in extremely poor recovery rates (these methods typically require special antibodies with low avidity). Therefore it was decided to integrate an affinity tag into the constructs. The choice of a suitable tag was complicated by the GPI anchor at the C-terminus and the need for an untouched N-terminus to preserve chemokine activity. Therefore, most commonly used protein tags that are attached at either the N- or the C-terminus could not be used. Cleavable N-terminal tags would have had to be integrated between the secretion signal sequence and the first amino acid of the mature chemokine, which proved technically difficult. Most cleavable tags also leave one or two amino acids behind at the N-terminus after cleavage, which was not acceptable with regards to chemokine function. For these reasons, the c-myc epitope tag was chosen as it could be integrated internally into the proteins preceding the GPI anchor, a commercially available affinity resin was available for purification and monoclonal antibodies were available for detection purposes. Through use of the commercially available affinity resin, sufficiently pure protein preparations were obtained that allowed subsequent functional studies. The proteins were not purified to homogeneity, but very pure protein preparations can enhance protein degradation and aggregation (Bondos and Bicknell 2003; Cromwell et al. 2006), the latter being a tendency which is strongly inherent to both membrane proteins and chemokines (Luster et al. 1995). Therefore, some level of impurity was acceptable for the purposes of the present study, also as impurities in the protein preparations could effectively be controlled by using the identically purified sEGFP-GPI control protein. Importantly, the purification protocol could be applied for the purification of all of the CXCL10 fusion proteins, the CXCL8 fusion proteins (compare 5.1) and the sEGFP-GPI control protein. Thus, the use of the c-myc epitope tag could greatly facilitate the expansion of the basic concept described in the present study to a broader context.

4.4 Purified GPI-anchored proteins can be used to paint primary endothelial cells

When untransfected CHO cells or endothelial cells were incubated with purified GPI-anchored fusion proteins, the proteins were incorporated into the target cell membranes as determined by surface staining using either FACS or immunofluorescence microscopy. Incorporation occurred only with GPI-anchored proteins and was therefore not due to interactions with cell surface molecules. This is at first sight in contrast to the fact that some endothelial cells are able to immobilize chemokines on their surface via GAG molecules - an essential prerequisite for leukocyte recruitment. However, the required GAG molecules are generally only upregulated as response to inflammatory stimuli (von

Hundelshausen et al. 2001). For example, we could detect binding of soluble CXCL10 to primary endothelial cells only after their pre-activation using IL-1β or TNF-α. Therefore, in our studies the GPI anchor was included to help facilitate the presentation of the chemokine fusion proteins on unactivated endothelial cells or tumor endothelial cells. Of note, GAG molecules required for normal chemokine presentation are often dysregulated in tumor endothelial cells, underlining the need for a GPI anchor for the proteins to function in a tumor setting (Sanderson et al. 2005).

As a second proof of the GPI anchorage, "painted" endothelial cells were treated with phosphatidyl-inositol-specific phospholipase C (PI-PLC), an enzyme which cuts the GPI anchor structure, thereby releasing the proteins from the cell surface. This treatment markedly reduced the surface signal after incorporation, verifying GPI anchorage of the proteins. The fact that the proteins could not be entirely removed from the cell surface by PI-PLC treatment may be explained by the relatively low enzyme concentration used in the experiments or by oligomerization effects of the incorporated proteins leading to retention of the protein complex on the surface.

4.5 CXCL10-mucin-GPI can recruit leukocytes *in vitro*

The central hypothesis of the present study was that CXCL10-mucin-GPI would, when it is injected into a tissue, integrate into cell membranes and enhance the recruitment of leukocytes carrying the CXCR3 receptor. Laminar flow assays were performed in order to test this hypothesis in a defined *in vitro* system. These assays were based on microscopic channels of rectangular geometry, in which the conditions found in the postcapillary microvascular bed could be closely mimicked. Primary microvascular endothelial cells were grown in the channels, pretreated with purified proteins and leukocytes were then perfused over the endothelial cell monolayer at a defined shear stress. Real-time video microscopy allowed the identification and categorization of adhesive events occurring between the leukocytes and the endothelial cells.

All assays were performed with non-activated, resting endothelial cells that normally do not support leukocyte adhesion, because CXCL10-mucin-GPI was designed to work under conditions where leukocyte recruitment is defective due to endothelial cell anergy. This is a phenomenon associated with tumor endothelium where upregulation of adhesion molecules on endothelial cells in reaction to proinflammatory cytokines fails, allowing the endothelial cells to remain in a resting-like state, and forcing interventional strategies to be efficient without endogenously upregulated endothelial adhesion molecules (Griffioen et al. 1996a; Griffioen et al. 1996b; Griffioen et al. 1998; Tromp et al. 2000; Dirkx et al. 2003).

Flow experiments were performed using NK cells as well as T cells as model leukocytes because both cell types have important functions in tumor rejection, and are potential targets of the CXCL10 chemokine fusion proteins. Studies involving NK cells were mostly performed using the human NK

cell line YT. Here it could be shown that endothelial cells treated with less than 1 nM CXCL10-mucin-GPI acquired the ability to bind freely flowing NK cells under conditions of physiologic flow, leading to an accumulation of NK cells on the endothelial cell layer. In contrast, NK cells did not adhere to endothelial cells treated with the sEGFP-GPI negative control protein, indicating that potential byproducts of the protein purification procedure or the incorporation of a GPI-anchored protein per se did not activate the endothelial cells in terms of adhesion molecule induction. Also CXCL10-GPI, a fusion protein lacking the mucin domain, could not induce significant amounts of adhesion. The presence of the mucin domain thus plays a central role in the recruitment of leukocytes by CXCL10-mucin-GPI. Treatment of the endothelial cells with soluble CXCL10, even at much higher concentrations than the GPI-anchored proteins, did also not induce adhesion of NK cells. This indicated that CXCL10 itself did not lead to an activation of the endothelial cells in terms of upregulation of adhesion molecules.

Nevertheless, the GPI-anchored CXCL10 fusion proteins may still have direct effects on endothelial cells with regards to proliferation and angiogenesis as CXCL10 is known to efficiently inhibit both processes (Angiolillo et al. 1995; Luster et al. 1998; Romagnani et al. 2001; Lasagni et al. 2003; Feldman et al. 2006; Campanella et al. 2010). Inhibition of angiogenesis can in turn control tumor growth, suggesting a potential additive antitumor effect of CXCL10-mucin-GPI. In mouse models it has recently been shown that angiostatic therapy can synergize with adoptive T cell therapy, leading to significantly enhanced tumor growth inhibition (Shrimali et al. 2010; Dings et al. 2011). A first indication for an antiproliferative activity of the CXCL10 fusion proteins was found in the present study when it was attempted to express CXCL10-GPI and CXCL10-mucin-GPI in endothelial cells. The expression of both proteins lead to a dramatically reduced proliferation in combination with a high rate of apoptosis, suggesting an inhibitory effect of the proteins on endothelial cell growth (data not shown). Thus, in CXCL10-mucin-GPI, the angiostatic activity of CXCL10 might synergize with the effects on leukocyte recruitment, making this reagent even more attractive for tumor therapy.

In the present study, no construct was generated that expressed the mucin domain alone without any chemokine head. Thus, it cannot be excluded that the observed effects were generated by the mucin domain itself rather than by the combination of a chemokine with the mucin domain. However, in previous studies it has been shown that the mucin domain alone does not have an effect on leukocyte recruitment (Imai et al. 1997; Fong et al. 2000). In addition, the CX3CL1 mucin domain can be functionally replaced with unrelated protein modules, as long as the chemokine domain is still protruded away from the cell membrane (Fong et al. 2000), making it unlikely that the mucin domain itself is responsible for the observed effects.

It was found that CXCL10-mucin-GPI was able to induce both rolling and tight adhesion of NK cells. This was an important finding as tight adhesion is considered to be a prerequisite for diapedesis of

leukocytes through the endothelium, which represents the final step of the recruitment cascade (Springer 1994). In combination with the results described in 3.2, where it was shown that the chemokine domain of the recombinant CXCL10 fusion proteins was able to stimulate the CXCR3 receptor on leukocytes, it seems possible that the observed tight adhesion to the endothelium was mediated in part by activation of the NK cells through the chemokine head leading to increased integrin affinity, while the presence of the mucin domain was required to initiate rolling adhesion.

Of note, this finding is in contrast to observations made with CX3CL1 itself. CX3CL1 directly induces tight adhesion in leukocytes, without involving rolling adhesion (Haskell et al. 1999). In addition, CX3CL1 does not upregulate integrin affinity, and adhesion between CX3CL1 and CX3CR1 works in the presence of pertussis toxin or when CX3CR1 is mutated so that it cannot transmit intracellular signals, underlining the independence of this protein pair from other adhesion molecules (Haskell et al. 1999). Haskell and colleagues have shown that this complete independence from other adhesion molecules does not necessarily hold true for combinations of other chemokines with the CX3CL1 mucin domain (Haskell et al. 2000). Under flow, such fusion proteins were all less efficient in binding leukocytes than the original CX3CL1 protein. However, Haskell et al. performed experiments with purified proteins immobilized on glass slides in the absence of other ligands such as ICAM-1. We also performed experiments in which the soluble CXCL10-mucin-Stop protein was immobilized on a glass surface. These experiments failed to demonstrate significant functionality of CXCL10-mucin-Stop alone (data not shown). Considering that in the present study CXCL10-mucin-GPI was found to be highly effective in an endothelial cell context, it seems likely that recombinant chemokine/mucin domain fusion proteins rely at least in part on the upregulation of integrin affinity by the chemokine head and require the presence of some degree of integrin counterparts on the endothelial side to convert rolling adhesion induced by the mucin domain into tight adhesion. Closer investigation of the differences between the mechanisms of adhesion induced by chemokine/mucin domain fusion proteins and the original CX3CL1 chemokine will be performed in future studies.

Another aspect influencing the efficiency of CXCL10-mucin-GPI is the cell type under study. While the protein was highly efficient in recruiting NK cells, no significant *in vitro* activity could be demonstrated when $CD8^+$ T cells were used. At physiologic flow, no adhesion of T cells to endothelial cells treated with CXCL10-mucin-GPI could be detected and even when the flow rate was lowered to subphysiologic levels, the number of adhesions observed with CXCL10-mucin-GPI did not differ from those observed with the control proteins. Of note, in this case the absolute numbers of adherent T cells were similar to the numbers of NK cells adhering at the same flow rate to endothelial cells treated with the control proteins, indicating that no general adhesion defect was present in the T cells. Little is known about the differences between NK cells and T cells regarding chemokine-mediated recruitment mechanisms at physiologic flow. To our knowledge no studies have been

published directly comparing these two cell types *in vitro*. In principle NK and T cells follow the classical scheme of leukocyte recruitment mediated by selectins, chemokines and integrins in combination with immunoglobulin superfamily molecules, although much more is known about T cells than NK cells (Bianchi et al. 1993; Laudanna and Alon 2005; Grégoire et al. 2007). Given the current knowledge about the chemokine system, it is however not surprising that the two cell types respond differently to identical stimuli. It has been shown that the same chemokine can differently influence the induction of tight adhesion of different lymphocyte subsets. In a study by D´Ambrosio and colleagues, CCL17 (a chemokine binding to CCR4) could induce tight adhesion of Th2, but not of Th1 $CD4^+$ T cells, although both cell types express the CCR4 receptor. In contrast, CCL22, another chemokine binding to the same receptor, could induce tight adhesion of both Th1 and Th2 cells. Similar effects have been observed for the CXCR3 ligands CXCL9 and CXCL11, and this mechanism has been proposed as an explanation for the question how a plethora of seemingly redundant chemokines can mediate specific effects (D'Ambrosio et al. 2002). A greater sensitivity of NK cells towards relatively low chemokine concentrations would also make sense from a biologic standpoint because NK cells, as part of the innate immune system, are designed to respond early in a developing infectious process. T cells, by contrast, are often recruited at later stages of the inflammation, when higher chemokine concentrations may be present as compared to the early phases. In experimental models of viral infection, it has also been shown that NK cell infiltration precedes infiltration with T cells, and that the recruited NK cells produce high levels of IFNγ – a cytokine known to induce CXCL10 expression (Hussell and Openshaw 1998).

The earlier experiments demonstrating that the CX3CL1 chemokine head can be functionally replaced with other chemokines were performed using either transfected K562 cells (an erythroleukemia line) or unsorted PBMCs, thus not allowing identification of the exact cell types recruited (Imai et al. 1997; Fong et al. 2000). Therefore, these experiments cannot provide clues as to if the efficiency of this approach varies among different leukocyte types.

Given the hypothesis that T cells and NK cells are differently sensitive towards recruitment by CXCL10-mucin-GPI, higher protein concentrations on the endothelium may be able to generate detectable effects of CXCL10-mucin-GPI also for T cells. In order to establish an experimental system with very high surface levels of CXCL10-mucin-GPI, we attempted to stably transfect immortalized endothelial cells with the recombinant constructs (data not shown). However, transfection with CXCL10-GPI or CXCL10-mucin-GPI lead to severely impaired proliferation of the cells in combination with a very high rate of apoptosis. Furthermore, the few clones that grew out under selection displayed only minimal CXCL10 surface levels (while the sEGFP-GPI protein was expressed at very high levels), indicating that cells with high CXCL10 expression levels were negatively selected. This

inhibitory effect of CXCL10 on endothelial cells is well documented in the literature and prevented use of the transfected cells in laminar flow assays (Angiolillo et al. 1995; Feldman et al. 2006).

Another means to increase surface levels of CXCL10-mucin-GPI would be to increase protein yields in the purification process. It was however not possible to isolate much higher amounts of protein with the protocol developed in the current study, mostly due to limitations at the cell culture level. Attempts to increase the expression levels of the GPI-anchored proteins by methotrexate treatment did not provide sufficient increases in protein levels. Therefore, future protein isolation protocols will need to make use of much higher cell numbers. As a first step in this direction, the transfected CHO cells were adapted growth in suspension (shortly described in 5.5). Here, 4-5 x more cells could be harvested from the same volume of medium compared to adherent culture. Additionally, suspension cells could be conveniently grown in spinner flasks, minimizing handling time and allowing the generation of much higher cell numbers. These improvements could in the future enable the isolation of significantly higher amounts of GPI-anchored proteins.

In addition to fostering selective leukocyte recruitment, the recombinant chemokines may also have other effects. CX3CL1 and CXCL10 have both been shown to activate NK cells leading to higher efficiency of target cell lysis (Taub et al. 1995; Saudemont et al. 2005; Zhang et al. 2006). To test if tumor treatment with the GPI-anchored proteins could also enhance NK killing, chromium release assays were performed, in which the ability of human NK cells to lyse target cells pretreated with CXCL10-mucin-GPI was determined (see 5.4). Freshly isolated primary NK cells with and without IL-2 activation were tested against two different target cell lines (K562 and RCC26). It was found that treatment of target cells with CXCL10-mucin-GPI or commercially available CXCL10 had no significant effect on lysis efficiencies compared to the buffer control, at least at the concentrations studied. Also here, higher amounts of protein might reveal previously undetected effects.

4.6 CXCL10-mucin-GPI can recruit leukocytes *in vivo*

The efficiency of CXCL10-mucin-GPI on leukocyte recruitment was not only assessed using *in vitro* systems, but also in a murine tumor model *in vivo*. Since the chemokine head in the fusion proteins was of human origin, it was first established that human CXCL10 is able to activate murine CXCR3. Here, human and murine CXCL10 were found to elicit identical levels of calcium mobilization and receptor internalization in $CXCR3^+$ murine T cells (see 5.2). In addition, CXCL10-mucin-GPI was found to efficiently induce the adhesion of primary murine NK cells *in vitro*, suggesting orthogonality of the fusion protein.

A subcutaneously implantable tumor model was used for *in vivo* experiments. Such a model was the most suitable for the present study as the aim was to provide proof of principle for the activity of CXCL10-mucin-GPI with regards to recruitment and not for therapeutic efficacy resulting in reduced

tumor growth or other endpoints. The cell line used for tumor implantation was derived from a spontaneously arising B cell lymphoma in mice expressing the c-myc oncogene under the control of the Igλ promoter (Kovalchuk et al. 2000). This would also allow direct verification of the results in the spontaneous model (which is currently underway).

The implanted tumors appeared well vascularized in H/E staining and thus constituted a good model system for the analysis of induced recruitment of leukocytes from the blood stream. Moreover, they displayed little signs of necrosis that could have interfered with the analyses.

Immunohistology was performed to detect $CD3^+$ infiltrates in the tumors using previously described antibodies (Vielhauer et al. 2009). Here, a pronounced infiltration was observed even in untreated tumors. This is in agreement with findings made in the spontaneous variant of the tumor model, where a strong infiltration of diseased lymph nodes with T cells was observed (Brenner, 2009; PhD thesis LMU). In the present study, it was found that secondary lymphoid structures were often resected together with the tumors. These structures contained large numbers of $CD3^+$ cells. Immunohistology was thus the only feasible way to analyze T cell infiltrates in the tumors as this technique allowed exclusion of these structures from analysis (see 5.3).

In order to assess tumor infiltration with T cells induced by CXCL10-mucin-GPI, the various proteins were injected into grown tumors, and subsequent leukocyte infiltrates were analyzed four hours later. Tumors treated with CXCL10-mucin-GPI harbored on average the highest numbers of $CD3^+$ cells, while tumors treated with the same molar amount of soluble CXCL10 or sEGFP-GPI on average contained about 33% less $CD3^+$ cells. Even 500 x higher molar amounts of soluble CXCL10 were less efficient than CXCL10-mucin-GPI. Nevertheless, the differences were not deemed statistically significant due to the low numbers of animals, and the large variances between single tumors of the same treatment condition. Thus, caution must be taken in interpreting the results. In future studies using modified experimental setups, the effects of the different CXCL10 species may prove significant. Notably, the low increase in infiltration by $CD3^+$ cells compared to NK cells (see below) reflected the results obtained *in vitro*, where CXCL10-mucin-GPI was efficient for the recruitment of NK cells, but not for T cells.

NK cells were detected immunohistologically with polyclonal antibodies against NKp46. These antibodies have been described for the detection of NK cells *in situ* by immunofluorescent staining of frozen sections (Walzer et al. 2007) and the staining was validated in our laboratory on formalin-fixed paraffin sections of spleens of C57/Bl6 mice (data not shown), where the same staining pattern was found as described by Walzer and colleagues on frozen sections (Grégoire et al. 2007; Walzer et al. 2007). To our knowledge, the current study is the first to describe the use of polyclonal NKp46-specific antibodies for the detection of NK cells in formalin-fixed paraffin sections. A recent

publication however showed the use of another NKp46-specific antibody on the same type of sections to detect NK cell infiltrates in tumors (Guerriero et al. 2011).

A relatively low infiltration of tumor centers with NKp46$^+$ cells was observed. In contrast, some tumors contained large amounts of NKp46$^+$ cells at the periphery. This highly unequal distribution of NK cells, although being an interesting finding, made it difficult to quantify NK cells infiltrates from immunohistological stainings. For this reason, and because of the relatively scarce evidence in the literature for the function and specificity of the polyclonal NKp46-antibodies, it was decided to quantify NK cell infiltrates by FACS. Importantly, the secondary lymphoid structures described above contained only few NKp46$^+$ cells, thereby allowing to use FACS for the quantification of NK cell infiltrates (see 5.3).

The trends observed for NK cell counts (defined as CD3$^-$ NK1.1$^+$ cells among the total cell counts) were much more pronounced than those seen for T cells. Tumors treated with CXCL10-mucin-GPI contained on average 8.5 x more NK cells than untreated tumors. Also, application of CXCL10-mucin-GPI was more effective than soluble CXCL10 at the same molar amount or even at 500-fold molar excess. The observation that CXCL10-mucin-GPI had a stronger effect on NK cell recruitment compared to T cell recruitment again mirrored the results of the *in vitro* experiments.

NK cells present in tumors treated with CXCL10-mucin-GPI or high amounts of soluble CXCL10 displayed an about 50% stronger surface staining for CXCR3 than NK cells recruited into untreated or sEGFP-GPI treated tumors (as assessed by the MFI values; data not shown). The signals on NK cells in tumors treated with low amounts of soluble CXCL10 (identical to CXCL10-mucin-GPI) ranged between the two extremes. This accumulation of strongly CXCR3-positive NK cells suggests that the cells were recruited via the CXCL10/CXCR3 axis. The degree of sensitivity of a given cell type towards a chemokine ligand also depends on the expression level of the receptor (D'Ambrosio et al. 2002). Thus, the recruited highly CXCR3-positive NK cells might constitute a strongly CXCL10-sensitive subset of NK cells that is consequently most effectively targeted by CXCL10. The time difference of four hours between the injection and the analysis might hereby be long enough for the NK cells to replenish surface CXCR3 that has been internalized upon recruitment (Meiser et al. 2008).

A series of questions remain to be answered regarding the *in vivo* mechanism of action of CXCL10-mucin-GPI. First, the evaluation of the potential therapeutic effect of CXCL10-mucin-GPI in terms of tumor growth is a central question. Here, also studies are planned using adoptive transfer of T or NK cells. Furthermore, in the current study we were not able to detect incorporated CXCL10-mucin-GPI proteins immunohistologically due to the low concentrations of purified proteins applied (data not shown). When higher amounts of purified proteins can be produced using the cell culture system described above and in 5.5, the detection of incorporated proteins *in situ* should become possible. This information would allow correlating the positions of leukocytes within the tumors to the

gradient of CXCL10-mucin-GPI. Thereby, the question if a stable CXCL10-mucin-GPI gradient can be used by recruited leukocytes for haptotaxis towards the tumor center may be answered, assessing another potentially important effect of CXCL10-mucin-GPI.

In summary, the current study showed that CXCL10-mucin-GPI can be used to enhance recruitment of $CXCR3^+$ leukocytes *in vitro* and strongly suggested that the positive effects hold true also *in vivo* in a tumor setting. Following this first proof of principle, the underlying concept of a chemokine head fused to the mucin domain of CX3CL1 and a GPI anchor signal sequence may be expanded into a broader family of reagents that allow targeted recruitment of cells into various tissues.

5 Addendum

5.1 Purification and characterization of CXCL8-mucin-GPI

The basic objective of this study was to establish the approach of a fusion protein consisting of a chemokine head, the mucin domain of CX3CL1 and a GPI anchor as a novel type of flexible reagents allowing the modification of various tissue micromilieus. Such reagents could have diverse applications ranging from tumor therapy to wound healing or ischemia reperfusion injuries. By utilizing different chemokine heads, the specificity of the respective fusion proteins could be redirected towards virtually any desired subset of cells, as long as the expression of the matching chemokine receptor is reasonably restricted to the desired cell type or types. As proof of concept, the CXCL10 fusion proteins were characterized in great detail as described in the last chapters. However, another set of fusion proteins was additionally generated, expressed and initially characterized that contained a human CXCL8 chemokine head at the N-terminus. The use of this chemokine should allow the recruitment of a subset of highly cytotoxic $CD8^+$ T cells along with neutrophils into tumor tissues (see 1.4). The compositions of the various proteins were identical to the ones of the corresponding CXCL10 fusion proteins except for the chemokine head. The proteins were generated as described in 2.2.3.3, yielding a set of fusion proteins that paralleled the set depicted in Figure 9 (page 55), including constructs with and without the mucin domain and with and without the GPI anchor signal sequence.

Essentially, the procedures which had been developed for the CXCL10 fusion proteins could also be applied for the CXCL8 proteins, including the use of the c-myc epitope tag for purification and detection purposes. A protocol for the solubilization of the proteins was developed using the assay described in 3.3. The results were comparable to those obtained for the CXCL10 proteins (data not shown), indicating that rather the general architecture of the proteins dictated the most efficient detergent than the single chemokine domains. Therefore, n-Dodecyl-β-D-maltoside could potentially be applied to solubilize all chemokine fusion proteins generated in the here described way, a finding which should facilitate broader application of this technique.

As an example, Figure 28 shows the expression (A), purification (B) and incorporation (C) of CXCL8-mucin-GPI. As depicted in panel A, CXCL8-mucin-GPI could readily be detected on the surface of transfected CHO cells. The same was true for cells transfected with CXCL8-GPI, while cells expressing the soluble CXCL8-Stop or CXCL8-mucin-Stop proteins could as expected not be stained (data not shown). These findings indicated that also the CXCL8 fusion proteins were correctly anchored to the cell membrane via their GPI anchor and not by nonspecific binding via the chemokine or the mucin

domains. As found also for the CXCL10 proteins, treatment with methotrexate could be used to eliminate cells with a low expression level (data not shown).

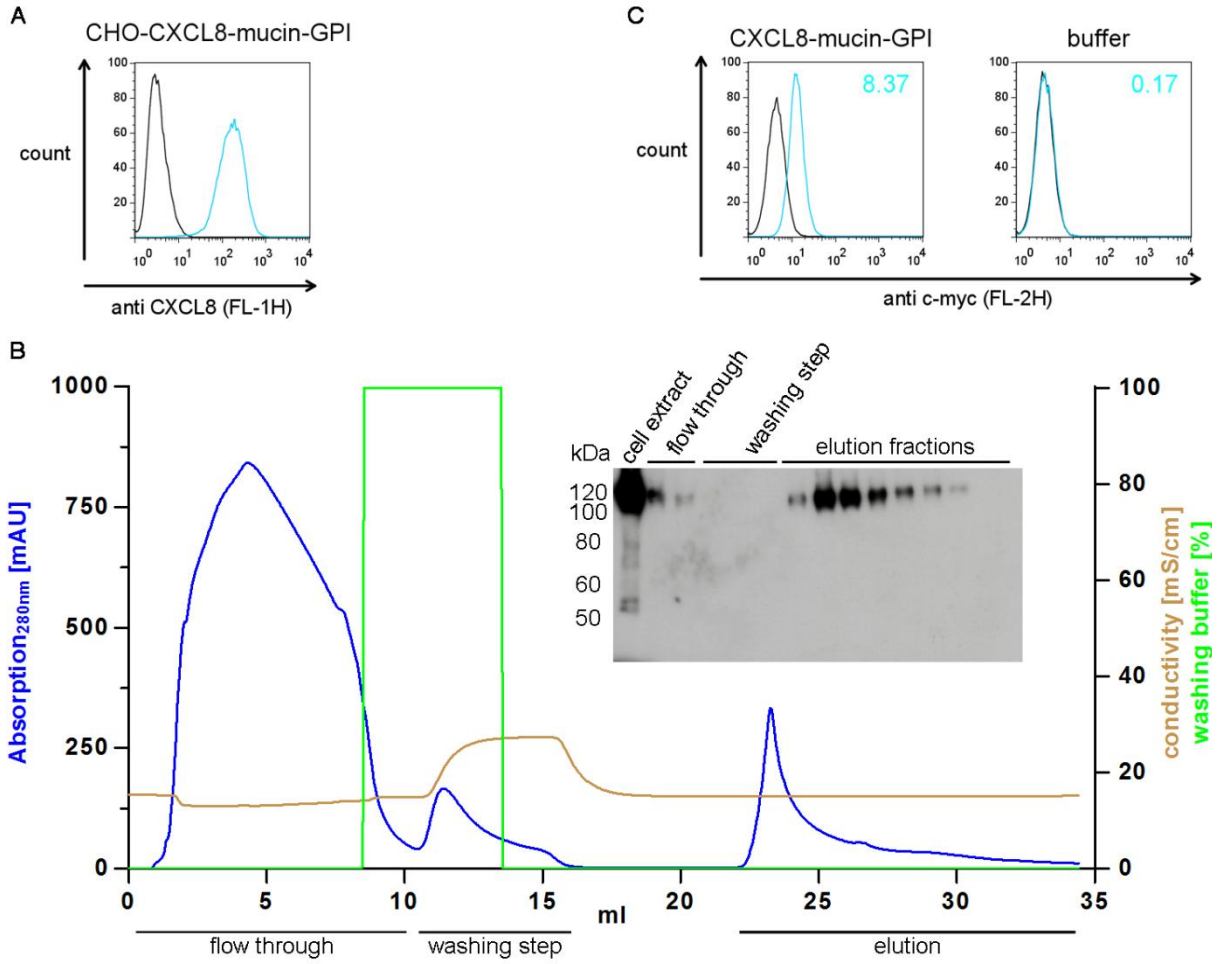

Figure 28: CXCL10-mucin-GPI can be expressed, purified and incorporated into endothelial cells using the procedures established for CXCL10-mucin-GPI. A: CXCL8-mucin-GPI can be detected on the surface of transfected CHO cells. Stably transfected CHO cells were incubated with CXCL8-specific antibodies (blue line) or isotype-matched control antibodies (black line). FITC-conjugated secondary antibodies were used to detect bound antibodies and the fluorescence intensity was measured by FACS. **B:** Solubilized CXCL8-mucin-GPI can be purified by affinity chromatography. Cell extracts from transfected CHO cells were applied to an anti c-myc affinity resin. Following a washing step at high salt concentration, proteins were eluted using c-myc peptides. The UV absorption as a measure of protein content (blue line) and the conductivity as a measure of salt concentration (brown line) were continuously measured. The green line represents the percentage of washing buffer applied to the column. Chromatography fractions were subjected to western blotting using CXCL8-specific antibodies (insert). **C:** Purified CXCL8-mucin-GPI incorporates into the cell membranes of micro-vascular endothelial cells. Microvascular endothelial cells (HMEC) were incubated with 0.36 nM of purified CXCL8-mucin-GPI or a buffer control, with both samples being diluted in medium at the same ratio. The cells were washed and incorporated proteins on the surface were detected by FACS analysis using anti c-myc primary and RPE-labeled secondary antibodies. The MFIs (geometric mean of isotype stained sample – geometric mean of anti c-myc stained sample) are given for each condition.

Panel B shows a chromatogram obtained during the purification of CXCL8-mucin-GPI using the same affinity resin as the one used for the purification of the CXCL10 proteins. Additionally, a corresponding western blot of the chromatography fractions is shown. Western blots of the CXCL8 proteins were performed using CXCL8-specific antibodies which were purified from culture supernatants of a hybridoma cell line. In the blots, CXCL8-mucin-GPI predominantly appeared in a dimeric form with an apparent molecular weight of about 120 kDa, while the monomeric form with 50-60 kDa was less abundant. The difference between the apparent molecular weights of monomeric CXCL10-mucin-GPI (45-50 kDa) and CXCL8-mucin-GPI (50-60 kDa) and also the relative amounts of monomeric versus dimeric forms were most likely due to the fact that western blots for CXCL10 were performed under reducing conditions, while the antibody against CXCL8 required non-reducing conditions. The western blot depicted in panel B shows that the majority of specific proteins could be recovered in the elution fractions with relatively little loss in the flow through, indicating that the large amount of proteins that did not bind to the column and was removed in the flow through and the washing step (see chromatogram) contained mostly contaminating proteins.

Panel C illustrates the ability of purified CXCL8-mucin-GPI proteins to incorporate into the cell membranes of endothelial cells. Microvascular endothelial cells were incubated with 0.36 nM CXCL8-mucin-GPI or a buffer control, both diluted in medium at the same volumetric percentage. Subsequently, the cells were washed and the presence of CXCL8-mucin-GPI on the surface of the endothelial cells was tested by FACS staining using anti c-myc primary and RPE-labeled secondary antibodies. The histograms show that incorporated CXCL10-mucin-GPI could be detected on the cell surface. The same was found for CXCL8-GPI (data not shown).

These experiments indicated that the principle outlined in this study could easily be expanded to constructs containing other chemokine domains than CXCL10, at least in terms of production of the proteins and incorporation of purified proteins into various cells. It will be an interesting question to be adressed in future studies whether recombinant proteins containing other chemokine heads are also bioactive.

5.2 Murine and human CXCL10 have identical effects on murine CXCR3$^+$ cells

In order to assess the effects of human and murine CXCL10 on murine cells, calcium mobilization and receptor internalization assays were performed, analogous to those applied in 3.2 to verify the bioactivity of the recombinant proteins. A murine T cell line (kindly provided by F. Lehmann, Helmholtz Zentrum Munich) was used as target cells, which had been shown to be CXCR3-positive (data not shown) and was available in sufficiently high numbers for the experiments.

For calcium mobilization assays, cells were loaded with the calcium-sensitive fluorescent dye Fluo-4 as described in 2.2.5.2.1. Using a FACS machine, the fluorescence of the cells was measured over

time. After 30 sec, commercially available human or murine CXCL10 at final concentrations of 1 µg/ml or a buffer control was added to the cells and the fluorescence was followed for an additional 3 min. Dead cells were identified by 7-AAD staining and excluded from the analysis.

Analysis of CXCR3 internalization was performed as described in 2.2.5.1.4. Briefly, murine T cells were incubated with 660 ng/ml of human or murine CXCL10 or a buffer control for 30 min at 37°C. Subsequently, the cell surface level of CXCR3 in each sample was determined using APC-labeled, CXCR3-specific antibodies. FACS was used to determine fluorescence intensities, while dead cells were identified by PI staining and excluded from the analysis. The results were expressed as percent CXCR3 surface signal with the fluorescence intensity of the buffer control defined as 100%. Figure 29 shows the results of both experiments.

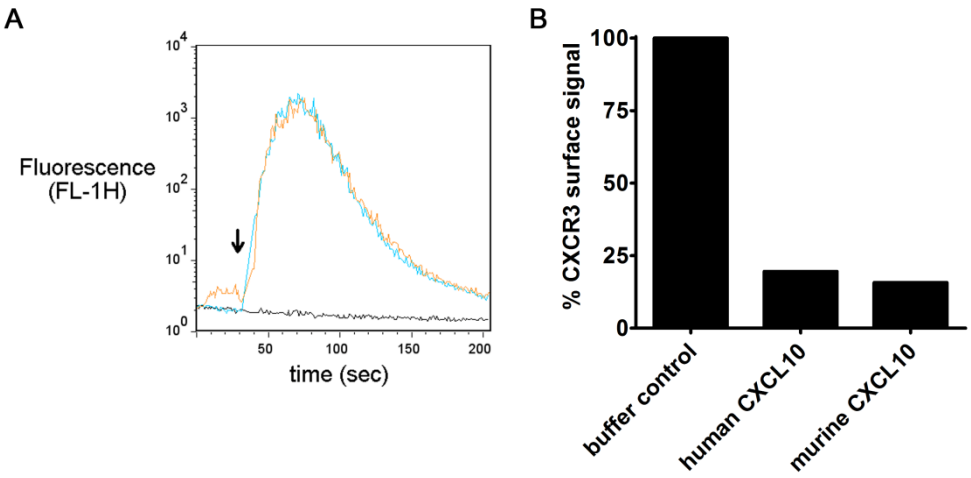

Figure 29: Human and murine CXCL10 elicit comparable levels of calcium mobilization and CXCR3 internalization on murine cells. A: Calcium mobilization. Murine CXCR3-positive cells were loaded with a calcium-sensitive fluorescent dye. The fluorescence in the population was continuously monitored by FACS. After 30 sec (black arrow), 1 µg/ml (115 nM) human (orange line) or murine (blue line) CXCL10 or a buffer control (black line) were added to the samples and the fluorescence was monitored. **B:** CXCR3 internalization. Murine $CXCR3^+$ T cells were incubated for 30 min with 660 ng/ml (76 nM) of human or murine CXCL10 or a buffer control and the CXCR3 surface levels were subsequently determined by FACS analysis. The fluorescence intensity in the buffer control was set as 100% and the levels of the other samples related to it.

Panel A depicts the results of the calcium mobilization analyses with the fluorescence intensities of single cells as a measure of intracellular calcium levels plotted against the time. A pronounced transient fluorescence signal was observed after addition of either human or murine CXCL10 (orange and blue line, respectively). In the buffer control (black line), no fluorescence signal was observed as had been expected. The curves obtained in the samples with murine and human CXCL10 were virtually identical, both in terms of maximal signal strength and signal duration. Thus, CXCL10 from both species elicited identical responses in terms of calcium mobilization, which indicated that both chemokines were similarly effective at triggering the CXCR3 receptor.

Panel B depicts the results of the analysis of CXCR3 internalization. Here, the CXCR3 surface levels were decreased to 19.6% after incubation with human CXCL10 and to 15.7% with murine CXCL10. According to our experience with similar experiments, the difference of 3.9% was within the experimental variation, although the experiment presented here was not repeated often enough to prove this assumption statistically.

In summary, human CXCL10 was as effective as the murine pendant in triggering the murine CXCR3 receptor as assessed by calcium mobilization and receptor internalization.

5.3 Additional immunohistological findings

In the immunohistological analysis of the subcutaneously implanted tumors (see 3.7) it was noted that at the margins of many tumors, secondary lymphatic organs had been resected together with the tumor. These organs clearly were not parts of the primary tumors. However, in order to analyze the influence of this finding on the analysis of infiltrates by FACS, immunohistological stainings were performed to detect $CD3^+$ and $NKp46^+$ cells. Figure 30 shows representative images of one of these structures.

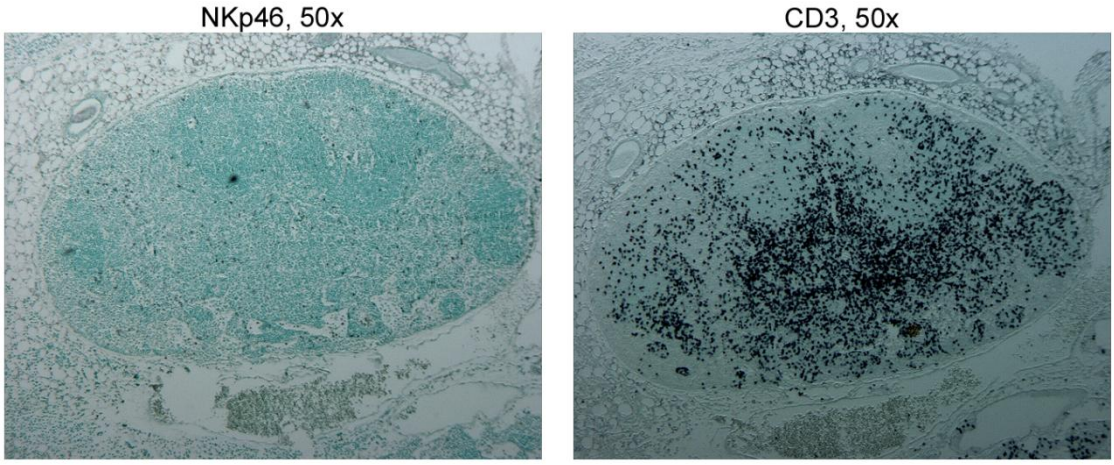

Figure 30: Secondary lymphatic organs co-resected with some subcutaneous tumors contain large numbers of T cells, but very few NK cells. Tumors were implanted subcutaneously in C57/Bl6 mice using the 291 cell line. Following excision, tumors were fixed with formalin and tumor sections were stained for the presence of $NKp46^+$ or $CD3^+$ cells. While the structures contained numerous $CD3^+$ cells (dark grey/ black staining), only very few $NKp46^+$ cells were found. Both images were acquired using 50 x magnification.

The staining showed that the described organs contained numerous $CD3^+$ cells, as it would be expected for a secondary lymphatic organ. Thus, the presence of these organs in the resected tumors ruled out the possibility to analyze T cell infiltrates by FACS. In contrast, only very few $NKp46^+$ cells were found to reside within the described organs, indicating that FACS analysis could still be used to characterize NK cell infiltration.

5.4 CXCL10-mucin-GPI on target cells does not enhance killing by NK cells

For NK cells, it has been shown that the presence of CX3CL1 on target cell surfaces can enhance tumor cell lysis (Zhang et al. 2006; Zhang et al. 2007). In addition, also CXCL10 has been shown to activate NK cells leading to higher amounts of granule exocytosis and enhanced target cell lysis (Taub et al. 1995; Taub et al. 1996). Therefore, it was hypothesized that the presence of CXCL10-mucin-GPI on target cells would also enhance NK cell mediated killing. This would represent an additional beneficial effect of the GPI-anchored protein in an adjuvant setting for tumor therapy, as treatment of the tumors with CXCL10-mucin-GPI might in this case not only enhance recruitment but also directly influence tumor cell clearance by recruited NK cells. Chromium release assays were conducted in order to test this hypothesis. In such assays, target cells are labeled with radioactive Chromium and subsequently incubated with effector cells. Cell-mediated lysis of the target cells results in release of Chromium into the medium, which can be quantified and expressed as percentage of target cell lysis.

Human NK cells were isolated from peripheral blood as described in 2.2.5.5 and experiments were performed using both freshly isolated cells and such that had been activated by an overnight incubation with 500 U/ml recombinant IL-2. Two different target cell lines were used: K562, a human erythroleukemia line, and RCC26, a renal cell carcinoma line, which were both kindly provided by Prof. E. Noessner, Helmholtz Zentrum Munich. The cells were labeled with $Na_2{}^{51}CrO_4$ and subsequently incubated with 0.24 nM of purified CXCL10-mucin-GPI, 14 nM of commercially available CXCL10 or a buffer control. The commercially available CXCL10 was used at a higher concentration than CXCL10-mucin-GPI in order to detect even modest effects mediated by the soluble protein. All samples were diluted in medium and contained the same percentage of chromatography buffer. Following treatment, the target cells were incubated for 4 h with different amounts of NK cells and the radioactivity of the supernatants was measured. The maximal radioactivity of the labeled cells of one well was additionally determined (100% lysis) and readings in the other samples were referred to this value. Figure 31 summarizes the lysis efficiencies for the differently treated target cells at different effector to target (E:T) ratios.

Freshly isolated NK cells were only able to lyse the K562 cell line, with lysis rates ranging from 60% to 4%, depending on the respective E:T ratio. The lysis rates could in this case be influenced neither by incubating the target cells with CXCL10-mucin-GPI nor by treating them with commercially available CXCL10. Activated NK cells, in contrast, mediated lysis of both RCC26 and K562 cells with lysis rates ranging from 75% to 19% for K562 and from 68% to 11% for RCC26. A much higher E:T ratio was required to achieve efficient lysis of RCC26 cells indicating that the stimulus delivered by these cells to the NK cells was weaker than in the case of K562.

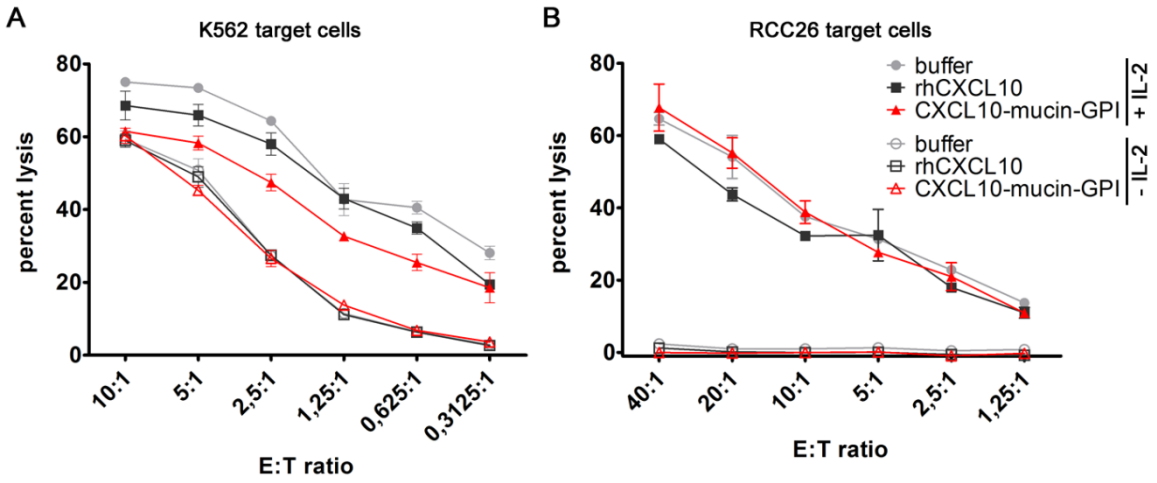

Figure 31: CXCL10-mucin-GPI does not enhance tumor cell lysis by human NK cells. Chromium release assays were performed to investigate the effect of CXCL10-mucin-GPI on NK cell mediated tumor cell lysis. Target cells (K562 in **A** or RCC26 in **B**) were labeled with $Na_2{}^{51}CrO_4$ and subsequently incubated with CXCL10-mucin-GPI (0.24 nM) or commercially available CXCL10 (14 nM). Freshly isolated human NK cells (open symbols) or such that had been activated overnight using 500 U/ml IL-2 (filled symbols) were added at different effector to target (E:T) ratios and the release of ^{51}Cr was used to quantify the percentage of target cell lysis using the maximal radioactivity of the respective target cells as reference. Symbols represent average values of duplicates +/- standard error of the mean (SEM).

The lysis values for RCC26 cells treated with CXCL10-mucin-GPI did not differ substantially from that of cells incubated with commercially available CXCL10 or the buffer control, indicating that the presence of CXCL10-mucin-GPI on these cells did not enhance the activating stimulus delivered to the NK cells. In the case of the K562 cells, target cells that had been incubated with CXCL10-mucin-GPI displayed the lowest lysis values (62% to 19%), followed by cells treated with normal CXCL10 (66% to 19%), while the highest values were found for the buffer control (75% to 28%). In summary, CXCL10-mucin-GPI on the target cell could not enhance tumor cell lysis by NK cells, at least not at the concentrations tested.

5.5 Adaptation of transfected CHO cells to large-scale suspension culture

In the experiments described in the chapter 3, relatively low amounts of the GPI-anchored proteins were used. These low amounts may have prevented the detection of some physiologic effects of the proteins, for example in the recruitment of T cells (see 3.6.4). However, the production of significantly higher amounts of proteins would require much higher amounts of primary cell culture material, which could not be produced at reasonable cost and effort using adherent cells as described in this study. Therefore, a suspension cell culture system was established as a first step in the direction of producing higher protein amounts. This system should allow the production of much higher amounts of transfected CHO cells in relation to the volume of medium than an adherent

system. Exponentially growing cells were transferred directly into CD CHO medium, a chemically defined serum free medium designed for growing CHO cells in suspension. The medium was exchanged every 3-4 days until the cells had adapted to the new medium. If clusters of cells formed during this time, the cells were singularized using Trypsin/EDTA. FACS analysis was used to ensure maintenance of transgene expression. A slight decrease of protein production could be seen upon transition into suspension growth, which could however be compensated by sorting the cells for high expression by FACS sorting (data not shown). Large numbers of cells were grown in 1 l spinner flasks. The flasks were inoculated with 1.4 x 10^5 cells/ml in a volume of 100 ml and continuously mixed at 50-60 rpm. The medium in the flask was doubled every 3-4 days by addition of fresh medium and the numbers of cells were monitored every day. Figure 32 shows the growth characteristic of a representative suspension culture.

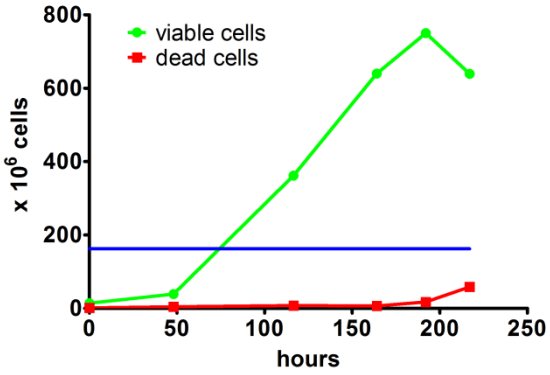

Figure 32: CHO cells grown in suspension culture yield over 4 x more cells than an adherent culture at the same expense of medium. A suspension culture system was established in order to produce larger amounts of cells at reasonable costs. The green line indicates the total numbers of viable cells in the spinner flask, the red line the numbers of dead cells identified by trypan blue staining. The blue line indicates the amount of cells that could be obtained using the same total volume of medium (650 ml) in adherent culture.

The figure indicates that the CHO cells displayed robust growth in suspension culture with up to 1.5 x 10^6 cells/ml. The cell counts usually reached a peak after 7-8 days (green line). At this time, the amount of cells that could be harvested was 4-5 x higher than if the cells had been grown in adherent culture using the same volume of medium (blue line; refers to 650 ml medium). Thus, the suspension culture system should represent a valuable tool for future studies, allowing the isolation of higher amounts of recombinant proteins from higher numbers of cells.

5.6 The GPI anchor signal sequence from DAF does not enhance incorporation

Different GPI-anchor signal sequences may differ in their efficiency to mediate GPI anchor attachment (Chen et al. 2001). If this transfer is inefficient, the proteins can exist as a mixture of transmembrane and GPI-anchored species. This has also been shown for the LFA-3 protein from

which the GPI anchor signal sequence used in the present study was taken (Hollander 1992). For this reason, DNA constructs were generated as described in 2.2.3.1.2 and 2.2.3.2.2 in which the signal sequence from DAF was used instead of the one from LFA-3, the rests of the respective constructs remaining identical to the constructs with the LFA-3 anchor sequence. The proteins were expressed in CHO cells and detected on their cell surface by FACS staining (data not shown). Since cleavage by PI-PLC, which is normally used to test if a given protein is GPI-anchored, was hampered by various effects as discussed above and transmembrane-anchored protein species could not be discriminated from GPI-anchored ones by western blotting or other established methods, the efficiency of incorporation was chosen as functional readout for the degree of GPI anchorage. As only GPI-anchored proteins have the ability to incorporate into cell membranes, the surface signal intensity after incorporation should correlate with the percentage of GPI-anchored proteins. To test this efficiency, CXCL10-mucin-DAFPI was exemplarily purified as described in 2.2.4.1.3 in the same way as and parallel to CXCL10-mucin-GPI (see 3.4). Specific concentrations of both proteins were obtained by ELISA and CHO cells were treated using 0.3 nM of both proteins. Subsequently, the cells were stained with anti c-myc primary and RPE-labeled secondary antibodies and fluorescence intensities were assessed by FACS. Figure 33 shows the results of the FACS staining.

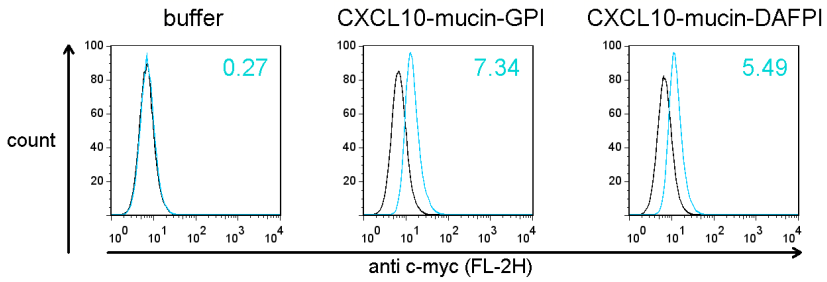

Figure 33: The GPI anchor signal sequence from DAF does not enhance incorporation compared to the signal sequence from LFA-3. In order to compare the reincorporation efficiencies of CXCL10-mucin-GPI and CXCL10-mucin-DAFPI (a protein containing the GPI anchor signal sequence from DAF instead of the one from LFA-3), CHO cells were treated with identical concentrations (0.3 nM) of purified CXCL10-mucin-GPI, CXCL10-mucin-DAFPI or a buffer control and subsequently analyzed by FACS staining for the presence of the GPI-anchored proteins on the cell surface using anti c-myc primary and RPE-labeled secondary antibodies. Histograms are gated on viable cells based on 7-AAD exclusion. Blue lines indicate staining with c-myc specific antibodies, black lines indicate staining with isotype control antibodies. The MFIs are given for every sample.

Both CXCL10-mucin-GPI and CXCL10-mucin-DAFPI incorporated with similar efficiency into the cell membranes of the CHO cells. The MFI was slightly lower for cells treated with CXCL10-mucin-DAFPI as compared to an identical concentration of CXCL10-mucin-GPI. Thus, it was concluded that the GPI anchor signal sequence from DAF was not more efficient in mediating GPI anchor attachment than the signal sequence from LFA-3.

5.7 DNA sequences of the recombinant fusion proteins

Start and stop codons in the respective constructs are underlined, available restriction sites are printed in bold.

Restriction sites	Genes or gene segments
GAATTC: *Eco*RI	CXCL10 gene
GTCGAC: *Sal*I	CXCL8 gene
GCTAGC: *Nhe*I	Double c-myc epitope tag
TCTAGA: *Xba*I	EGFP gene
ACGCGT: *Mlu*I	GPI signal sequence from DAF
	GPI signal sequence from LFA-3
	Mucin domain from CX3CL1
	Secretion signal sequence from TIMP-1

>CXCL10-GPI

GAATTCCCAGTCTCAGCACCATGAATCAAACTGCCATTCTGATTTGCTGCCTTATCTTTCTGACTCTAAGTGGCA
TTCAAGGAGTACCTCTCTCTAGAACTGTACGCTGTACCTGCATCAGCATTAGTAATCAACCTGTTAATCCAAGGT
CTTTAGAAAAACTTGAAATTATTCCTGCAAGCCAATTTTGTCCACGTGTTGAGATCATTGCTACAATGAAAAAG
AAGGGTGAGAAGAGATGTCTGAATCCAGAATCGAAGGCCATCAAGAATTTACTGAAAGCAGTTAGCAAGGAA
AGGTCTAAAAGATCTCCTGCTAGAGAACAGAAGCTGATCAGCGAGGAGGACCTGGAGCAGAAGTTGATCAGC
GAGGAGGACCTGGCTAGAACAACCTGTATCCCAAGCAGCGGTCATTCAAGACACAGATATGCACTTATACCCA
TACCATTAGCAGTAATTACAACATGTATTGTGCTGTATATGAATGTATTATGA**GTCGAC**

>CXCL10-mucin-GPI

GAATTCCCAGTCTCAGCACCATGAATCAAACTGCCATTCTGATTTGCTGCCTTATCTTTCTGACTCTAAGTGGCA
TTCAAGGAGTACCTCTCTCTAGAACTGTACGCTGTACCTGCATCAGCATTAGTAATCAACCTGTTAATCCAAGGT
CTTTAGAAAAACTTGAAATTATTCCTGCAAGCCAATTTTGTCCACGTGTTGAGATCATTGCTACAATGAAAAAG
AAGGGTGAGAAGAGATGTCTGAATCCAGAATCGAAGGCCATCAAGAATTTACTGAAAGCAGTTAGCAAGGAA
AGGTCTAAAAGATCTCCTGCTAGAAATGGCGGCACCTTCGAGAAGCAGATCGGCGAGGTGAAGCCCAGGACC
ACCCCTGCCGCCGGGGGAATGGACGAGTCTGTGGTCCTGGAGCCCGAAGCCACAGGCGAAAGCAGTAGCCTG
GAGCCGACTCCTTCTTCCCAGGAAGCACAGAGGGCCCTGGGGACCTCCCCAGAGCTGCCGACGGGTGTGACT
GGTTCCTCAGGGACCAGGCTCCCCCCGACGCCAAAGGCTCAGGATGGAGGGCCTGTGGGCACGGAGCTTTTC
CGAGTGCCTCCCGTCTCCACTGCCGCCACGTGGCAGAGTTCTGCTCCCCACCAACCTGGGCCCAGCCTCTGGGC
TGAGGCAAAGACCTCTGAGGCCCCGTCCACCCAGGACCCCTCCACCCAGGCCTCCACTGCGTCCTCCCCAGCCC
CAGAGGAGAATGCTCCGTCTGAAGGCCAGCGTGTGTGGGGTCAGGGGCAGAGCCCCAGGCCAGAGAACTCT
CTGGAGCGGGAGGAGATGGGTCCCGTGCCAGCGCACACGGATGCCTTCCAGGACTGGGGGCCTGGCAGCAT
GGCCCACGTCTCTGTGGTCCCTGTCTCCTCAGAAGGGACCCCCAGCAGGGAGCCAGTGGCTTCAGGCAGCTGG
ACCCCTAAGGCTGAGGAACCCATCCATGCCACCATGGACCCCCAGAGGCTGGGCGTCCTTATCACTCCTGTCCC
TGACGCCCAGGCTGCCACCCGGAGGCAGGCTAGAGAACAGAAGCTGATCAGCGAGGAGGACCTGGAGCAGA
AGTTGATCAGCGAGGAGGACCTG**GCTAGC**ACAACCTGTATCCCAAGCAGCGGTCATTCAAGACACAGATATGC
ACTTATACCCATACCATTAGCAGTAATTACAACATGTATTGTGCTGTATATGAATGTATTATGA**GTCGAC**

>CXCL10-Stop

GAATTCCCAGTCTCAGCACCATGAATCAAACTGCCATTCTGATTTGCTGCCTTATCTTTCTGACTCTAAGTGGCA
TTCAAGGAGTACCTCTCTCTAGAACTGTACGCTGTACCTGCATCAGCATTAGTAATCAACCTGTTAATCCAAGGT
CTTTAGAAAAACTTGAAATTATTCCTGCAAGCCAATTTTGTCCACGTGTTGAGATCATTGCTACAATGAAAAAG
AAGGGTGAGAAGAGATGTCTGAATCCAGAATCGAAGGCCATCAAGAATTTACTGAAAGCAGTTAGCAAGGAA
AGGTCTAAAAGATCTCCTGCTAGAGAACAGAAGCTGATCAGCGAGGAGGACCTGGAGCAGAAGTTGATCAGC
GAGGAGGACCTGTA**GTCGAC**

>CXCL10-mucin-Stop

GAATTCCCAGTCTCAGCACCATGAATCAAACTGCCATTCTGATTTGCTGCCTTATCTTTCTGACTCTAAGTGGCA
TTCAAGGAGTACCTCTCTCTAGAACTGTACGCTGTACCTGCATCAGCATTAGTAATCAACCTGTTAATCCAAGGT
CTTTAGAAAAACTTGAAATTATTCCTGCAAGCCAATTTTGTCCACGTGTTGAGATCATTGCTACAATGAAAAAG
AAGGGTGAGAAGAGATGTCTGAATCCAGAATCGAAGGCCATCAAGAATTTACTGAAAGCAGTTAGCAAGGAA
AGGTCTAAAAGATCTCCTGCTAGAAATGGCGGCACCTTCGAGAAGCAGATCGGCGAGGTGAAGCCCAGGACC
ACCCCTGCCGCCGGGGGAATGGACGAGTCTGTGGTCCTGGAGCCCGAAGCCACAGGCGAAAGCAGTAGCCTG
GAGCCGACTCCTTCTTCCCAGGAAGCACAGAGGGCCCTGGGGACCTCCCCAGAGCTGCCGACGGGTGTGACT
GGTTCCTCAGGGACCAGGCTCCCCCCGACGCCAAAGGCTCAGGATGGAGGGCCTGTGGGCACGGAGCTTTTC
CGAGTGCCTCCCGTCTCCACTGCCGCCACGTGGCAGAGTTCTGCTCCCCACCAACCTGGGCCCAGCCTCTGGGC
TGAGGCAAAGACCTCTGAGGCCCCGTCCACCCAGGACCCCTCCACCCAGGCCTCCACTGCGTCCTCCCCAGCCC
CAGAGGAGAATGCTCCGTCTGAAGGCCAGCGTGTGTGGGGTCAGGGGCAGAGCCCCAGGCCAGAGAACTCT
CTGGAGCGGGAGGAGATGGGTCCCGTGCCAGCGCACACGGATGCCTTCCAGGACTGGGGGCCTGGCAGCAT
GGCCCACGTCTCTGTGGTCCCTGTCTCCTCAGAAGGGACCCCCAGCAGGGAGCCAGTGGCTTCAGGCAGCTGG
ACCCCTAAGGCTGAGGAACCCATCCATGCCACCATGGACCCCCAGAGGCTGGGCGTCCTTATCACTCCTGTCCC
TGACGCCCAGGCTGCCACCCGGAGGCAGGCTAGAGAACAGAAGCTGATCAGCGAGGAGGACCTGGAGCAGA
AGTTGATCAGCGAGGAGGACCTGTA**GTCGAC**

>CXCL10-DAFPI

GAATTCCCAGTCTCAGCACCATGAATCAAACTGCCATTCTGATTTGCTGCCTTATCTTTCTGACTCTAAGTGGCA
TTCAAGGAGTACCTCTCTCTAGAACTGTACGCTGTACCTGCATCAGCATTAGTAATCAACCTGTTAATCCAAGGT
CTTTAGAAAAACTTGAAATTATTCCTGCAAGCCAATTTTGTCCACGTGTTGAGATCATTGCTACAATGAAAAAG
AAGGGTGAGAAGAGATGTCTGAATCCAGAATCGAAGGCCATCAAGAATTTACTGAAAGCAGTTAGCAAGGAA
AGGTCTAAAAGATCTCCTGCTAGAGAACAGAAGCTGATCAGCGAGGAGGACCTGGAGCAGAAGTTGATCAGC
GAGGAGGACCTGGCTAGAGGAAGTGGAACCACTTCAGGTACTACCCGTCTTCTATCTGGGCACACGTGTTTCA
CGTTGACAGGTTTGCTTGGGACGCTAGTAACCATGGGCTTGCTGACTTAG**GTCGAC**

>CXCL10-mucin-DAFPI

GAATTCCCAGTCTCAGCACCATGAATCAAACTGCCATTCTGATTTGCTGCCTTATCTTTCTGACTCTAAGTGGCA
TTCAAGGAGTACCTCTCTCTAGAACTGTACGCTGTACCTGCATCAGCATTAGTAATCAACCTGTTAATCCAAGGT
CTTTAGAAAAACTTGAAATTATTCCTGCAAGCCAATTTTGTCCACGTGTTGAGATCATTGCTACAATGAAAAAG
AAGGGTGAGAAGAGATGTCTGAATCCAGAATCGAAGGCCATCAAGAATTTACTGAAAGCAGTTAGCAAGGAA
AGGTCTAAAAGATCTCCTGCTAGAAATGGCGGCACCTTCGAGAAGCAGATCGGCGAGGTGAAGCCCAGGACC
ACCCCTGCCGCCGGGGGAATGGACGAGTCTGTGGTCCTGGAGCCCGAAGCCACAGGCGAAAGCAGTAGCCTG
GAGCCGACTCCTTCTTCCCAGGAAGCACAGAGGGCCCTGGGGACCTCCCCAGAGCTGCCGACGGGTGTGACT
GGTTCCTCAGGGACCAGGCTCCCCCCGACGCCAAAGGCTCAGGATGGAGGGCCTGTGGGCACGGAGCTTTTC
CGAGTGCCTCCCGTCTCCACTGCCGCCACGTGGCAGAGTTCTGCTCCCCACCAACCTGGGCCCAGCCTCTGGGC
TGAGGCAAAGACCTCTGAGGCCCCGTCCACCCAGGACCCCTCCACCCAGGCCTCCACTGCGTCCTCCCCAGCCC
CAGAGGAGAATGCTCCGTCTGAAGGCCAGCGTGTGTGGGGTCAGGGGCAGAGCCCCAGGCCAGAGAACTCT
CTGGAGCGGGAGGAGATGGGTCCCGTGCCAGCGCACACGGATGCCTTCCAGGACTGGGGGCCTGGCAGCAT
GGCCCACGTCTCTGTGGTCCCTGTCTCCTCAGAAGGGACCCCCAGCAGGGAGCCAGTGGCTTCAGGCAGCTGG
ACCCCTAAGGCTGAGGAACCCATCCATGCCACCATGGACCCCCAGAGGCTGGGCGTCCTTATCACTCCTGTCCC
TGACGCCCAGGCTGCCACCCGGAGGCAGGCTAGAGAACAGAAGCTGATCAGCGAGGAGGACCTGGAGCAGA
AGTTGATCAGCGAGGAGGACCTGGCTAGAGGAAGTGGAACCACTTCAGGTACTACCCGTCTTCTATCTGGGCA
CACGTGTTTCACGTTGACAGGTTTGCTTGGGACGCTAGTAACCATGGGCTTGCTGACTTAG**GTCGAC**

>sEGFP-GPI

GAATTCATGGCCCCCTTTGAGCCCCTGGCTTCTGGCATCCTGTTGTTGCTGTGGCTGATAGCCCCC**ACGCGT**GC
CATGGTGAGCAAGGGCGAGGAGCTGTTCACCGGGGTGGTGCCCATCCTGGTCGAGCTGGACGGCGACGTAA
ACGGCCACAAGTTCAGCGTGTCCGGCGAGGGCGAGGGCGATGCCACCTACGGCAAGCTGACCCTGAAGTTCA
TCTGCACCACCGGCAAGCTGCCCGTGCCCTGGCCCACCCTCGTGACCACCCTGACCTACGGCGTGCAGTGCTTC
AGCCGCTACCCCGACCACATGAAGCAGCACGACTTCTTCAAGTCCGCCATGCCCGAAGGCTACGTCCAGGAGC
GCACCATCTTCTTCAAGGACGACGGCAACTACAAGACCCGCGCCGAGGTGAAGTTCGAGGGCGACACCCTGG
TGAACCGCATCGAGCTGAAGGGCATCGACTTCAAGGAGGACGGCAACATCCTGGGGCACAAGCTGGAGTACA
ACTACAACAGCCACAACGTCTATATCATGGCCGACAAGCAGAAGAACGGCATCAAGGTGAACTTCAAGATCCG
CCACAACATCGAGGACGGCAGCGTGCAGCTCGCCGACCACTACCAGCAGAACACCCCCATCGGCGACGGCCC
CGTGCTGCTGCCCGACAACCACTACCTGAGCACCCAGTCCGCCCTGAGCAAAGACCCCAACGAGAAGCGCGAT
CACATGGTCCTGCTGGAGTTCGTGACCGCCGCCGGGATCACTCTCGGCATGGACGAGCTGTACAAG**TCTAGA**G
AACAGAAGCTGATCAGCGAGGAGGACCTGGAGCAGAAGTTGATCAGCGAGGAGGACCTG**GCTAGC**ACAACC
TGTATCCCAAGCAGCGGTCATTCAAGACACAGATATGCACTTATACCCATACCATTAGCAGTAATTACAACATG
TATTGTGCTGTATATGAATGTATTATGA**GTCGAC**

>CXCL8-GPI

GAATTGAAGGAACCATCTCACTGTGTGTAAACATGACTTCCAAGCTGGCCGTGGCTCTCTTGGCAGCCTTCCTG
ATTTCTGCAGCTCTGTGTGAAGGTGCAGTTTTGCCAAGGAGTGCTAAAGAACTTAGATGTCAGTGCATAAAGA
CATACTCCAAACCTTTCCACCCCAAATTTATCAAAGAACTGAGAGTGATTGAGAGTGGACCACACTGCGCCAAC
ACAGAAATTATTGTAAAGCTTTCTGATGGAAGAGAGCTCTGTCTGGACCCCAAGGAAAACTGGGTGCAGAGG
GTTGTGGAGAAGTTTTTGAAGAGGGCTGAGAATTCA**TCTAGA**GAACAGAAGCTGATCAGCGAGGAGGACCTG
GAGCAGAAGTTGATCAGCGAGGAGGACCTG**GCTAGC**ACAACCTGTATCCCAAGCAGCGGTCATTCAAGACAC
AGATATGCACTTATACCCATACCATTAGCAGTAATTACAACATGTATTGTGCTGTATATGAATGTATTATGA**GTC**
GAC

>CXCL8-mucin-GPI

GAATTGAAGGAACCATCTCACTGTGTGTAAACATGACTTCCAAGCTGGCCGTGGCTCTCTTGGCAGCCTTCCTG
ATTTCTGCAGCTCTGTGTGAAGGTGCAGTTTTGCCAAGGAGTGCTAAAGAACTTAGATGTCAGTGCATAAAGA
CATACTCCAAACCTTTCCACCCCAAATTTATCAAAGAACTGAGAGTGATTGAGAGTGGACCACACTGCGCCAAC
ACAGAAATTATTGTAAAGCTTTCTGATGGAAGAGAGCTCTGTCTGGACCCCAAGGAAAACTGGGTGCAGAGG
GTTGTGGAGAAGTTTTTGAAGAGGGCTGAGAATTCA**TCTAGA**AATGGCGGCACCTTCGAGAAGCAGATCGGC
GAGGTGAAGCCCAGGACCACCCCTGCCGCCGGGGGAATGGACGAGTCTGTGGTCCTGGAGCCCGAAGCCAC
AGGCGAAAGCAGTAGCCTGGAGCCGACTCCTTCTTCCCAGGAAGCACAGAGGGCCCTGGGGACCTCCCCAGA
GCTGCCGACGGGTGTGACTGGTTCCTCAGGGACCAGGCTCCCCCCGACGCCAAAGGCTCAGGATGGAGGGCC
TGTGGGCACGGAGCTTTTCCGAGTGCCTCCCGTCTCCACTGCCGCCACGTGGCAGAGTTCTGCTCCCCACCAAC
CTGGGCCCAGCCTCTGGGCTGAGGCAAAGACCTCTGAGGCCCCGTCCACCCAGGACCCCTCCACCCAGGCCTC
CACTGCGTCCTCCCCAGCCCCAGAGGAGAATGCTCCGTCTGAAGGCCAGCGTGTGTGGGGTCAGGGGCAGAG
CCCCAGGCCAGAGAACTCTCTGGAGCGGGAGGAGATGGGTCCCGTGCCAGCGCACACGGATGCCTTCCAGGA
CTGGGGGCCTGGCAGCATGGCCCACGTCTCTGTGGTCCCTGTCTCCTCAGAAGGGACCCCCAGCAGGGAGCCA
GTGGCTTCAGGCAGCTGGACCCCTAAGGCTGAGGAACCCATCCATGCCACCATGGACCCCCAGAGGCTGGGC
GTCCTTATCACTCCTGTCCCTGACGCCCAGGCTGCCACCCGGAGGCAG**GCTAGA**GAACAGAAGCTGATCAGCG
AGGAGGACCTGGAGCAGAAGTTGATCAGCGAGGAGGACCTG**GCTAGC**ACAACCTGTATCCCAAGCAGCGGTC
ATTCAAGACACAGATATGCACTTATACCCATACCATTAGCAGTAATTACAACATGTATTGTGCTGTATATGAAT
GTATTATGA**GTCGAC**

>CXCL8-Stop

GAATTGAAGGAACCATCTCACTGTGTGTAAACATGACTTCCAAGCTGGCCGTGGCTCTCTTGGCAGCCTTCCTG
ATTTCTGCAGCTCTGTGTGAAGGTGCAGTTTTGCCAAGGAGTGCTAAAGAACTTAGATGTCAGTGCATAAAGA
CATACTCCAAACCTTTCCACCCCAAATTTATCAAAGAACTGAGAGTGATTGAGAGTGGACCACACTGCGCCAAC
ACAGAAATTATTGTAAAGCTTTCTGATGGAAGAGAGCTCTGTCTGGACCCCAAGGAAAACTGGGTGCAGAGG
GTTGTGGAGAAGTTTTTGAAGAGGGCTGAGAATTCA**TCTAGA**GAACAGAAGCTGATCAGCGAGGAGGACCTG
GAGCAGAAGTTGATCAGCGAGGAGGACCTGTA**GTCGAC**

>CXCL8-mucin-Stop

GAATTGAAGGAACCATCTCACTGTGTGTAAACATGACTTCCAAGCTGGCCGTGGCTCTCTTGGCAGCCTTCCTG
ATTTCTGCAGCTCTGTGTGAAGGTGCAGTTTTGCCAAGGAGTGCTAAAGAACTTAGATGTCAGTGCATAAAGA
CATACTCCAAACCTTTCCACCCCAAATTTATCAAAGAACTGAGAGTGATTGAGAGTGGACCACACTGCGCCAAC
ACAGAAATTATTGTAAAGCTTTCTGATGGAAGAGAGCTCTGTCTGGACCCCAAGGAAAACTGGGTGCAGAGG
GTTGTGGAGAAGTTTTTGAAGAGGGCTGAGAATTCA**TCTAGA**AATGGCGGCACCTTCGAGAAGCAGATCGGC
GAGGTGAAGCCCAGGACCACCCCTGCCGCCGGGGGAATGGACGAGTCTGTGGTCCTGGAGCCCGAAGCCAC
AGGCGAAAGCAGTAGCCTGGAGCCGACTCCTTCTTCCCAGGAAGCACAGAGGGCCCTGGGGACCTCCCCAGA
GCTGCCGACGGGTGTGACTGGTTCCTCAGGGACCAGGCTCCCCCCGACGCCAAAGGCTCAGGATGGAGGGCC
TGTGGGCACGGAGCTTTTCCGAGTGCCTCCCGTCTCCACTGCCGCCACGTGGCAGAGTTCTGCTCCCCACCAAC
CTGGGCCCAGCCTCTGGGCTGAGGCAAAGACCTCTGAGGCCCCGTCCACCCAGGACCCCTCCACCCAGGCCTC
CACTGCGTCCTCCCCAGCCCCAGAGGAGAATGCTCCGTCTGAAGGCCAGCGTGTGTGGGGTCAGGGGCAGAG
CCCCAGGCCAGAGAACTCTCTGGAGCGGGAGGAGATGGGTCCCGTGCCAGCGCACACGGATGCCTTCCAGGA
CTGGGGGCCTGGCAGCATGGCCCACGTCTCTGTGGTCCCTGTCTCCTCAGAAGGGACCCCCAGCAGGGAGCCA
GTGGCTTCAGGCAGCTGGACCCCTAAGGCTGAGGAACCCATCCATGCCACCATGGACCCCCAGAGGCTGGGC
GTCCTTATCACTCCTGTCCCTGACGCCCAGGCTGCCACCCGGAGGCAG**GCTAGA**GAACAGAAGCTGATCAGCG
AGGAGGACCTGGAGCAGAAGTTGATCAGCGAGGAGGACCTG**TAGTCGAC**

5.8 Abbreviations and symbols

Symbols, numbers	
µCi	micro-Curie
µF	microfarad
µg	microgram
µl	microliter
µm	micrometer
µM	micromolar
µmol	micromole
2-ME	2-mercaptoethanol
7-AAD	7-aminoactinomycin D
A	
aa	amino acid
APC	allophycocyanin
APS	ammoniumpersulfate
B	
BCA	bicinchonic acid
bFGF	basic fibroblast growth factor
BiTE	bispecific T cell engager
bp	basepairs
BRIJ 35	trade name; tricosaethylene glycol ether
BSA	bovine serum albumin
C	
C	celsius
C12E8	octaethylene glycol monododecyl ether
CD	cluster of differentiation
CD CHO	chemically defined CHO medium
cDNA	copy deoxyribonucleic acid
CHO	Chinese hamster ovary
cm	centimeter
CpG	cytosine-guanine
CTLA-4	cytotoxic T lymphocyte associated antigen 4
CV	column volumes
D	
DAF	decay accelerating factor
DC	dendritic cell
DDM	n-Dodecyl-β-D-maltoside
dFCS	dialyzed fetal calf serum
Dhfr	dihydrofolate reductase
DMEM	Dulbecco´s modified eagle medium
DMSO	dimethyl sulfoxide
DNA	deoxyribonucleic acid
dNTP	deoxyribonuleoside triphosphate
dyn	dynes
E	
ECGM	Endothelial cell growth medium
ECGS	Endothelial cell growth supplement
ECL	enhanced chemiluminsecence
EDTA	ethylenediaminetetraacetic acid
EGFP	enhanced green fluorescent protein
EGFR	epidermal growth factor receptor
EGTA	ethylene glycol tetraacetic acid
ELISA	enzyme linked immunosorbent assay
EpCAM	epithelial cell adhesion molecule
ER	endoplasmatic reticulum
F	
FACS	fluorescence activated cell scanning
Fc	fragment, crystallizable
FCS	fetal calf serum
FDA	food and drug administration
FITC	fluorescein isothiocyanate
FPLC	fast protein liquid chromatography
FSC	forward scatter
fw	forward
G	
g	gram
GAG	glycosaminoglycan
GM-CSF	granulocyte macrophage colony stimulating factor
GPI	glycosylphosphatidylinositol
GPI-PLD	glycosylphosphatidylinositol-specific phospholipase D
H	
h	hour
H/E	hematoxylin / eosin
HAM-F12	Ham´s F12
HBSS	Hank´s balanced salt solution
HDBEC	human dermal microvascular endothelial cells from blood vessels
HEPES	4-(2-hydroxyethyl)-1-piperazineethanesulfonic acid
HMEC	human microvascular endothelial cells
HRP	horseradish peroxidase
HT	hypoxanthine / thymidine
I	
ICAM	intercellular adhesion molecule
IHC	immunohistochemistry
IF	immunofluorescence microscopy
IFN	interferon
Ig	immunoglobulin
IgG_{low}	low IgG content
IL	interleukin
K	
kDa	kilo-Daltons
L	
LB	lysogeny broth
LFA-3	lymphocyte function antigen 3
M	
M	molar
mAU	milli-absorption units
MEM	minimum essential medium
MFI	mean fluorescence intensity
mg	milligram
MHC I	major histocompatibility complex I
min	minutes
ml	milliliter

mm	millimeter
mM	millimolar
mmol	millimole
mRNA	messenger ribonucleic acid
mS	milli-Siemens
N	
NEAA	non-essential amino acids
ng	nanogram
NK	natural killer
nm	nanometer
nM	nanomolar
nmol	nanomole
NMR	nuclear magnetic resonance
NP40	nonidet P40
O	
Octyl-glucoside	n-Octyl-β-D-glucopyranoside
OD	optical density
P	
P/S	penicillin / streptomycin
PAGE	polyacrylamide gelelectrophoresis
PBMCs	peripheral blood mononuclear cells
PBS	phosphate buffered saline
PCR	polymerase chain reaction
PFA	paraformaldehyde
pH	potentia hydrogenia
PIPES	piperazine-N,N′-bis(2-ethanesulfonic acid)
PI-PLC	phosphatidylinositol-specific phospholipase C
pM	picomolar
pmol	picomole
PVDF	polyvinylidene fluoride
R	
RCC	renal cell carcinoma
rh	recombinant human
RNA	ribonucleic acid
RPE	R-Phycoerythrin
rpm	rounds per minute
RPMI	Roswell Park Memorial Institute
rProtA	recombinant protein A
rt	room temperature
rv	reverse
S	
s	secreted
SDS	sodium dodecyl sulfate
sec	seconds
SSC	sideward scatter
T	
TBE	Tris/Borate/EDTA
TBS	Tris-buffered saline
TBST	Tris-buffered saline with Tween20
TCR	T cell receptor
TEM	transendothelial migration
TEMED	N,N,N',N'-tetramethyl-ethane-1,2-diamine
TGF-β	transforming growth factor β
Th	T helper
TIL	tumor-infiltrating lymphocyte
TIMP-1	tissue inhibitor of matrix metalloproteases 1
TNF	tumor necrosis factor
Treg	T regulatory
Tris	tris(hydroxymethyl)aminomethane
Triton X-100h	Triton X-100, hydrogenated
U	
U	units
UV	ultraviolet
V	
V	volts
v/v	volume per volume
VCAM	vascular endothelial cell adhesion molecule
VEGF	vascular endothelial growth factor
W	
w/v	weight per volume
WB	western blotting
WHO	world health organization

6 References

Angiolillo, A. L., C. Sgadari, et al. (1995). "Human interferon-inducible protein 10 is a potent inhibitor of angiogenesis in vivo." *The Journal of experimental medicine* **182**(1): 155-162.

Arai, S., R. Meagher, et al. (2008). "Infusion of the allogeneic cell line NK-92 in patients with advanced renal cell cancer or melanoma: a phase I trial." *Cytotherapy* **10**(6): 625-632.

Azzouz, N. and Y. Capdeville (1992). "Structural comparisons between the soluble and the GPI-anchored forms of the Paramecium temperature-specific 156G surface antigen." *Biol Cell* **75**(3): 217-223.

Baggiolini, M. and I. Clark-Lewis (1992). "Interleukin-8, a chemotactic and inflammatory cytokine." *FEBS letters* **307**(1): 97-101.

Baggiolini, M., A. Walz, et al. (1989). "Neutrophil-activating peptide-1/interleukin 8, a novel cytokine that activates neutrophils." *The Journal of clinical investigation* **84**(4): 1045-1049.

Baldwin, E. T., I. T. Weber, et al. (1991). "Crystal structure of interleukin 8: symbiosis of NMR and crystallography." *Proceedings of the National Academy of Sciences* **88**(2): 502-506.

Bazan, J. F., K. B. Bacon, et al. (1997). "A new class of membrane-bound chemokine with a CX3C motif." *Nature* **385**(6617): 640-644.

Beck, A., T. Wurch, et al. (2010). "Strategies and challenges for the next generation of therapeutic antibodies." *Nature reviews. Immunology* **10**(5): 345-352.

Becker, Y. (1993). "Dendritic cell activity against primary tumors: an overview." *In Vivo* **7**(3): 187-191.

Bianchi, G., M. Sironi, et al. (1993). "Migration of natural killer cells across endothelial cell monolayers." *The Journal of Immunology* **151**(10): 5135-5144.

Bingle, L., N. J. Brown, et al. (2002). "The role of tumour-associated macrophages in tumour progression: implications for new anticancer therapies." *The Journal of pathology* **196**(3): 254-265.

Bodnar, R. J., C. C. Yates, et al. (2009). "IP-10 induces dissociation of newly formed blood vessels." *J Cell Sci* **122**(Pt 12): 2064-2077.

Bondos, S. E. and A. Bicknell (2003). "Detection and prevention of protein aggregation before, during, and after purification." *Anal Biochem* **316**(2): 223-231.

Booth, V., D. W. Keizer, et al. (2002). "The CXCR3 binding chemokine IP-10/CXCL10: structure and receptor interactions." *Biochemistry* **41**(33): 10418-10425.

Borghaei, H., M. R. Smith, et al. (2009). "Immunotherapy of cancer." *European journal of pharmacology* **625**(1-3): 41-54.

Borroni, E. M., A. Mantovani, et al. (2010). "Chemokine receptors intracellular trafficking." *Pharmacology & Therapeutics* **127**(1): 1-8.

Bradford, M. M. (1976). "A rapid and sensitive method for the quantitation of microgram quantities of protein utilizing the principle of protein-dye binding." *Anal Biochem* **72**: 248-254.

Brown, D. and G. L. Waneck (1992). "Glycosyl-phosphatidylinositol-anchored membrane proteins." *Journal of the American Society of Nephrology : JASN* **3**(4): 895-906.

Bumgarner, G. W., J. C. Zampell, et al. (2005). "Modified cell ELISA to determine the solubilization of cell surface proteins: Applications in GPI-anchored protein purification." *Journal of biochemical and biophysical methods* **64**(2): 99-109.

Campanella, G. S. V., R. A. Colvin, et al. (2010). "CXCL10 Can Inhibit Endothelial Cell Proliferation Independently of CXCR3." *PloS one* **5**(9): e12700.

Campbell, J. J., S. Qin, et al. (2001). "Unique subpopulations of CD56+ NK and NK-T peripheral blood lymphocytes identified by chemokine receptor expression repertoire." *Journal of immunology* **166**(11): 6477-6482.

Cella, M., D. Jarrossay, et al. (1999). "Plasmacytoid monocytes migrate to inflamed lymph nodes and produce large amounts of type I interferon." *Nature medicine* **5**(8): 919-923.

Cerneus, D. P., E. Ueffing, et al. (1993). "Detergent insolubility of alkaline phosphatase during biosynthetic transport and endocytosis. Role of cholesterol." *The Journal of biological chemistry* **268**(5): 3150-3155.

Chen, R., J. J. Knez, et al. (2001). "Comparative efficiencies of C-terminal signals of native glycophosphatidylinositol (GPI)-anchored proproteins in conferring GPI-anchoring." *Journal of cellular biochemistry* **84**(1): 68-83.

Cho, D., D. R. Shook, et al. (2010). "Cytotoxicity of activated natural killer cells against pediatric solid tumors." *Clinical cancer research : an official journal of the American Association for Cancer Research* **16**(15): 3901-3909.

Chung, C. W., R. M. Cooke, et al. (1995). "The three-dimensional solution structure of RANTES." *Biochemistry* **34**(29): 9307-9314.

Cinamon, G., V. Shinder, et al. (2001). "Shear forces promote lymphocyte migration across vascular endothelium bearing apical chemokines." *Nature immunology* **2**(6): 515-522.

Clark, W. H., Jr., D. E. Elder, et al. (1989). "Model predicting survival in stage I melanoma based on tumor progression." *J Natl Cancer Inst* **81**(24): 1893-1904.

Clemente, C. G., M. C. Mihm, Jr., et al. (1996). "Prognostic value of tumor infiltrating lymphocytes in the vertical growth phase of primary cutaneous melanoma." *Cancer* **77**(7): 1303-1310.

Coley, W. B. (1910). "The Treatment of Inoperable Sarcoma by Bacterial Toxins (the Mixed Toxins of the Streptococcus erysipelas and the Bacillus prodigiosus)." *Proc R Soc Med* **3**(Surg Sect): 1-48.

Colvin, R. A., G. S. Campanella, et al. (2004). "Intracellular domains of CXCR3 that mediate CXCL9, CXCL10, and CXCL11 function." *The Journal of biological chemistry* **279**(29): 30219-30227.

Cooper, M. A., T. A. Fehniger, et al. (2001). "The biology of human natural killer-cell subsets." *Trends in immunology* **22**(11): 633-640.

Corcione, A., E. Ferretti, et al. (2009). "CX3CR1 Is Expressed by Human B Lymphocytes and Meditates CX3CL1 Driven Chemotaxis of Tonsil Centrocytes." *PloS one* **4**(12): e8485.

Cornish, R. J. (1928). "Flow in a Pipe of Rectangular Cross-Section." *Proceedings of the Royal Society of London. Series A* **120**(786): 691-700.

Cromwell, M. E., E. Hilario, et al. (2006). "Protein aggregation and bioprocessing." *AAPS J* **8**(3): E572-579.

D'Ambrosio, D., C. Albanesi, et al. (2002). "Quantitative Differences in Chemokine Receptor Engagement Generate Diversity in Integrin-Dependent Lymphocyte Adhesion." *The Journal of Immunology* **169**(5): 2303-2312.

Danielsen, T. and E. K. Rofstad (1998). "VEGF, bFGF and EGF in the angiogenesis of human melanoma xenografts." *Int J Cancer* **76**(6): 836-841.

De Luca, A., A. Carotenuto, et al. (2008). "The role of the EGFR signaling in tumor microenvironment." *J Cell Physiol* **214**(3): 559-567.

Di Carlo, E., G. Forni, et al. (2001). "The intriguing role of polymorphonuclear neutrophils in antitumor reactions." *Blood* **97**(2): 339-345.

Dings, R. P., K. B. Vang, et al. (2011). "Enhancement of T-cell-mediated antitumor response: angiostatic adjuvant to immunotherapy against cancer." *Clinical cancer research : an official journal of the American Association for Cancer Research* **17**(10): 3134-3145.

Dirkx, A. E., M. G. Oude Egbrink, et al. (2003). "Tumor angiogenesis modulates leukocyte-vessel wall interactions in vivo by reducing endothelial adhesion molecule expression." *Cancer research* **63**(9): 2322-2329.

DiVietro, J. A., M. J. Smith, et al. (2001). "Immobilized IL-8 triggers progressive activation of neutrophils rolling in vitro on P-selectin and intercellular adhesion molecule-1." *Journal of immunology* **167**(7): 4017-4025.

Donahue, T., T. Haut, et al. (2003). "Mechanosensitivity of bone cells to oscillating fluid flow induced shear stress may be modulated by chemotransport." *Journal of Biomechanics* **36**(9): 1363-1371.

Dufour, J. H., M. Dziejman, et al. (2002). "IFN-gamma-inducible protein 10 (IP-10; CXCL10)-deficient mice reveal a role for IP-10 in effector T cell generation and trafficking." *Journal of immunology* **168**(7): 3195-3204.

Edman, P. (1949). "A method for the determination of amino acid sequence in peptides." *Arch Biochem* **22**(3): 475.

Ehlert, J. E., C. A. Addison, et al. (2004). "Identification and partial characterization of a variant of human CXCR3 generated by posttranscriptional exon skipping." *Journal of immunology* **173**(10): 6234-6240.

Everson, T. C. (1964). "Spontaneous regression of cancer." *Annals of the New York Academy of Sciences* **114**(2): 721-735.

Feldman, E. D., D. M. Weinreich, et al. (2006). "Interferon gamma-inducible protein 10 selectively inhibits proliferation and induces apoptosis in endothelial cells." *Annals of surgical oncology* **13**(1): 125-133.

Ferradini, L., A. Mackensen, et al. (1993). "Analysis of T cell receptor variability in tumor-infiltrating lymphocytes from a human regressive melanoma. Evidence for in situ T cell clonal expansion." *The Journal of clinical investigation* **91**(3): 1183-1190.

Figel, A. M., D. Brech, et al. (2011). "Human renal cell carcinoma induces a dendritic cell subset that uses T-cell crosstalk for tumor-permissive milieu alterations." *The American journal of pathology* **179**(1): 436-451.

Fong, A. M., H. P. Erickson, et al. (2000). "Ultrastructure and function of the fractalkine mucin domain in CX(3)C chemokine domain presentation." *The Journal of biological chemistry* **275**(6): 3781-3786.

Fong, A. M., L. A. Robinson, et al. (1998). "Fractalkine and CX3CR1 mediate a novel mechanism of leukocyte capture, firm adhesion, and activation under physiologic flow." *The Journal of experimental medicine* **188**(8): 1413-1419.

Foussat, A., A. Coulomb-L'Hermine, et al. (2000). "Fractalkine receptor expression by T lymphocyte subpopulations and in vivo production of fractalkine in human." *European journal of immunology* **30**(1): 87-97.

Friedl, P. and B. Weigelin (2008). "Interstitial leukocyte migration and immune function." *Nature immunology* **9**(9): 960-969.

Garbi, N., B. Arnold, et al. (2004). "CpG motifs as proinflammatory factors render autochthonous tumors permissive for infiltration and destruction." *Journal of immunology* **172**(10): 5861-5869.

Garcia-Lopez, M. A., F. Sanchez-Madrid, et al. (2001). "CXCR3 chemokine receptor distribution in normal and inflamed tissues: expression on activated lymphocytes, endothelial cells, and dendritic cells." *Lab Invest* **81**(3): 409-418.

Geller, M. A., S. Cooley, et al. (2011). "A phase II study of allogeneic natural killer cell therapy to treat patients with recurrent ovarian and breast cancer." *Cytotherapy* **13**(1): 98-107.

Gerber, L. D., K. Kodukula, et al. (1992). "Phosphatidylinositol glycan (PI-G) anchored membrane proteins. Amino acid requirements adjacent to the site of cleavage and PI-G attachment in the COOH-terminal signal peptide." *The Journal of biological chemistry* **267**(17): 12168-12173.

Gimbrone, M. A., Jr., S. B. Leapman, et al. (1972). "Tumor dormancy in vivo by prevention of neovascularization." *The Journal of experimental medicine* **136**(2): 261-276.

Grégoire, C., L. Chasson, et al. (2007). "The trafficking of natural killer cells." *Immunological reviews* **220**(1): 169-182.

Griffioen, A. W., C. A. Damen, et al. (1996a). "Tumor angiogenesis is accompanied by a decreased inflammatory response of tumor-associated endothelium." *Blood* **88**(2): 667-673.

Griffioen, A. W., C. A. Damen, et al. (1996b). "Endothelial intercellular adhesion molecule-1 expression is suppressed in human malignancies: the role of angiogenic factors." *Cancer research* **56**(5): 1111-1117.

Griffioen, A. W., C. A. Damen, et al. (1999). "Angiogenesis inhibitors overcome tumor induced endothelial cell anergy." *Int J Cancer* **80**(2): 315-319.

Griffioen, A. W., S. C. Tromp, et al. (1998). "Angiogenesis modulates the tumour immune response." *International journal of experimental pathology* **79**(6): 363-368.

Grone, H. J., C. Weber, et al. (1999). "Met-RANTES reduces vascular and tubular damage during acute renal transplant rejection: blocking monocyte arrest and recruitment." *The FASEB journal : official publication of the Federation of American Societies for Experimental Biology* **13**(11): 1371-1383.

Guerriero, J. L., D. Ditsworth, et al. (2011). "DNA Alkylating Therapy Induces Tumor Regression through an HMGB1-Mediated Activation of Innate Immunity." *The Journal of Immunology* **186**(6): 3517-3526.

Hancock, W. W., B. Lu, et al. (2000). "Requirement of the chemokine receptor CXCR3 for acute allograft rejection." *The Journal of experimental medicine* **192**(10): 1515-1520.

Haraldsen, G., D. Kvale, et al. (1996). "Cytokine-regulated expression of E-selectin, intercellular adhesion molecule-1 (ICAM-1), and vascular cell adhesion molecule-1 (VCAM-1) in human microvascular endothelial cells." *The Journal of Immunology* **156**(7): 2558-2565.

Harcourt, J., R. Alvarez, et al. (2006). "Respiratory Syncytial Virus G Protein and G Protein CX3C Motif Adversely Affect CX3CR1+ T Cell Responses." *The Journal of Immunology* **176**(3): 1600-1608.

Haskell, C. A., M. D. Cleary, et al. (1999). "Molecular uncoupling of fractalkine-mediated cell adhesion and signal transduction. Rapid flow arrest of CX3CR1-expressing cells is independent of G-protein activation." *The Journal of biological chemistry* **274**(15): 10053-10058.

Haskell, C. A., M. D. Cleary, et al. (2000). "Unique role of the chemokine domain of fractalkine in cell capture. Kinetics of receptor dissociation correlate with cell adhesion." *The Journal of biological chemistry* **275**(44): 34183-34189.

Haskell, C. A., W. W. Hancock, et al. (2001). "Targeted deletion of CX3CR1 reveals a role for fractalkine in cardiac allograft rejection." *The Journal of clinical investigation* **108**(5): 679-688.

Hess, C., T. K. Means, et al. (2004). "IL-8 responsiveness defines a subset of CD8 T cells poised to kill." *Blood* **104**(12): 3463-3471.

Hiroi, Y., R. Chen, et al. (2000). "Cloning of murine glycosyl phosphatidylinositol anchor attachment protein, GPAA1." *Am J Physiol Cell Physiol* **279**(1): C205-212.

Hodi, F. S., S. J. O'Day, et al. (2010). "Improved survival with ipilimumab in patients with metastatic melanoma." *N Engl J Med* **363**(8): 711-723.

Hoessli, D. C. and P. J. Robinson (1998). "GPI-anchors and cell membranes: a special relationship." *Trends in Cell Biology* **8**(2): 87-89.

Hollander, N. (1992). "Membrane dynamics of the phosphatidylinositol-anchored form and the transmembrane form of the cell adhesion protein LFA-3." *Journal of Biological Chemistry* **267**(8): 5663-5667.

Holmgren, L., M. S. O'Reilly, et al. (1995). "Dormancy of micrometastases: balanced proliferation and apoptosis in the presence of angiogenesis suppression." *Nature medicine* **1**(2): 149-153.

Homans, S. W., M. A. Ferguson, et al. (1988). "Complete structure of the glycosyl phosphatidylinositol membrane anchor of rat brain Thy-1 glycoprotein." *Nature* **333**(6170): 269-272.

Hossler, P., S. F. Khattak, et al. (2009). "Optimal and consistent protein glycosylation in mammalian cell culture." *Glycobiology* **19**(9): 936-949.

Huang, H., Y. Liu, et al. (2002). "Synergistic effect of adoptive T-cell therapy and intratumoral interferon gamma-inducible protein-10 transgene expression in treatment of established tumors." *Cellular immunology* **217**(1-2): 12-22.

Hundhausen, C., D. Misztela, et al. (2003). "The disintegrin-like metalloproteinase ADAM10 is involved in constitutive cleavage of CX3CL1 (fractalkine) and regulates CX3CL1-mediated cell-cell adhesion." *Blood* **102**(4): 1186-1195.

Hussell, T. and P. J. Openshaw (1998). "Intracellular IFN-gamma expression in natural killer cells precedes lung CD8+ T cell recruitment during respiratory syncytial virus infection." *Journal of General Virology* **79**(11): 2593-2601.

Iliopoulou, E. G., P. Kountourakis, et al. (2010). "A phase I trial of adoptive transfer of allogeneic natural killer cells in patients with advanced non-small cell lung cancer." *Cancer immunology, immunotherapy : CII* **59**(12): 1781-1789.

Imai, T., K. Hieshima, et al. (1997). "Identification and molecular characterization of fractalkine receptor CX3CR1, which mediates both leukocyte migration and adhesion." *Cell* **91**(4): 521-530.

Jabeen, T., P. Leonard, et al. (2008). "Structure of mouse IP-10, a chemokine." *Acta crystallographica. Section D, Biological crystallography* **64**(Pt 6): 611-619.

Jinquan, T., C. Jing, et al. (2000). "CXCR3 expression and activation of eosinophils: role of IFN-gamma-inducible protein-10 and monokine induced by IFN-gamma." *Journal of immunology* **165**(3): 1548-1556.

Joensuu, H., A. Anttonen, et al. (2002). "Soluble syndecan-1 and serum basic fibroblast growth factor are new prognostic factors in lung cancer." *Cancer research* **62**(18): 5210-5217.

Jones, D. A., L. V. McIntire, et al. (1994). "A two-step adhesion cascade for T cell/endothelial cell interactions under flow conditions." *The Journal of clinical investigation* **94**(6): 2443-2450.

June, C. H. (2007). "Adoptive T cell therapy for cancer in the clinic." *The Journal of clinical investigation* **117**(6): 1466-1476.

Jung, S., J. Aliberti, et al. (2000). "Analysis of fractalkine receptor CX(3)CR1 function by targeted deletion and green fluorescent protein reporter gene insertion." *Molecular and cellular biology* **20**(11): 4106-4114.

Kantoff, P. W., C. S. Higano, et al. (2010). "Sipuleucel-T immunotherapy for castration-resistant prostate cancer." *N Engl J Med* **363**(5): 411-422.

Kawakami, Y., S. Eliyahu, et al. (1994). "Cloning of the gene coding for a shared human melanoma antigen recognized by autologous T cells infiltrating into tumor." *Proceedings of the National Academy of Sciences of the United States of America* **91**(9): 3515-3519.

Kirkwood, J., M. Strawderman, et al. (1996). "Interferon alfa-2b adjuvant therapy of high-risk resected cutaneous melanoma: the Eastern Cooperative Oncology Group Trial EST 1684." *Journal of Clinical Oncology* **14**(1): 7-17.

Klebanoff, C. A., N. Acquavella, et al. (2011). "Therapeutic cancer vaccines: are we there yet?" *Immunological reviews* **239**(1): 27-44.

Klein, N. J., G. I. Shennan, et al. (1992). "Alteration in glycosaminoglycan metabolism and surface charge on human umbilical vein endothelial cells induced by cytokines, endotoxin and neutrophils." *J Cell Sci* **102 (Pt 4)**: 821-832.

Kohrgruber, N., M. Groger, et al. (2004). "Plasmacytoid dendritic cell recruitment by immobilized CXCR3 ligands." *Journal of immunology* **173**(11): 6592-6602.

Kovalchuk, A. L., C.-F. Qi, et al. (2000). "Burkitt Lymphoma in the Mouse." *The Journal of experimental medicine* **192**(8): 1183-1190.

Kukreti, S., K. Konstantopoulos, et al. (1997). "Molecular mechanisms of monocyte adhesion to interleukin-1beta-stimulated endothelial cells under physiologic flow conditions." *Blood* **89**(11): 4104-4111.

Kuschert, G. S., F. Coulin, et al. (1999). "Glycosaminoglycans interact selectively with chemokines and modulate receptor binding and cellular responses." *Biochemistry* **38**(39): 12959-12968.

Laemmli, U. K. (1970). "Cleavage of structural proteins during the assembly of the head of bacteriophage T4." *Nature* **227**(5259): 680-685.

Lasagni, L., M. Francalanci, et al. (2003). "An alternatively spliced variant of CXCR3 mediates the inhibition of endothelial cell growth induced by IP-10, Mig, and I-TAC, and acts as functional receptor for platelet factor 4." *The Journal of experimental medicine* **197**(11): 1537-1549.

Laudanna, C. and R. Alon (2005). "Right on the spot. Chemokine triggering of integrin–mediated arrest of rolling leukocytes." *Thrombosis and Haemostasis*.

Lawrence, M. B., L. V. McIntire, et al. (1987). "Effect of flow on polymorphonuclear leukocyte/endothelial cell adhesion." *Blood* **70**(5): 1284-1290.

Lawrence, M. B. and T. A. Springer (1991). "Leukocytes roll on a selectin at physiologic flow rates: distinction from and prerequisite for adhesion through integrins." *Cell* **65**(5): 859-873.

Leen, A. M., C. M. Rooney, et al. (2007). "Improving T cell therapy for cancer." *Annual review of immunology* **25**: 243-265.

Legler, D. F., M. A. Doucey, et al. (2005). "Differential insertion of GPI-anchored GFPs into lipid rafts of live cells." *The FASEB journal : official publication of the Federation of American Societies for Experimental Biology* **19**(1): 73-75.

Leibson, P. J. (1997). "Signal Transduction during Natural Killer Cell Activation: Inside the Mind of a Killer." *Immunity* **6**(6): 655-661.

Lesterhuis, W. J., J. B. A. G. Haanen, et al. (2011). "Cancer immunotherapy – revisited." *Nat Rev Drug Discov* **10**(8): 591-600.

Levy, E. M., M. P. Roberti, et al. (2011). "Natural killer cells in human cancer: from biological functions to clinical applications." *Journal of biomedicine & biotechnology* **2011**: 676198.

Li, A., S. Dubey, et al. (2003). "IL-8 directly enhanced endothelial cell survival, proliferation, and matrix metalloproteinases production and regulated angiogenesis." *Journal of immunology* **170**(6): 3369-3376.

Linke, R., A. Klein, et al. (2010). "Catumaxomab: clinical development and future directions." *MAbs* **2**(2): 129-136.

Loetscher, M., B. Gerber, et al. (1996). "Chemokine receptor specific for IP10 and mig: structure, function, and expression in activated T-lymphocytes." *The Journal of experimental medicine* **184**(3): 963-969.

Loetscher, M., P. Loetscher, et al. (1998). "Lymphocyte-specific chemokine receptor CXCR3: regulation, chemokine binding and gene localization." *European journal of immunology* **28**(11): 3696-3705.

Luster, A. D., R. D. Cardiff, et al. (1998). "Delayed wound healing and disorganized neovascularization in transgenic mice expressing the IP-10 chemokine." *Proc Assoc Am Physicians* **110**(3): 183-196.

Luster, A. D., S. M. Greenberg, et al. (1995). "The IP-10 chemokine binds to a specific cell surface heparan sulfate site shared with platelet factor 4 and inhibits endothelial cell proliferation." *The Journal of experimental medicine* **182**(1): 219-231.

Luster, A. D. and P. Leder (1993). "IP-10, a -C-X-C- chemokine, elicits a potent thymus-dependent antitumor response in vivo." *The Journal of experimental medicine* **178**(3): 1057-1065.

Luster, A. D., J. C. Unkeless, et al. (1985). "Gamma-interferon transcriptionally regulates an early-response gene containing homology to platelet proteins." *Nature* **315**(6021): 672-676.

Mackay, C. R. (2008). "Moving targets: cell migration inhibitors as new anti-inflammatory therapies." *Nature immunology* **9**(9): 988-998.

Manes, T. D., J. S. Pober, et al. (2006). "Endothelial cell-T lymphocyte interactions: IP-10 stimulates rapid transendothelial migration of human effort but not central memory CD4+ T cells. Requirements for shear stress and adhesion molecules." *Transplantation* **82**(1 Suppl): S9-14.

Mantovani, A., R. Bonecchi, et al. (2006). "Tuning inflammation and immunity by chemokine sequestration: decoys and more." *Nature reviews. Immunology* **6**(12): 907-918.

Marquardt, N., E. Wilk, et al. (2010). "Murine CXCR3+CD27bright NK cells resemble the human CD56bright NK-cell population." *European journal of immunology* **40**(5): 1428-1439.

McEver, R. P. and C. Zhu (2010). "Rolling cell adhesion." *Annu Rev Cell Dev Biol* **26**: 363-396.

McGovern, V. J. (1975). "Spontaneous regression of melanoma." *Pathology* **7**(2): 91-99.

McLaughlin, P., A. J. Grillo-Lopez, et al. (1998). "Rituximab chimeric anti-CD20 monoclonal antibody therapy for relapsed indolent lymphoma: half of patients respond to a four-dose treatment program." *J Clin Oncol* **16**(8): 2825-2833.

Medof, M. E., T. Kinoshita, et al. (1984). "Inhibition of complement activation on the surface of cells after incorporation of decay-accelerating factor (DAF) into their membranes." *The Journal of experimental medicine* **160**(5): 1558-1578.

Medof, M. E., S. Nagarajan, et al. (1996). "Cell-surface engineering with GPI-anchored proteins." *The FASEB journal : official publication of the Federation of American Societies for Experimental Biology* **10**(5): 574-586.

Meiser, A., A. Mueller, et al. (2008). "The chemokine receptor CXCR3 is degraded following internalization and is replenished at the cell surface by de novo synthesis of receptor." *Journal of immunology* **180**(10): 6713-6724.

Meyer, C., A. Sevko, et al. (2011). "Chronic inflammation promotes myeloid-derived suppressor cell activation blocking antitumor immunity in transgenic mouse melanoma model." *Proceedings of the National Academy of Sciences*.

Middleton, J., S. Neil, et al. (1997). "Transcytosis and surface presentation of IL-8 by venular endothelial cells." *Cell* **91**(3): 385-395.

Mizoue, L. S., J. F. Bazan, et al. (1999). "Solution structure and dynamics of the CX3C chemokine domain of fractalkine and its interaction with an N-terminal fragment of CX3CR1." *Biochemistry* **38**(5): 1402-1414.

Müller, D. and R. E. Kontermann (2010). "Bispecific Antibodies for Cancer Immunotherapy." *BioDrugs* **24**(2): 89-98.

Mukai, S., J. Kjaergaard, et al. (1999). "Infiltration of tumors by systemically transferred tumor-reactive T lymphocytes is required for antitumor efficacy." *Cancer research* **59**(20): 5245-5249.

Murphy, K. M., P. Travers, et al. (2007). Janeway´s Immunobiology 7th edition. New York, Garland Science.

Musolino, A., N. Naldi, et al. (2008). "Immunoglobulin G fragment C receptor polymorphisms and clinical efficacy of trastuzumab-based therapy in patients with HER-2/neu-positive metastatic breast cancer." *J Clin Oncol* **26**(11): 1789-1796.

Naito, Y., K. Saito, et al. (1998). "CD8+ T cells infiltrated within cancer cell nests as a prognostic factor in human colorectal cancer." *Cancer research* **58**(16): 3491-3494.

Notohamiprodjo, M., R. Djafarzadeh, et al. (2006). "Generation of GPI-linked CCL5 based chemokine receptor antagonists for the suppression of acute vascular damage during allograft transplantation." *Protein engineering, design & selection : PEDS* **19**(1): 27-35.

O'Connor, E., B. Eisenhaber, et al. (2005). "Species specific membrane anchoring of nyctalopin, a small leucine-rich repeat protein." *Human Molecular Genetics* **14**(13): 1877-1887.

Pages, F., J. Galon, et al. (2010). "Immune infiltration in human tumors: a prognostic factor that should not be ignored." *Oncogene* **29**(8): 1093-1102.

Palucka, K., H. Ueno, et al. (2011). "Recent Developments in Cancer Vaccines." *The Journal of Immunology* **186**(3): 1325-1331.

Parkinson, D., J. Abrams, et al. (1990). "Interleukin-2 therapy in patients with metastatic malignant melanoma: a phase II study." *Journal of Clinical Oncology* **8**(10): 1650-1656.

Paul, S., B. Acres, et al. (2007). "Cancer vaccines: challenges and outlook in the field." *IDrugs* **10**(5): 324-328.

Peled, A., V. Grabovsky, et al. (1999). "The chemokine SDF-1 stimulates integrin-mediated arrest of CD34(+) cells on vascular endothelium under shear flow." *The Journal of clinical investigation* **104**(9): 1199-1211.

Phillipson, M., B. Heit, et al. (2006). "Intraluminal crawling of neutrophils to emigration sites: a molecularly distinct process from adhesion in the recruitment cascade." *The Journal of experimental medicine* **203**(12): 2569-2575.

Piali, L., C. Weber, et al. (1998). "The chemokine receptor CXCR3 mediates rapid and shear-resistant adhesion-induction of effector T lymphocytes by the chemokines IP10 and Mig." *European journal of immunology* **28**(3): 961-972.

Pober, J. S. (1987). "Effects of tumour necrosis factor and related cytokines on vascular endothelial cells." *Ciba Found Symp* **131**: 170-184.

Pockaj, B. A., R. M. Sherry, et al. (1994). "Localization of 111indium-labeled tumor infiltrating lymphocytes to tumor in patients receiving adoptive immunotherapy. Augmentation with cyclophosphamide and correlation with response." *Cancer* **73**(6): 1731-1737.

Proudfoot, A. E., T. M. Handel, et al. (2003). "Glycosaminoglycan binding and oligomerization are essential for the in vivo activity of certain chemokines." *Proceedings of the National Academy of Sciences of the United States of America* **100**(4): 1885-1890.

Proudfoot, A. E., C. A. Power, et al. (2001). "Cellular assays of chemokine receptor activation." *Curr Protoc Pharmacol* **Chapter 12**: Unit12 14.

Proudfoot, A. E., C. A. Power, et al. (2010). "Anti-chemokine small molecule drugs: a promising future?" *Expert Opinion on Investigational Drugs* **19**(3): 345-355.

Proudfoot, A. E. I., C. A. Power, et al. (1996). "Extension of Recombinant Human RANTES by the Retention of the Initiating Methionine Produces a Potent Antagonist." *Journal of Biological Chemistry* **271**(5): 2599-2603.

Qin, S., J. B. Rottman, et al. (1998). "The chemokine receptors CXCR3 and CCR5 mark subsets of T cells associated with certain inflammatory reactions." *The Journal of clinical investigation* **101**(4): 746-754.

Quezada, S. A., K. S. Peggs, et al. (2011). "Shifting the equilibrium in cancer immunoediting: from tumor tolerance to eradication." *Immunological reviews* **241**(1): 104-118.

Reisinger, V. and L. A. Eichacker (2008). "Isolation of membrane protein complexes by blue native electrophoresis." *Methods Mol Biol* **424**: 423-431.

Robertson, M. J. (2002). "Role of chemokines in the biology of natural killer cells." *Journal of leukocyte biology* **71**(2): 173-183.

Romagnani, P., F. Annunziato, et al. (2001). "Cell cycle-dependent expression of CXC chemokine receptor 3 by endothelial cells mediates angiostatic activity." *The Journal of clinical investigation* **107**(1): 53-63.

Rosenberg, S. A., M. T. Lotze, et al. (1985). "Observations on the systemic administration of autologous lymphokine-activated killer cells and recombinant interleukin-2 to patients with metastatic cancer." *N Engl J Med* **313**(23): 1485-1492.

Rosenberg, S. A., B. S. Packard, et al. (1988). "Use of tumor-infiltrating lymphocytes and interleukin-2 in the immunotherapy of patients with metastatic melanoma. A preliminary report." *N Engl J Med* **319**(25): 1676-1680.

Rosenberg, S. A., P. Spiess, et al. (1986). "A new approach to the adoptive immunotherapy of cancer with tumor-infiltrating lymphocytes." *Science* **233**(4770): 1318-1321.

Rot, A. (1993). "Neutrophil attractant/activation protein-1 (interleukin-8) induces in vitro neutrophil migration by haptotactic mechanism." *European journal of immunology* **23**(1): 303-306.

Ruffell, B., A. Au, et al. (2011). "Leukocyte composition of human breast cancer." *Proceedings of the National Academy of Sciences*.

Ruggeri, L., M. Capanni, et al. (2002). "Effectiveness of donor natural killer cell alloreactivity in mismatched hematopoietic transplants." *Science* **295**(5562): 2097-2100.

Ryschich, E., V. Kerkadze, et al. (2006). "Active leukocyte crawling in microvessels assessed by digital time-lapse intravital microscopy." *The Journal of surgical research* **135**(2): 291-296.

Sanderson, R. D., Y. Yang, et al. (2005). "Enzymatic remodeling of heparan sulfate proteoglycans within the tumor microenvironment: growth regulation and the prospect of new cancer therapies." *Journal of cellular biochemistry* **96**(5): 897-905.

Sato, E., S. H. Olson, et al. (2005). "Intraepithelial CD8+ tumor-infiltrating lymphocytes and a high CD8+/regulatory T cell ratio are associated with favorable prognosis in ovarian cancer." *Proceedings of the National Academy of Sciences of the United States of America* **102**(51): 18538-18543.

Saudemont, A., N. Jouy, et al. (2005). "NK cells that are activated by CXCL10 can kill dormant tumor cells that resist CTL-mediated lysis and can express B7-H1 that stimulates T cells." *Blood* **105**(6): 2428-2435.

Sauty, A., R. A. Colvin, et al. (2001). "CXCR3 internalization following T cell-endothelial cell contact: preferential role of IFN-inducible T cell alpha chemoattractant (CXCL11)." *Journal of immunology* **167**(12): 7084-7093.

Schroeder, R. J., S. N. Ahmed, et al. (1998). "Cholesterol and sphingolipid enhance the Triton X-100 insolubility of glycosylphosphatidylinositol-anchored proteins by promoting the formation of detergent-insoluble ordered membrane domains." *The Journal of biological chemistry* **273**(2): 1150-1157.

Schwartzentruber, D. J., D. H. Lawson, et al. (2011). "gp100 peptide vaccine and interleukin-2 in patients with advanced melanoma." *N Engl J Med* **364**(22): 2119-2127.

Sebastiani, S., P. Allavena, et al. (2001). "Chemokine receptor expression and function in CD4+ T lymphocytes with regulatory activity." *Journal of immunology* **166**(2): 996-1002.

Seidel, C., A. Sundan, et al. (2000). "Serum syndecan-1: a new independent prognostic marker in multiple myeloma." *Blood* **95**(2): 388-392.

Shamri, R., V. Grabovsky, et al. (2005). "Lymphocyte arrest requires instantaneous induction of an extended LFA-1 conformation mediated by endothelium-bound chemokines." *Nature immunology* **6**(5): 497-506.

Shrimali, R. K., Z. Yu, et al. (2010). "Antiangiogenic agents can increase lymphocyte infiltration into tumor and enhance the effectiveness of adoptive immunotherapy of cancer." *Cancer research* **70**(15): 6171-6180.

Shulman, Z., V. Shinder, et al. (2009). "Lymphocyte crawling and transendothelial migration require chemokine triggering of high-affinity LFA-1 integrin." *Immunity* **30**(3): 384-396.

Signoret, N., A. Pelchen-Matthews, et al. (2000). "Endocytosis and recycling of the HIV coreceptor CCR5." *The Journal of cell biology* **151**(6): 1281-1294.

Slamon, D. J., B. Leyland-Jones, et al. (2001). "Use of Chemotherapy plus a Monoclonal Antibody against HER2 for Metastatic Breast Cancer That Overexpresses HER2." *New England Journal of Medicine* **344**(11): 783-792.

Smith, P. K., R. I. Krohn, et al. (1985). "Measurement of protein using bicinchoninic acid." *Anal Biochem* **150**(1): 76-85.

Springer, T. A. (1994). "Traffic signals for lymphocyte recirculation and leukocyte emigration: the multistep paradigm." *Cell* **76**(2): 301-314.

Strieter, R. M., S. L. Kunkel, et al. (1995). "Interferon gamma-inducible protein 10 (IP-10), a member of the C-X-C chemokine family, is an inhibitor of angiogenesis." *Biochemical and biophysical research communications* **210**(1): 51-57.

Strieter, R. M., S. L. Kunkel, et al. (1988). "Monokine-induced gene expression of a human endothelial cell-derived neutrophil chemotactic factor." *Biochemical and biophysical research communications* **156**(3): 1340-1345.

Sylvester, R. J., M. A. Brausi, et al. (2010). "Long-term efficacy results of EORTC genito-urinary group randomized phase 3 study 30911 comparing intravesical instillations of epirubicin, bacillus Calmette-Guerin, and bacillus Calmette-Guerin plus isoniazid in patients with intermediate- and high-risk stage Ta T1 urothelial carcinoma of the bladder." *Eur Urol* **57**(5): 766-773.

Tanaka, Y., D. H. Adams, et al. (1993). "T-cell adhesion induced by proteoglycan-immobilized cytokine MIP-1 beta." *Nature* **361**(6407): 79-82.

Taub, D., J. Ortaldo, et al. (1996). "Beta chemokines costimulate lymphocyte cytolysis, proliferation, and lymphokine production." *Journal of leukocyte biology* **59**(1): 81-89.

Taub, D., T. Sayers, et al. (1995). "Alpha and beta chemokines induce NK cell migration and enhance NK- mediated cytolysis." *The Journal of Immunology* **155**(8): 3877-3888.

Towbin, H., T. Staehelin, et al. (1979). "Electrophoretic transfer of proteins from polyacrylamide gels to nitrocellulose sheets: procedure and some applications." *Proceedings of the National Academy of Sciences of the United States of America* **76**(9): 4350-4354.

Tromp, S. C., M. G. oude Egbrink, et al. (2000). "Tumor angiogenesis factors reduce leukocyte adhesion in vivo." *International immunology* **12**(5): 671-676.

Turtle, C. J. and S. R. Riddell (2011). "Genetically retargeting CD8+ lymphocyte subsets for cancer immunotherapy." *Current Opinion in Immunology* **23**(2): 299-305.

Umehara, H., E. T. Bloom, et al. (2004). "Fractalkine in vascular biology: from basic research to clinical disease." *Arteriosclerosis, thrombosis, and vascular biology* **24**(1): 34-40.

van der Bruggen, P., C. Traversari, et al. (1991). "A gene encoding an antigen recognized by cytolytic T lymphocytes on a human melanoma." *Science* **254**(5038): 1643-1647.

Vielhauer, V., R. Allam, et al. (2009). "Efficient renal recruitment of macrophages and T cells in mice lacking the duffy antigen/receptor for chemokines." *The American journal of pathology* **175**(1): 119-131.

von Hundelshausen, P., K. S. Weber, et al. (2001). "RANTES deposition by platelets triggers monocyte arrest on inflamed and atherosclerotic endothelium." *Circulation* **103**(13): 1772-1777.

Walmsley, A. R., F. Zeng, et al. (2001). "Membrane topology influences N-glycosylation of the prion protein." *EMBO J* **20**(4): 703-712.

Walz, A., P. Peveri, et al. (1987). "Purification and amino acid sequencing of NAF, a novel neutrophil-activating factor produced by monocytes." *Biochemical and biophysical research communications* **149**(2): 755-761.

Walzer, T., M. Blery, et al. (2007). "Identification, activation, and selective in vivo ablation of mouse NK cells via NKp46." *Proceedings of the National Academy of Sciences of the United States of America* **104**(9): 3384-3389.

WHO (2011). "Cancer Fact Sheet No. 297."

Wiener, M. C. (2004). "A pedestrian guide to membrane protein crystallization." *Methods* **34**(3): 364-372.

Wu, D., C. K. Huang, et al. (2000). "Roles of phospholipid signaling in chemoattractant-induced responses." *J Cell Sci* **113**(17): 2935-2940.

Wu, N. Z., B. Klitzman, et al. (1992). "Diminished leukocyte-endothelium interaction in tumor microvessels." *Cancer research* **52**(15): 4265-4268.

Wurm, F. M. (2008). Manufacture of Recombinant Biopharmaceutical Proteins by Cultivated Mammalian Cells in Bioreactors. Modern Biopharmaceuticals, Wiley-VCH Verlag GmbH**:** 723-759.

Xie, J. H. (2003). "Antibody-mediated blockade of the CXCR3 chemokine receptor results in diminished recruitment of T helper 1 cells into sites of inflammation." *Journal of leukocyte biology* **73**(6): 771-780.

Yoshimura, T., K. Matsushima, et al. (1987). "Neutrophil chemotactic factor produced by lipopolysaccharide (LPS)- stimulated human blood mononuclear leukocytes: partial characterization and separation from interleukin 1 (IL 1)." *The Journal of Immunology* **139**(3): 788-793.

Zhang, X., H. Wei, et al. (2007). "Activation of human natural killer cells by recombinant membrane-expressed fractalkine on the surface of tumor cells." *Oncol Rep* **17**(6): 1371-1375.

Zhang, X., H. Wei, et al. (2006). "Involvement of interaction between Fractalkine and CX3CR1 in cytotoxicity of natural killer cells against tumor cells." *Oncol Rep* **15**(2): 485-488.

Zhao, D. X., Y. Hu, et al. (2002). "Differential expression of the IFN-gamma-inducible CXCR3-binding chemokines, IFN-inducible protein 10, monokine induced by IFN, and IFN-inducible T cell alpha chemoattractant in human cardiac allografts: association with cardiac allograft vasculopathy and acute rejection." *Journal of immunology* **169**(3): 1556-1560.

7 Acknowledgements

There are many people who I owe a debt of deep gratitude as they have made this work possible. First of all, I want to thank my thesis advisor, Peter J. Nelson. Thank you for giving me the opportunity to work on a fascinating project like this one in the first place, and later for your great support with all the smaller and bigger problems that arose in the years I spent on the project. I am also very grateful for all the chances you gave me to broaden my immunological knowledge and for your help with the transition to a new professional perspective. I always felt perfectly supported, which is not to be taken for granted.

I also want to thank the reviewers of my thesis for taking the time and effort to evaluate my writing.

None of the work presented here would have been possible without the help of my great great (yes, 2x great) colleagues. Be it that I could always count on the truly professional help with experiments that I got from the best cell-culture-protein-isolation-cloning-and-all-other-tasks technicians I ever met or be it the many cups of coffee that helped me through lab days. And not to be forgotten the many times I was supplied with vitamins or self-made treats – when I someday know how to cook I will pay you back. So thank you Alex, Anna, Anke, Christine, Dilip, Farah, Laura, Moni, Sophia, Susan and Sylke. You are a great team. And my special thanks go to my AEW Nicki. You know how much I owe you - mentioning every single point would fill this page. Thank you so much. Oh, and Sophia, thanks for trusting in my consulting skills. I also learned a lot in doing this.

I also want to thank Elfriede Noessner, who taught me a lot of skills, was always open for discussion and supported me wherever she could, not least by giving me the chance to routinely work in the Helmholtz Zentrum. Also her group deserves my gratitude for being great collaborators, providing me with so many cells and pieces of advice and the feeling to be always welcome. Thanks also to the graduate college of the SFB TR-36 for many fascinating hours and events.

It was also a great pleasure to work with Ralph Mocikats group, especially to mention Lorenz Bankel, who made the *in vivo* studies possible and who was one of the best organized collaborators I have met.

Speaking of which – All the other groups in the Klinische Biochemie also provided their share to the success of this study. It is great to know that one can anytime walk into any lab and there will be someone who is happy to help you with his expertise. Keep this spirit up!

Thanks also to Frank Lehmann for providing me with the murine T cells.

Yes, there is a life outside the lab, so in the following words I want to thank the people who enriched my inter-experimental life.

Thanks to all my great friends – Captain, Jenne, Steph and Steffi to name just very few of them – for the many great hours and days. You´ve been a great crew.

A huge big thank you also goes to my fantastic parents and sisters, who I can count on in every second, who made my studies possible and also greatly supported me in the time of this thesis.

And last but not least I want to thank Claudia – for little dances and smiles, her great phantasy and so much else. I am so glad to have found you.

In summary, the reasons detailed above indicate that people mentioned above are great. Thank you.

EHRENWÖRTLICHE VERSICHERUNG

Ich versichere hiermit ehrenwörtlich, dass ich die vorliegende Dissertation selbstständig angefertigt habe, mich außer der angegebenen keiner weiteren Hilfsmittel bedient und alle Erkenntnisse, die aus dem Schrifttum ganz oder annähernd übernommen sind, als solche kenntlich gemacht und nach ihrer Herkunft unter Bezeichnung der Fundstelle einzeln nachgewiesen habe.

München, den ....

(Unterschrift)

ERKLÄRUNG

Hiermit erkläre ich, dass die vorliegende Dissertation nicht, ganz oder in wesentlichen Teilen, einer anderen Prüfungskommission vorgelegt worden ist. Ich habe mich nicht anderweitig einer Doktorprüfung unterzogen.

München, den ....

(Unterschrift)